NTNU – Trondheim
Norwegian University of
Science and Technology

A Sedimentary Investigation of the Lower Triassic Formations and their Underlying Permo-Carboniferous Units across Spitsbergen, Svalbard

Valentin Zuchuat

Petroleum Geosciences
Submission date: June 2014
Supervisor: Atle Mørk, IGB
Co-supervisor: Snorre Olaussen, UNIS

Norwegian University of Science and Technology
Department of Geology and Mineral Resources Engineering

NTNU – Trondheim
Norwegian University of
Science and Technology

UNIS
The University Centre in Svalbard

A Sedimentary Investigation of the Lower Triassic Formations and their Underlying Permo-Carboniferous Units across Spitsbergen, Svalbard

Valentin Zuchuat

Petroleum Geosciences
Submission date: June 2014
Supervisor: Atle Mørk, NTNU
Co-supervisor: Snorre Olaussen, The University Centre in Svalbard (UNIS)

Norwegian University of Science and Technology
Faculty of Engineering Science and Technology
Department of Geology and Mineral Resources Engineering

Abstract

This study documents and discusses the detailed sedimentology of the Triassic Vikinghøgda and Vardebukta Formations, and their underlying units, of the Permian Kapp Starostin Formation in central and western Spitsbergen, and Lower Carboniferous Hornsundneset and Sergeevfjellet Formations in southern Spitsbergen.

In addition to high-resolution sampling, for further palynological and isotopic analysis purposes, nine detailed sedimentary sections have been measured and logged. These include mountains of Marmierfjellet, Høgskulefjellet, Kongressfjellet in central Spitsbergen, the coastal section at Festningen in western Spitsbergen and mountains of Kovalevskajafjellet, Lidfjellet and Sergeevfjellet on the Sørkapp-Hornsund High. Log and sample GPS coordinates have been recorded using the UTM 33x grid zone.

Based on the field data and analyses of 19 thin sections, 17 sedimentary facies have been identified. These have been grouped into one of four facies associations, based on their vertical and lateral genetic relations, as: (I) Braided river. (II) “Cold” offshore transition. (III) Upper shoreface shallow marine. (IV) “Warm” water offshore transition.

The topmost strata of the Kapp Starostin Formation suggest a lateral shallowing-up trend within their depositional environment, with the appearance of storm-influenced beds. A lower spiculitic content within these sediments is observed towards the east. The boundary between the Kapp Starostin Formation and the Vardebukta/Vikinghøgda Formations, is interpreted as a major transgressive event with no evidence of any break in the sedimentation being observed in the correlated sections. An unexpected “apparent” shallowing-up sequence, which contradicts the typical deepening-up scheme observed in text-book-like transgressive deposits is also seen. The occurrence of a rapid transgression at the base of the Vardebukta/Vikinghøgda Formations could explain the existence of such a sequence at this boundary. This study also documents the occurrence

of major thickness variations, within the Deltadalen Member between Marmierfjellet and Kongressfjellet in central Spitsbergen This may potentially be interpreted as being related to the existence of unmapped, low angle thrusts within the Triassic shales of the lowest member of the Vikinghøgda Formation.

The conglomeratic Brevassfjellet Beds and the *Myalina* limestones of Dienerian age overlie the Lower Carboniferous Hornsundneset Formation at Lidfjellet and the Sergeevfjellet Formation at Sergeevfjellet and Kovalevskajafjellet in Sørkapp. The soft shales of the Vardebukta Formation cap these conglomeratic beds. Both Brevassfjellet Beds and *Myalina* limestones show lateral and vertical differences within their internal architecture, as a consequence of 4D amplitude and frequency variations of the flow energy.

Five amendments to the existing C13G geological map of the Hornsund area are suggested: (I) Extension of the Hornsundneset Formation to the boundary with the Triassic sediments at the foot of the northern ridge of Lidfjellet. (II) The occurrence of the Sergeevfjellet Formation between the Hornsundneset Formation and the Brevassfjellet Beds on Kovalevskajafjellet. (III) The relocation of the normal fault mapped on northern ridge of Sergeevfjellet to its southern ridge. (IV) The mapping of a normal fault on Savičtoppen as a potential continuation of the normal fault existing on Sergeevfjellet. (V) The existence of two unmapped thrusts or *décollement niveaux* on the western slopes of Sergeevfjellet

.

Key Words: facies description, lithostratigraphical boundary, Hornsundneset Fm., Sergeevfjellet Fm., Kapp Starostin Fm. Vardebukta Fm., Vikinghøgda Fm., central, western, south Spitsbergen

Acknowledgments

The person I would like to acknowledge the most has offered me the unique opportunity to combine two of my true passions: studying geology and experiencing the Arctic. His outstanding availability to discuss and his kindness have been of great help to me in achieving my goals. For that, I would like to thank you very much, Atle. I also extend my thanks to my co-supervisor at the University Centre in Svalbard, Professor Snorre Olaussen, as well as Professor Hans Arne Nakrem at the University of Oslo and Professor Nils-Martin Hanken at the University of Tromsø for their useful help and comments.

My loyal field-squire and true friend, PhD candidate Gareth Lord, is also to be gratefully acknowledged for his indispensable assistance during the days out in the field, as well as in the process of writing this thesis. His penchant for the good things has been of great help as well, whenever a break became necessary.

I would also like to thank SINTEF Petroleum Research and the University Centre in Svalbard for their crucial logistic support, as well as the Norwegian Petroleum Directorate, in the persons of Terje Solbakk and Bo Haugen, who joined us for nine unforgettably humid days in Hornsund.

Finally, I would like to thank my dear parents, who offered me the chance to live my dream up north and for the their endless encouragements. I would also like to extend my thanks to Laure, Mats, Scott and Nathaniel, who supported me during these two years in Trondheim.

Thank you.

Index

List of Figures

List of Tables

Preface

This thesis is the final assignment of the international master program MSG2 Petroleum Geology, delivered to the Norwegian University of Science and Technology (NTNU), in collaboration with the University Centre in Svalbard (UNIS). It started initially as part of a potential new joint project between SINTEF Petroleum Research, NTNU and the University of Bergen, in the persons of Professor II Atle Mørk and Professor Gunn Mangerud.

While the main project would focus on the exact location of the Permian-Triassic Boundary within the stratigraphy of Svalbard, which, so far, remains undefined, the thesis consists of a detailed sedimentary study of the lowermost strata of the Triassic Vikinghøgda and Vardebukta Formations and the uppermost beds of their underlying Permian and Carboniferous units, respectively in central, western and south Spitsbergen, in order to better understand the transition across these different lithostratigraphical boundaries. It holds a value of 30 credits and is associated with an earlier project report, a concise literature review of the Permian-Triassic Boundary, its causes and its consequences, as well as the problems resulting of the official definition of the Boundary with the First Appearance Date (FAD) of the conodont *Hindeodus Parvus*.

Data analysed and discussed herein has been collected during the field season of summer 2013 only. While data has been gathered throughout independent expeditions in central and western Spitsbergen, with the logistic help and safety support of the UNIS, the expedition to south Spitsbergen has been conducted in partnership with the Norwegian Petroleum Directorate. Palynology samples, intended for further high-resolution biostratigraphical studies, have been extensively collected at every location. The lithostratigraphical approach of this thesis, alone, can't solve the persistent chronostratigraphical uncertainties of the Permian-Triassic Boundary on Svalbard, but combined with these upcoming new palynological results, will provide important information and a better understanding of the changes happening across both lithostratigraphical and chronostratigraphical boundaries.

1. Introduction

The exceptional high arctic archipelago of Svalbard (Fig. 1) has been resonating in the head of geologists as a call to adventure since Baltazar Mathias Keilhau lead the first Norwegian geological expedition in 1827 (Sysselmannen 2008). Over the last thirty years, Svalbard has seen the interests of earth scientists increasing exponentially as it became a great analogue for the oil and gas provinces of the Barents Sea. Outcropping between 74°N and 81°N, the rocks present on these boreal islands, free of any dense vegetation, offer geoscientists a tremendous playground to carry out their research.

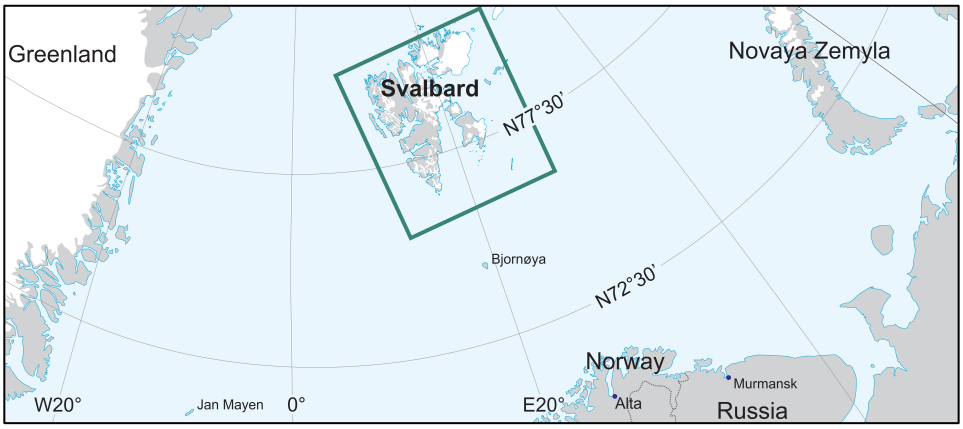

Fig. 1 – Map of Svalbard and its neighbouring regions (from Lord 2013).

This thesis will analyse and discuss the detailed sedimentology of the uppermost beds of the Carboniferous Hornsundneset Fm. and Sergeevfjellet fms., the Permian Kapp Starostin Fm. and the lowermost strata of the Triassic Vardebukta and Vikinghøgda fms..

2. Svalbard Geological setting

Since the Precambrian, almost the entire geological time has been recorded in the rocks of Svalbard, with the convenience of some hiatuses (Dallmann (ed.) 1999). However, the landmass that is known today as Svalbard hasn't always been located in the neighbourhood of polar latitudes. Indeed, it has been drifting northwards from the equator since the Devonian (Fig. 2) (Elvevold *et al.* 2007, Golonka 2011). Note that, during the Jurassic and the Cretaceous, the drifting velocity is relatively slow compared with the previous Paleozoic and Triassic and the following Cenozoic velocities: from the end of Triassic until the end Cretaceous-Tertiary Boundary, it only moves from approximately 50°N to about 60°N.

As a consequence of this journey towards more boreal regions, sedimentary processes and depositional environments, heavily influenced by the evolution of climatic conditions, have been changing. The alternation of different rocks sculpting the landscape of Svalbard testifies to this tortuous history, punctuated by five major tectonic events: the Grenvillian (Upper Mesoproterozoic), the Caledonian (Ordovician-Silurian), The Ellesmerian or Svalbardian (Upper Devonian), the Variscan (Middle Carboniferous) and the Alpine orogeny (Lower Cenozoic) (Dallmann (ed.) 1999).

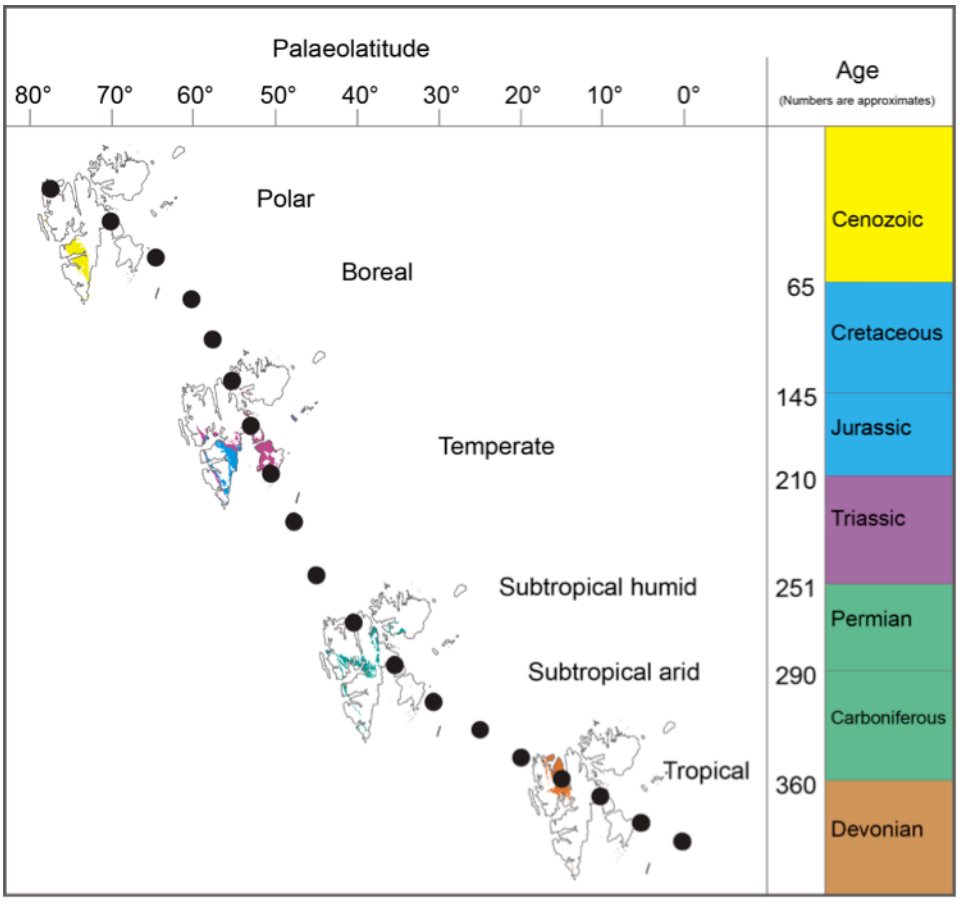

Fig. 2 – Time-lapse of the northwards drift of Svalbard (from Elvevold *et al.* 2007 and Lord 2013).

As shown in Fig. 3, the geology of Svalbard consists of a poly-metamorphic pre-Devonian basement called *Hecla Hoek* covered by nine sedimentary groups and one Mesozoic dolerite inclusion (Diabasodden Suite). Otha (1994) resumes the formation of *Hecla Hoek* in four periods, obtained by radiometric dating Archean[1] to Early Proterozoic ages:

[1] The geological significance of these rocks is still not completely understood.

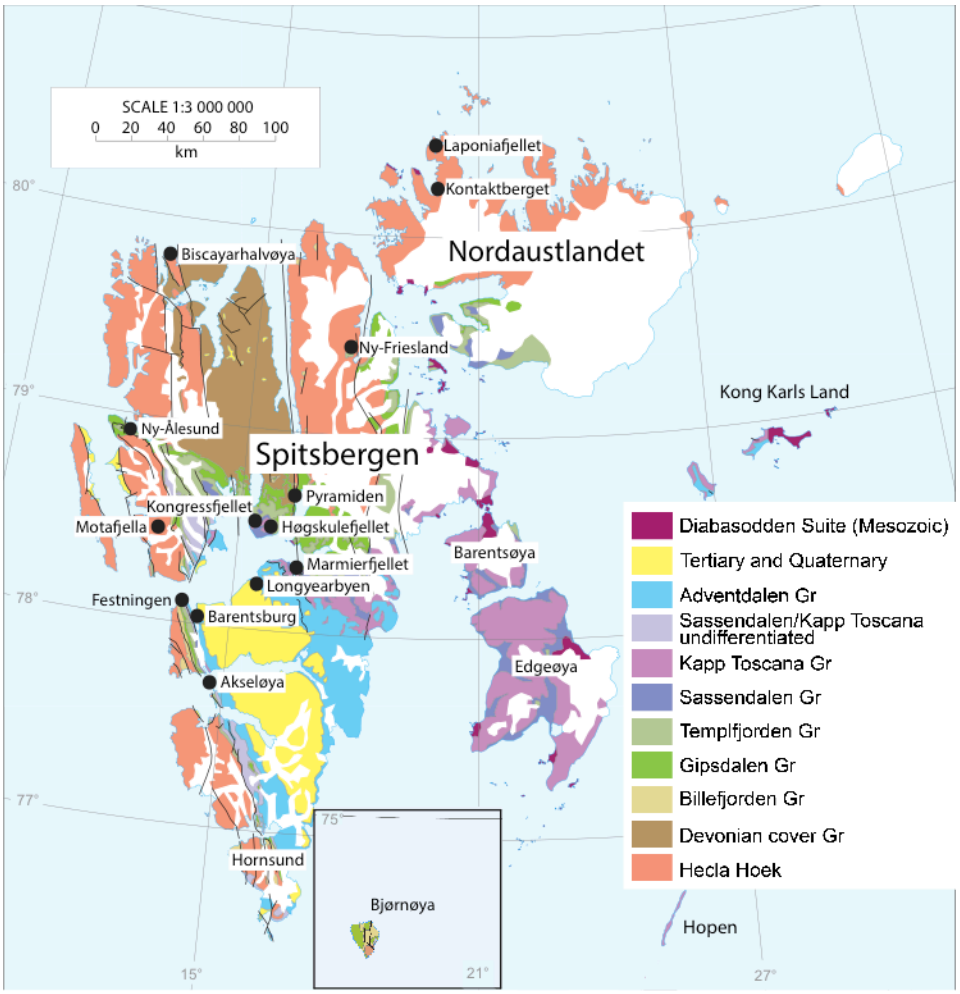

Fig. 3 – Geological map of Svalbard (from Dallmann (ed.) 1999, localities added).

(i) 3.2 Gya at Biscayarhalvøya, (Peucat *et al.* 1989), 2.1 Gya at Motalafjella (Bernard-Griffiths *et al.* 1993),

(ii) Svecofennian ages: 1.67-1.75 Gya at Ny-Friesland (Gee 1991, Gee *et al.* 1992, 1994),

(iii) Grenvillian Orogeny event: 1.27 Gy-910 Mya, 961±17Mya at Laponiafjellet, 939±8 Mya at Kontaktberget (Gee *et al.*1995),

(iv) a) Early Caledonian event (Middle-Late Cambrian), b) Late Caledonian event (Middle-Late Silurian) and c) a post-orogeny Devonian graben formation

The existence of Late Proterozoic basic and felsic rocks on the northern coast is also mentioned by Otha (1994), without providing any more information other than they are coeval with the Upper Proterozoic Baikalian event (850-650 Mya) (Khomentovsky 2002), the Siberian equivalent of the Baltican Timanide Orogeny (Gee & Pease 2004). On Svalbard, this Late Precambrian period is referred as the "Deposition of Neoproterozoic Murchisonfjorden and Lomfjorden Supergroups and Vendian to Ordovician Hinlopenstretet Supergroup" by Johansson *et al.* (2005).

The Devonian period is characterized by the termination of the Caledonian orogeny, followed by the formation of the European Variscan belt ensuing from the collision of Baltica and Laurentia continents (Friend *et al.* 2000). The principal Ellesmerian episodes are contemporary of this period (Ziegler 1988). The *Old Red* sediments are deposited and deformed in a molasses-type, wedge-shaped foreland basin setting concomitantly with these consecutive tectonic events, especially during the Upper Devonian Svalbardian folding (Piepjohn *et al.* 2000).

During the Carboniferous period, the tectonic regime changes. An extensional tectonism replaces the compressive-transpressive setting, developing grabens and tilted fault blocks (Dallmann (ed.)

1999). The Sørkapp-Hornsund High is seen as a consequence of these Svalbardian (Upper Devonian) and Adriabukta (Lower or Mid-Carboniferous) tectonic events (Dallmann 1992). The clastic input that formed the Billefjorden Gp. diminishes by the end of Carboniferous. Consequently and until the Early Permian, the tropical to warm-water column becoming free of any detrital material, carbonate platforms start to develop on Svalbard (Gipsdalen Gp.) (Reid *et al.* 2007, Blomeier *et al.* 2011). Several evaporitic episodes interrupt these complex carbonate sequences.

Since the geological units going through the Permian-Triassic Boundary (PTB) are the main topic of this thesis, the Permian and Triassic stratigraphy will be developed in greater details further on.

The Jurassic period sees the sediments of the Adventdalen Gp. being deposited in a deeper marine setting, overlain by Lower Cretaceous shallower successions. The dolerite intrusion of the Diabasodden Suite within the Upper Paleozoic and Mesozoic strata is a direct consequence of the opening of the North Atlantic Ocean during the Upper Jurassic and the Lower Cretaceous (Dallmann (ed.) 1999). The Late Cretaceous is not present on Svalbard because of a tectonic uplift.

The Atlantic Ocean continues its inexorable opening throughout the Cenozoic. During the Paleocene-Eocene periods and despite this regional divergent tectonic context, the Spitsbergen and the Molloy dextral transform faults systems start separating Greenland

and Svalbard (Torsvik *et al.* 2001, Engen *et al.* 2008). This localised multiphased convergent-transpressive stress regime is the cause of the development of the West Spitsbergen Fold-and-Thrust Belt (WSFTB), accumulating a margin-perpendicular shortening of approximately 20-40 km (Braathen *et al.* 1999, Dallmann (ed.) 1999, Leever *et al.* 2011). As a result, most of the Upper Paleozoic and Mesozoic rocks in the western part of Spitsbergen, including basement units, are heavily thrusted and folded. Meanwhile, complex sedimentary basins are formed, among which the most important is the asymmetric Central Tertiary Basin to the East of the WSFTB (Müller & Spielhagen 1990).

The Cenozoic deformation province can be divided as follow: (i) a western zone characterized by folds and thrusts, involving basement rocks, (ii) a central zone of thin-skinned fold-thrust units overlying a Permian evaporitic *décollement* horizon, and (iii) an eastern zone representing a foreland province (Bergh *et al.* 1997, Braathen *et al.* 1999).

These main structural lineaments follow a general NNW-SSE trend. This orientation tendency has been observed to the edge of the continental margin (Myhre & Eldholm 1988, Faleide *et al.* 2008). One of the most impressive examples of these complex deformation structures is visible on the northwest face of Midterhukfjellet (Fig. 4). The Middle Triassic ductile shales of the Bravaisberget Fm. are disharmonically deformed, while the more

competent rocks of the Permian Kapp Starostin, the Lower Triassic Vardebukta and Tvillingodden fms. and the Upper Triassic-Jurassic Kapp Toscana Gr. are characterized by a longer folding wave length (see Maher *et al.* (1986) for a detailed kinematic study of this area).

The WSFTB contrasts with the relatively undeformed sub-horizontal strata, characteristic of the central and eastern areas of Spitsbergen, as well as the eastern islands of Edgeøya, Barentsøya and Wilhelmøya. Note that, between Spitsbergen and these islands, the major structural lineaments are N-S oriented, while they become NE-SW oriented when continuing offshore Svalbard (Gabrielsen *et al.* 1990, Faleide *et al.* 2008). According to Faleide *et al.* (2008) however, the faulting and the basin formation to the East of Svalbard is related to an Upper Paleozoic failed rifting period.

Svalbard has undergone two uplift phases: (i) >36-10Mya and (ii) <10Mya (Dörr *et al.* 2013). The intensity of both uplift periods reduces towards the East. Volcanic rocks (Miocene and Pliocene transitional olivine basalts and Quaternary off-ridge alkali basalts) have also been reported in NW Spitsbergen (Dallmann (ed.) 1999).

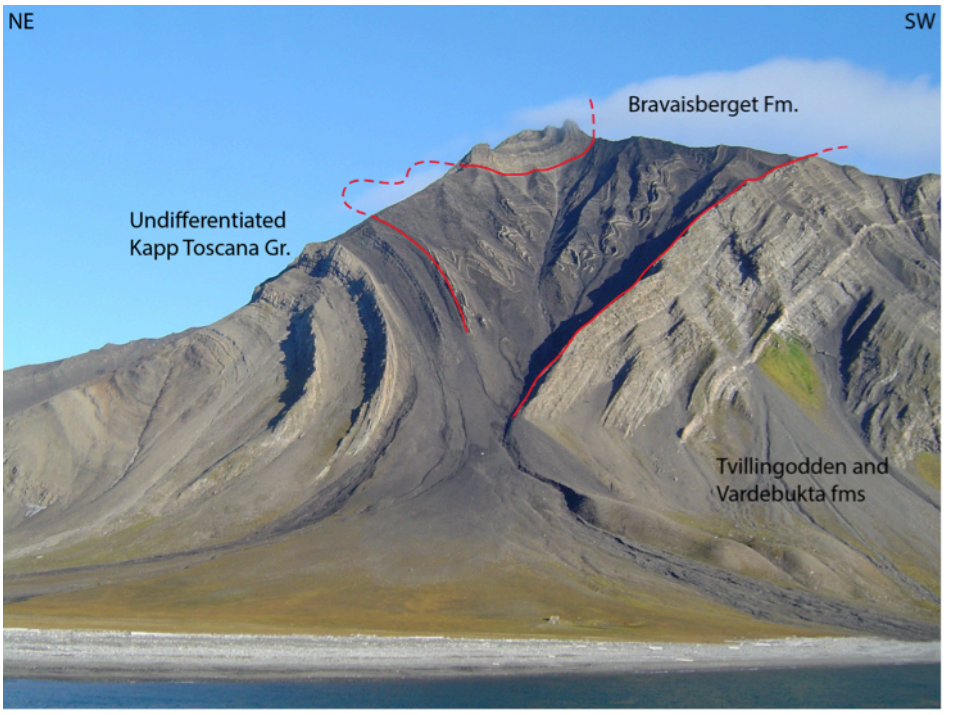

Fig. 4 – Folding in Midtrerhuktafjellet, Van Keulenfjorden (Photo from Ólafur Ingólfsson, stratigraphy added after Maher *et al.* (1986)).

2.1. Lithostratigraphy of the Permian-Triassic Boundary units

Even if the title of this subchapter refers to the Permian and the Triassic ages, it doesn't encompass the complexity of the basal contact of the Vardebukta Fm. throughout Svalbard. Indeed, towards the West of the Sørkapp-Hornsund High, the Triassic shales of the Vardebukta Fm. don't rest on the Permian units of the Kapp Starostin Fm., but on sandstones of Visean/?Serpukhovian age (Lower Carboniferous, palynology results, Dallmann *et al.* 1999, Scheibner *et al.* 2012), belonging to the Billefjorden Group. Therefore, these two Carboniferous

formations present on the High will also be described in this subchapter.

2.1.1. Carboniferous units on the Sørkapp-Hornsund High

The precise structural history of the Sørkapp Hornsund High remains not thoroughly understood. The basement units have been uplifted during by the Upper Devonian Svalbardian event and its complementary Adriabukta event (Dallmann 1999, Bergh *et al* 2011). On the West of the High itself, the Triassic Brevassfjellet Beds, a basal conglomerate of the Vardebukta Fm. (Worsley & Mørk 1978, Mørk *et al.* 1999b), rest on two different units of Lower Carboniferous age: (i) the Hornsundneset Fm., which directly lies on *Hecla Hoek* rocks, and (ii) the Sergeevfjellet Fm. (Lipiarski & Čmiel 1984, Wendorff 1985, Dallmann *et al.* 1999) (Fig. 5, Fig. 6). Both of them belong to the Upper Billefjorden Group.

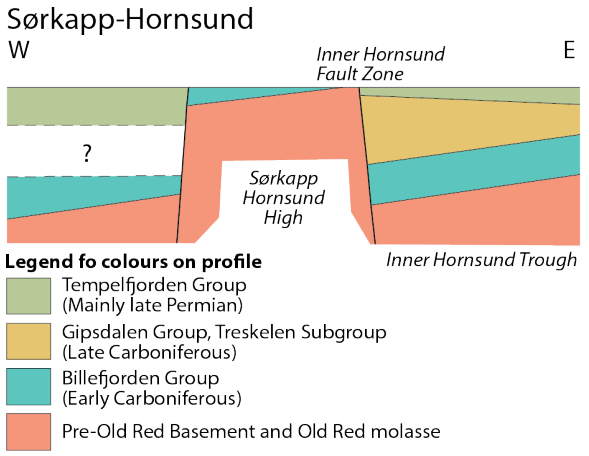

Fig. 5 – Schematic cross section through the Paleozoic units of Sørkapp-Hornsund High (from Dallmann *et al.* 1999).

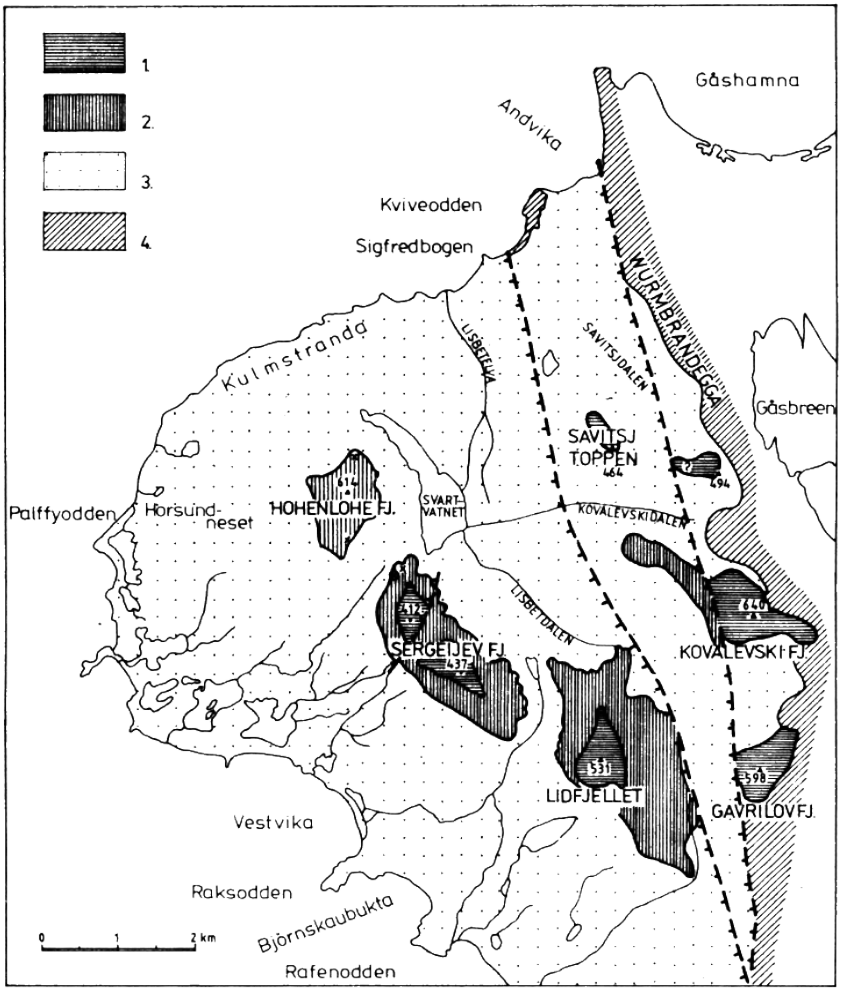

Fig. 6 – Geological map of the Hornsundneset area. 1 – Triassic; 2 – Sergeevfjellet Fm.; 3 – Hornsundneset Fm.; 4 – Hecla Hoek (from Lipiarski & Čmiel 1984).

The Hornsundneset Fm. is a stack of light-coloured, medium to fine, monomictic, quartz-rich sandstone, deposited braided rivers flowing towards E-SE directions, interbedded with dark siltstone and a few coal seams (Gjelberg & Steel 1981, Lipiarski & Čmiel 1984, Wendorff 1985). Its type section is located at Hohenlohefjellet, in Hornsund (Fig. 7, left). A thin quartz

conglomerate defines its lower boundary. It grossly fines upwards towards the overlying Sergeevfjellet Fm. (Dallmann *et al* 1999). The thickness of that formation ranges from approximately 700m at Hornsundneset, where the strata are gently dipping, to 1100m at Austernebba and at Knattbergetin in the foldbelt itself, with sub-vertical to overturned beds (Wendorff 1985, Dallmann *et al.* 1999).

The name Sergeevfjellet Fm. originates from the mountain where is has been defined in Hornsund, just south of Hohenlohefjellet (Fig. 7, right). It has exclusively been reported from the Hornsundneset area. The lower boundary of this formation is defined by Dallmann *et al*. (1999) “at the base of the first fining-upward sandstone unit that ends up with a distinct shale interval”. These fine-grained, cream-coloured quartz-rich fluvial sandstones are often interbedded by clear siltstone, carbonaceous shales and coal layers (Gjelberg & Steel 1981, Lipiarski & Čmiel 1984, Wendorff 1985). The depositional environment has been interpreted as braided rivers with a major floodplain influence. The thickness of this formation reaches a maximum value of 260m (Dallmann *et al*. 1999).

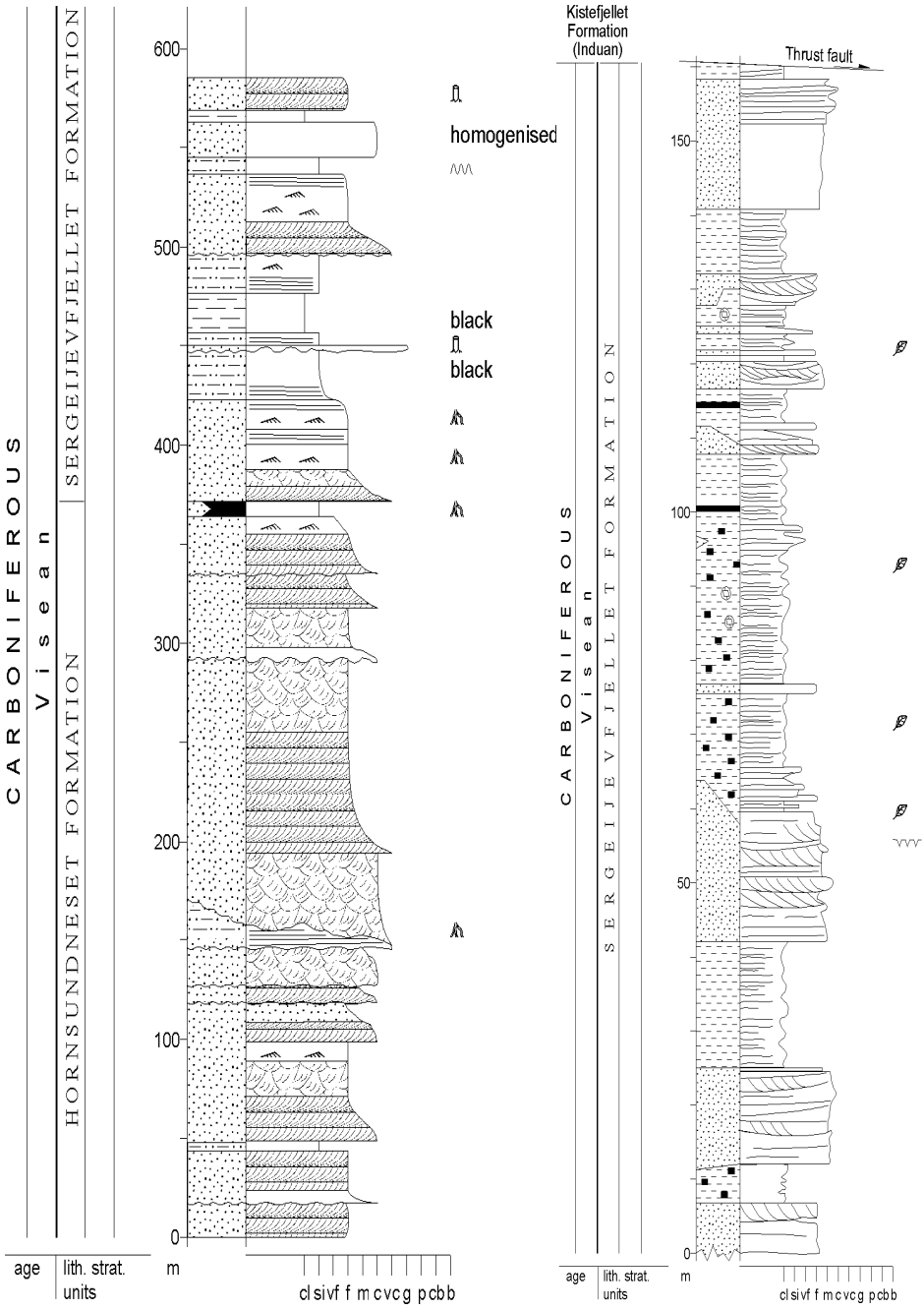

Fig. 7 – Left: type section of the Hornsundneset Fm. Right: type section of the Sergeevfjellet Fm. (from Dallmann *et al.* 1999).

Fig. 7 (continues) – Legend for the sedimentary logs (from Dallmann (ed.) 1999).

LEGEND FOR STRATIGRAPHIC TYPE SECTIONS

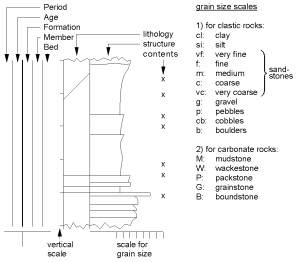

LITHOLOGY:

1. Siliciclastic rocks

- Breccia
- Conglomerate
- Gravelstone/gritstone
- Pebbly sandstone
- Sandstone
- Silty sandstone
- Siltstone
- Sandy shale
- Shale, mudstone, claystone
- Sandy chert
- Chert
- Paper shale

2. Mixed carbonate-siliciclastic rocks

- Calcite-cemented sandstone
- Dolomite-cemented sandstone
- Calcareous shale
- Dolomitic shale
- Sandy limestone
- Silty limestone
- Clayey limestone
- Cherty limestone
- Sandy, dolomitic limestone
- Sandy, calcitic dolomite
- Sandy dolomite
- Siderite-cemented sandstone

3. Carbonate rocks

- Limestone, calcareous ...
- Dolomite, dolomitic ...
- Dolomitic limestone
- Calcitic dolomite
- Siderite

4. Other layered lithologies

- Gypsum & anhydrite
- Coal
- Dolerite sill / dyke
- Basalt lava

5. Secondary lithological content

- Cherty nodules
- Calcareous nodules
- Dolomitic nodules
- Sideritic nodules
- Gypsiferous/anhydritic nodules
- Pyritic nodules
- Septarian nodules
- Phosphate nodules
- Sandstone lens
- Clay-ironstone or siltstone nodules
- Conglomerate beds
- Polymict conglomerate beds
- Mud flakes
- Mud clasts
- Sandy
- Silty
- Shaley
- Cherty
- Calcareous
- Dolomitic
- Sideritic
- Gypsiferous/anhydritic
- Halitic
- Coaly, coal lenses or fragments
- Bentonite
- Glauconite
- Quartzite
- Caliche

STRUCTURE:

- Trough cross-bedding, undifferentiated
- Trough/planar cross-bedding, adjusted to appearance in outcrop
- Tabular/planar cross-bedding
- Herringbone cross-bedding
- Bioherm/reef

- MPS Maximum particle size (cm)
- Beds distinct
- Unbedded
- Cross bedding, ripple lamination
- Ripple structures
- Climbing ripple lamination
- Dunes
- Flaser bedding/lenticular bedding
- Wave ripples
- Wavy lamination
- Planar lamination
- Cone in cone
- Convolute lamination and soft-sediment deformation
- Flow structures
- Karst
- Stylolites
- Mud cracks
- Hiatus/erosion surface
- Loading
- Hummocky bedding/lamination

FOSSILS AND PARTICLES:

1. Vertebrate fossils

- Vertebrates
- Fish remains

2. Invertebrate fossils

- Calcispheres
- Corals
- Bivalves
- Rudists
- Gastropods
- Brachiopods
- *Lingula*
- Bryozoans
- Trilobites
- Sponges
- Foraminifera, undifferentiated
- Foraminifera, benthic
- Foraminifera, encrusting
- Foraminifera, planktonic
- Fusulinids
- *Orbitolina*
- Ostracods
- Molluscs
- Cephalopods, mostly belemnites
- Ammonoids
- Echinoderms
- Crinoids
- *Palaeoaplysina*

3. Plant fossils

- Laminar stromatolites
- Columnar stromatolites
- Encrusting algae
- Green algae
- Red algae
- Phylloid algae
- Algae lamination
- *Girvanella*
- Stromatoporids
- *Stigmaria*
- Plant fragments
- Tree trunks
- Roots

4. Trace fossils

- Burrows, horizontal
- Burrows, vertical
- Burrows, undifferentiated
- Increasing bioturbation
- *Arenicolites*
- Trails
- *Ophiomorpha*
- *Rhizocorallium*
- *Skolithos*
- *Terebellina*
- *Thalassinoides*
- *Zoophycos*
- *Chondrites*
- *Palaeophycus, planolites*
- *Diplocraterion*

5. Others

- Fossils, undifferentiated
- *Microcodium*
- *Tubiphytes*
- Coquina beds
- Ooids
- Oncoids
- Pellets
- Peloids
- Bioclasts
- Intraclasts
- Lithoclasts

VARIOUS:

- Break
- Fault
- c Covered section

2.1.2. Permian units

During the Permian, while the Ural orogeny is at its peak, the Uralian seaway is closing (Blomeier *et al.* 2011) (Fig. 8a), isolating the boreal water from the Tethys Ocean. As a consequence, the influx of clastic sediments in the system increases again, before dwindling during the Wordian-Wuchiapingian (Reid *et al* 2007). Eventually, the cold-water, fossil-rich, cherty-spiculitic, bioturbated shales and limestones of the Kapp Starostin Fm. are deposited on Svalbard following the onset of a transgression, as part of the so-called “Permian Chert Event” (Beauchamp & Baud 2002). The similar warm-to-cool water shift is documented in the Sverdrup Basin by Reid *et al.* (2007).

The thickness of the Kapp Starostin Fm. formation fluctuates between the different places of Svalbard. From 460 m in the St. Jonsfjorden Trough, it pinches out towards the Sørkapp-Hornsund High, where only a few meters have been recorded in the area of the Treskelen peninsula (Malkowski 1982, Lipiarski & Čmiel 1984, Wendorff 1985, Birkenmajer 1977, 1990, Dallmann *et al.* 1999). The responsibility of some active tectonic regarding this wedge geometry and the absence of the Kapp Starostin Fm. around the Sørkapp-Hornsund High remains unclear, as a pure (non-)depositional episode can’t be excluded (Worsley & Mørk 1978). The upper part of the Kapp Starostin Fm. is proposed to be of Wuchiapingien age, based on the Sr-isotopic composition of brachiopods shells (Ehrenberg *et al.* 2010). However, the

stratigraphic development of this formation remains nebulous (Dallmann *et al.* 1999).

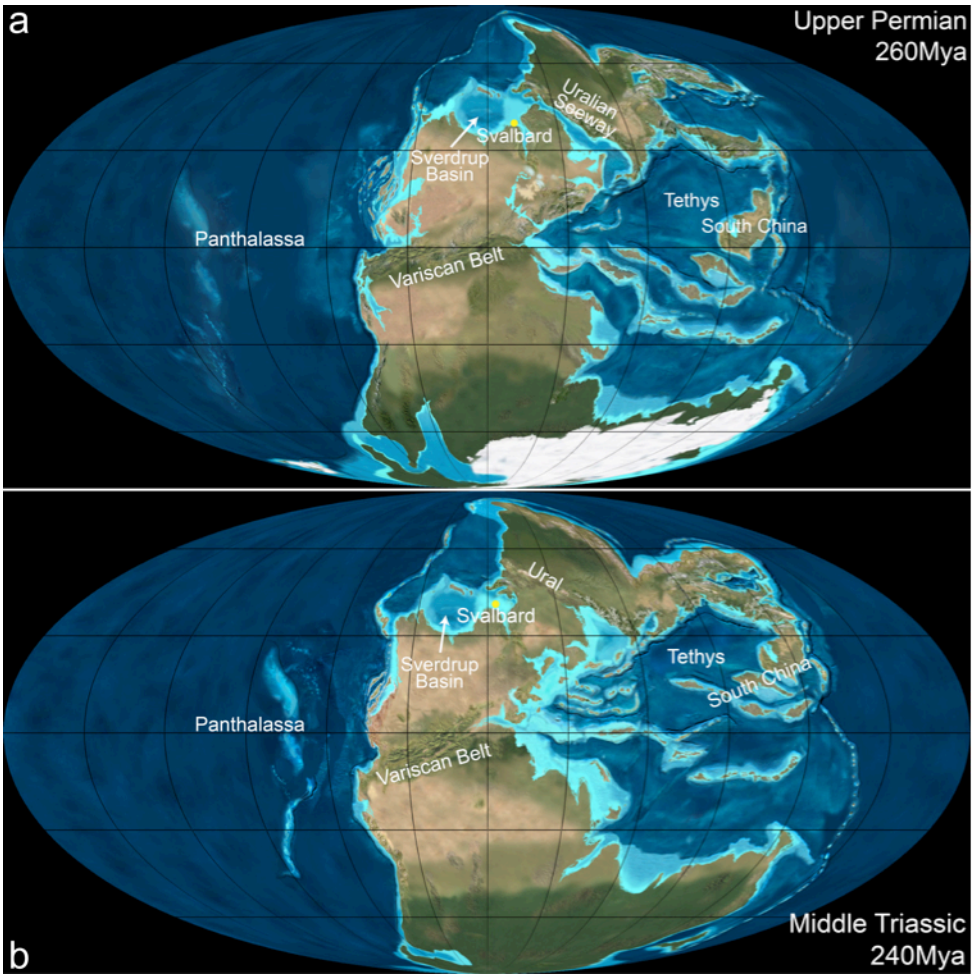

Fig. 8 – a. Paleogeography of the Late Permian (from Backley 2013: jan.ucc.nau.edu, geographical names added). b. Paleogeography of the Middle Triassic (from Backley 2013: jan.ucc.nau.edu, geographical names added). Note the closure of the Uralian Seaway, isolating the boreal water from the Tethys Ocean.

The type section of the Kapp Starostin Fm. is located at Festningen (Fig. 9). Its lower base is defined by the bioclastic limestone bed of the Vøringen Mb., rich in corals, brachiopods, bryozoans and crinoids. The deepening up trend towards lower

energy spiculite-rich deposits is supported by the study of bryozoans and trace fossils (Nakrem 1994, Uchman *et al.* in prep.). The Vøringen Mb. is overlain by the deep marine shelf, clastic, spiculitic shales of the Svenskeega Mb., which terminates with a marker bioclastic limestone bed. The Hovtinden Mb. is the topmost unit of the Kapp Starostin Fm. at Festningen. Note that these beds consist of SiO_2-cemented silty shales, that contain less spiculite than the Svenskeega Mb.

Two other glauconitic sandstone dominated members exist at the top of the Kapp Starostin Fm. (Dallmann *et al*. 1999): the Revtanna Mb. in the East of the Sørkapp-Hornsund High and the Stensiöfjellet Mb. in the central Spitsbergen. The Tokrossøya Fm., on the SW side of the Sørkapp-Hornsund High, is described as the epicontinental marine representative of the Tempelfjorden Gp. Arenaceous spiculitic chert dominates its lower part, while arenaceous cherty limestones and calcareous siltstones are characterizing its upper part. Other fossil-rich members are defined in the Nordaustlandet regions (Palanderbukta Mb. and Selanderneset Mb.). On Bjørnøya, the Miseryfjellet Fm. is the lateral equivalent of the Kapp Starostin Fm.

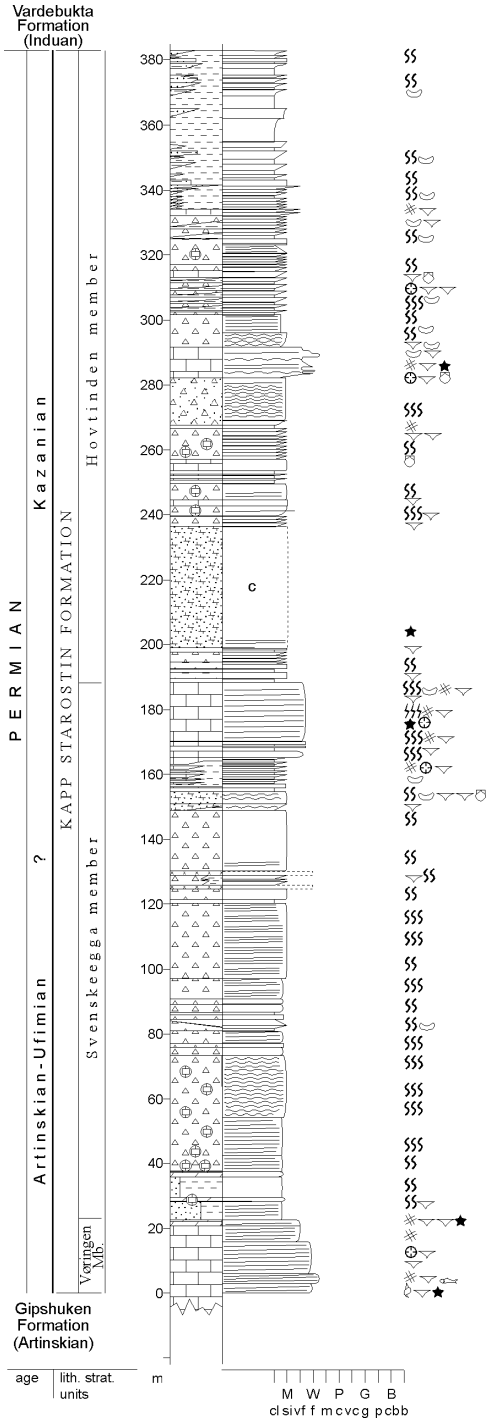

Fig. 9 – Kapp Starostin type section, Festningen (from Dallmann *et al.* 1999). See Fig. 7 for legend.

2.1.3. Triassic units

Laying comfortably on the Permian Kapp Starostin Fm., the Triassic succession of Svalbard consists of (Fig. 8b), high sedimentation rate, siliciclastic sequences. Nine finning-up transgressive and coarsening-up regressive cycles have been recoded in this fast subsiding basin (Mørk *et al.* 1989, Vigran *et al.* 2014). Two groups are defined in the Triassic sedimentary record of Svalbard and the Barents Sea: The Lower to Middle Triassic Sassendalen Gp. and the Upper Triassic to Middle Jurassic Kapp Toscana Gp. (Fig. 10).

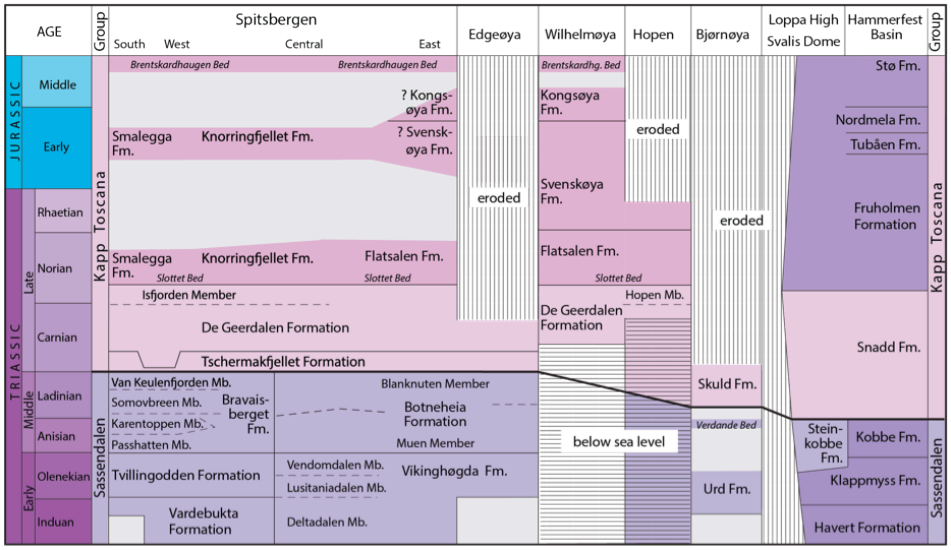

Fig. 10 – Correlation chart of the Sassendalen and the Kapp Toscana groups on Svalbard and in the Norwegian Barents Sea (from Mørk *et al.* 2013).

Since the rock strata are sub-vertical within the WSFTB, the alternations of hard and soft units lead to particular shorelines geometry. The non-siliceous soft shales strata form embayment while the hard sandstones beds stick out towards the sea. These sequence boundaries are notably visible at Festningen, Akseløya

and Kapp Toscana (Fig. 11a). Since the bedding is sub-horizontal on central and eastern Spitsbergen, these lithology changes are marked by the alternation of sandstone cliffs and more gently shally slopes. However, the Middle Triassic, organic-rich shales of the Blanknuten Mb. (Botneheia Fm.) do form cliff, as notably observed at Muen, on the Western coast of Edgeøya (Krajewski 2008) (Fig.11b).

The Lower Triassic Sassendalen Gp. of Svalbard consists of the Vardebukta and the Tvillingodden fms. in western and southern Spitsbergen defined by Buchan *et al.* (1965), and of the Vikinghøgda Fm. in central and eastern Svalbard, described by Mørk *et al.* (1999a) with a new type section in Deltadalen. The Vardebukta Fm. is 292 m thick at Festningen (Fig. 12 left), while it only reaches 16 m on the Sørkapp-Hornsund High. The Tvillingodden Fm. is 200-250 m high at Festningen (type section) and follows the same southwards pinching-out geometry towards the Sørkapp-Hornsund High. The Vikinghøgda is somewhat more isopachous, ranging between 250 m in Deltadalen, central Spitsbergen (Fig. 12 right) and 200-220 m in eastern Spitsbergen (Mørk *et al.* 1999b).

Fig. 11 – a. Aerial view of the Festningen area (from Norsk Polarinstitutt). The Triassic succession of transgressive-regressive sequences results in an alternation of soft shales coarsening upwards to hard sandstones. Since the erosion is less important on the harder and coarser units than on the finer and softer strata, the harder the rock is, the further in the sea it extends (based on Mørk *et al.* 1989 and Mørk *et al.* 1999b). b. Cliff forming shales of the Botneheia Fm. at Muen, west coast of Edgeøya. The canyon width reaches approximately 50m (photo V. Zuchuat, stratigraphy after Krajewski (2008)). →

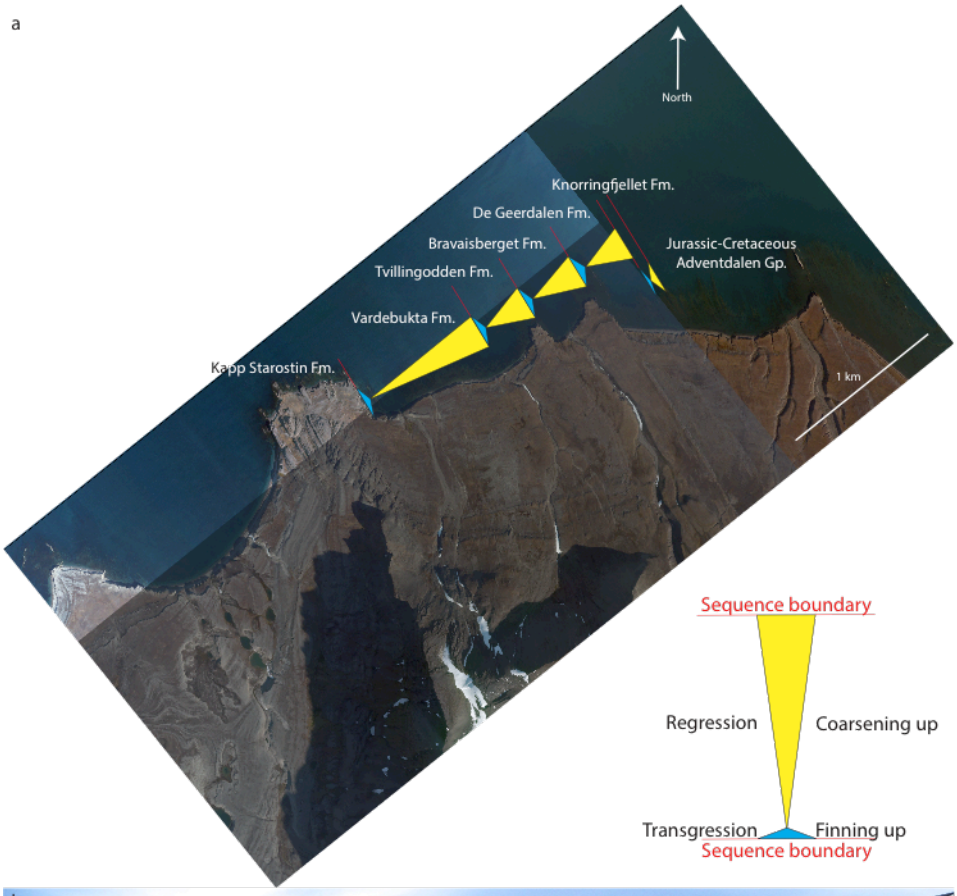
a
North
Knorringfjellet Fm.
De Geerdalen Fm.
Bravaisberget Fm.
Tvillingodden Fm.
Vardebukta Fm.
Kapp Starostin Fm.
Jurassic-Cretaceous
Adventdalen Gp.
1 km
Sequence boundary
Regression
Coarsening up
Transgression
Finning up
Sequence boundary

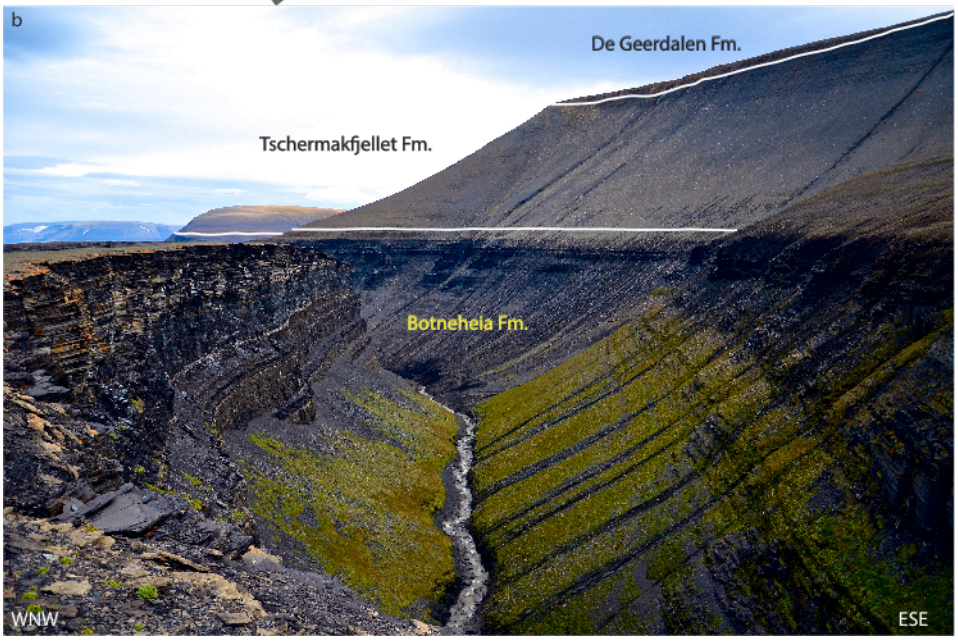
b
De Geerdalen Fm.
Tschermakfjellet Fm.
Botnehela Fm.
WNW
ESE

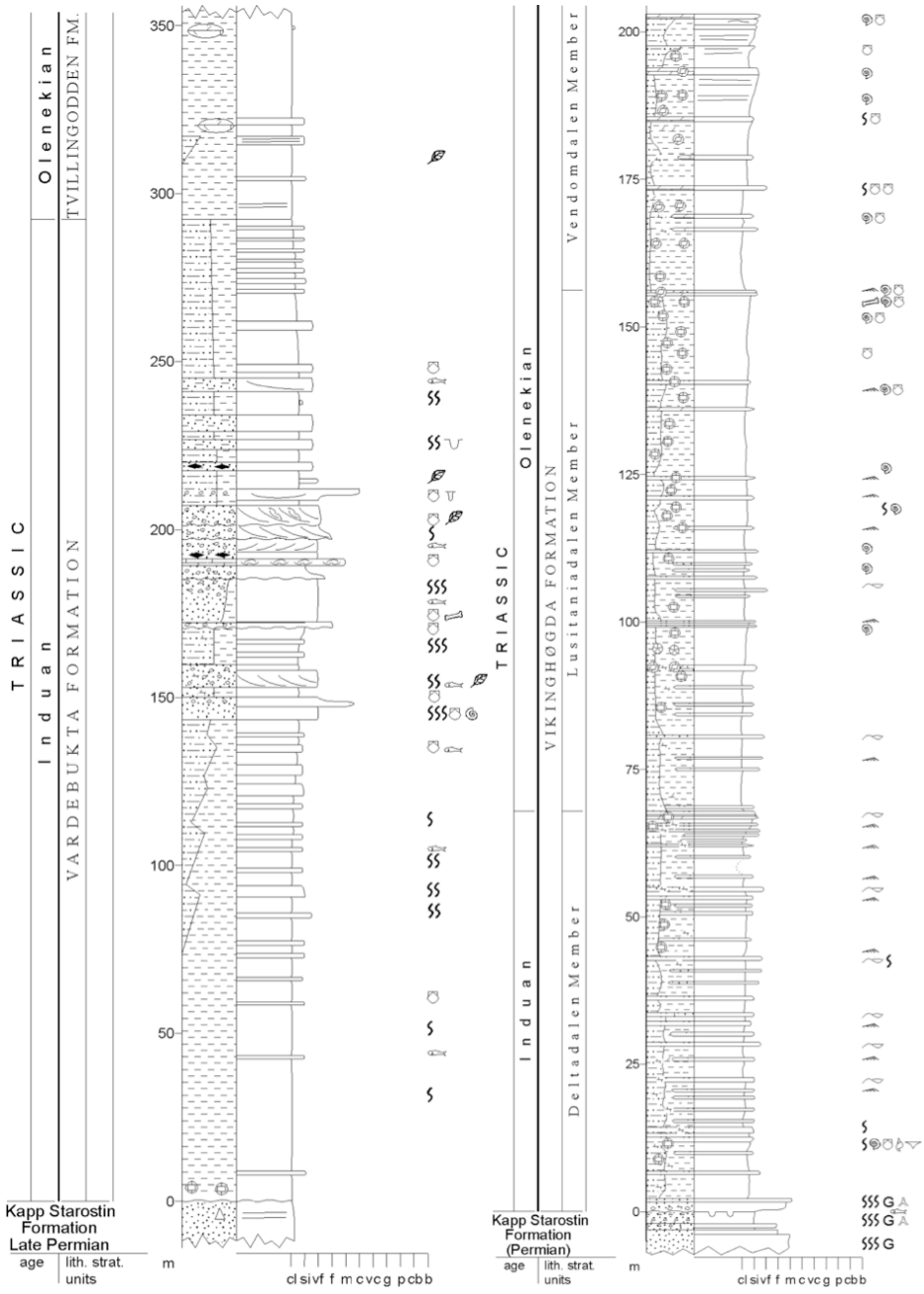

Fig. 12 – Left: Type section of the Vardebukta Fm., Festningen. Right: Type section of the Vikinghøgda Fm., Deltadalen (the top strata of the Vendomalen Mb. is missing) (from Mørk *et al.* 1999b). See Fig. 7 for legend.

The Vardebukta Fm. is divided into two members: the Selmaneset Mb. and the Siksaken Mb. The Vikinghøgda Fm. consists of three members: the Deltadalen Mb., the Lusitaniadalen Mb. and the Vendomalen Mb. Both the Vardebukta and the Vikinghøgda fms. consist of alternations of non-siliceous, dark grey, variably bioturbated, changeably organic-rich shales and hummocky cross-laminated siltstone beds, interpreted as storm-influenced deposits. Several calcareous erratically nodular layers have also been reported within these two formations. Some of them sparsely contain remains of *Otoceras boreale* ammonites, bivalves, bryozoans, conodonts or fish bones (Nakrem & Mørk 1991). The quantity of fossils and bioturbations, sand content and the thickness of these storm beds increase significantly towards the top of these formations (Buchan *et al.* 1965, Mørk *et al.* 1982, 1989, Wignall *et al.* 1998).

A general deeper depositional environmental trend is observed from the West to the East of Svalbard. The Vardebukta Fm. is characterized by a "shallow-marine, coastal environment with prograding deltaic lobes", while the deeper shelf mudstones deposits form the Vikinghøgda Fm. (Mørk *et al.* 1999b). The Sørkapp-Hornsund High and other positive structures are onlapped later during the Dienerian or the Olenekian (Worsley & Mørk 1978, Nakrem & Mørk 1991, Worsley 2008, Hellem & Worsley unpublished). Yet, the accurate stratigraphic evolution of the Sørkapp-Hornsund High remains obscure. This is especially true regarding the presence of the Birkenmajer's (1977)

“Brevassfjellet *Myalina* Beds”, redefined as the basal Triassic polymictic conglomerate bed(s) of the Kistefjellet Mb. In the studied area, the underlying units are fluvial influenced deposits of the Hornsundneset and Sergeevfjellet fms. of Visean age, Carboniferous (Lipiarski & Čmiel 1984, Wendorff 1985, Birkenmajer 1990, Dallmann *et al.* 1999). It is overlain by shales and siltstones (Worsley & Mørk 1978, Mørk *et al.* 1982, Mørk *et al.* 1999b). This is regarded as the lateral equivalent of the Vardebukta Fm.

During the Lower Triassic, these siltstone/sandstone and changeably organic-rich dark shales are deposited in alternation under coastal fluvio-deltaic to shallow marine environment, influenced by a westwards-eastwards coastline progradation (Mørk *et al*. 1982, Mørk *et al.* 1999b). In the Late Lower Triassic and the early Middle Triassic (Anisian, Ladinian), sediments deriving from the Ural Mountains are deposited in the now Russian part of the Barents Sea. Albeit the western delta system lingers reasonably stable throughout time, the great Uralian deltaic system progrades north-westwards (Riis *et al.* 2008, Golonka 2011) and, by the end Carnian, leads to a delta-plain environment over much of the northern Barents Shelf (Lord *et al.* in prep.). On Edgeøya, the lower part of the Vikinghøgda Fm. is absent (Mørk *et al.* 1999b). Even though clasts of Permian age have been reported at the base of the Triassic shales, it is not clear whether sediments were deposited and eroded or simply not deposited until the Olenekian, (Mørk *et al.* 1982). On Hopen, the uppermost De

Geerdalen Fm. is the first exposed unit (Kapp Toscana Gp. Late Carnian age). Thick fluvial sandstones with interbedded continental deposits characterize this formation (Riis *et al.* 2008). However, laying 965 m below sea level, one has reported Triassic marine shales of unknown stratigraphic affiliation, underlain by hard siliceous shales of Permian age (Dallmann *et al.* in prep.).

The base of the Vardebukta and Vikinghøgda Fms. become younger towards the South and the East. It is therefore diachronous. Although the contact between the Kapp Starostin Fm. and the Vardebukta Fm. is obvious and clearly recognizable in the field, it is more problematic to identify the boundary suggested by Mørk *et al.* (1999a) at the base of the Vikinghøgda Fm. Especially since no proofs of erosional surface have been documented throughout Spitsbergen so far (Buchan *et al.* 1965, Mørk *et al.* 1982, Nabbefeld *et al.* 2010, Vigran *et al.* 2014). Nevertheless, the postulate of a submarine non-depositional hiatus close to the boundary is not undeniably demonstrated nor excluded yet. However, only the second negative $\delta^{13}C$ peaks is measured at Tschermakfjellet in comparison of the two negative peaks at Festningen (Wignall *et al.* 1998, Dustira *et al.* 2013). This possible sedimentary gap in central and eastern Spitsbergen is a matter of interest, as a hiatus usually is more likely to exist at the proximal margins of the basin (Vardebukta) and not in the more distal, intra-basinal part of the system (Vikinghøgda) (Grasby & Beauchamp 2008, Beauchamp *et al.* 2009), unless topography is involved. Notwithstanding, the Buchanan Lake section in the

Sverdrup Basin shows a gradual diminution of $\delta^{13}C$, synonym of incessant sedimentation (Grasby & Beauchamp 2008). An abrupt change in the isotopic curves (a rapid and unforeseen negative migration of the isotopic values) indicates erosion instead.

3. The Permian-Triassic Boundary

3.1. Definition

The Permian-Triassic boundary corresponds to one of the *Big Five* Mass Extinctions (ME) that the Earth has experienced. 95% of all marine and terrestrial living species are taken away (Raup 1979, Erwin 1989, Sepkoski 1989)! However, Foster and Twitchett (2014) have just shown that a relatively high functional diversity has persisted at the global scale. Several radiochronological methods have been used to date it. The approximated age of the PTB is 252.3 Mya using U-Pb (Mundil *et al.* 2010) and 249.25±0.14 Mya using $^{40}Ar/^{39}Ar$ (Reichow *et al.* 2009). Yin *et al.* (2001) formally define the PTB by the appearance of the conodont *Hindeodus parvus* (Fig. 12). Its GSSP is located at the base of "Bed 27c of Meishan section D, Changxing County, Zhejiang Province, South China". This condensed limestone section was deposited under very slow sedimentation rate conditions, contrasting with the high sedimentation rate, siliciclastic sequences observed in the Arctic. Located just above the base of the LT1n normal polarity interval (Szurlies 2007, Hounslow *et al.* 2008a, Hounslow & Muttoni 2010), it postdates the actual mass extinction event, the $\delta^{13}C$ minimum and other momentous events, such as the $\delta^{18}O$ and $\delta^{34}S$ migrations. The respective negative

shift of these climatic proxies ranges between 4-7‰, 2-6‰ and 15‰, while the $^{87}Sr/^{86}Sr$ ratio increases as a result of a major and dramatic climatic change (Baud *et al.* 1989, Martin & MacDougall 1995, Hallam & Wignall 1997, Wignall *et al.* 1998, Veizer *et al.* 1999, Korte *et al.* 2004a, 2004b, Newton *et al.* 2004, Bjerager *et al.* 2006, Grasby & Beauchamp 2008, Korte & Kozur 2010, Joachimsk *et al.* 2012, Sun *et al.* 2012, Kaiho *et al.* 2012, Clarkson *et al.* 2013, Dustira *et al.* 2013, Schneebeli-Hermann *et al.* 2013, Shen *et al.* 2013, Takahashi *et al.* 2013).

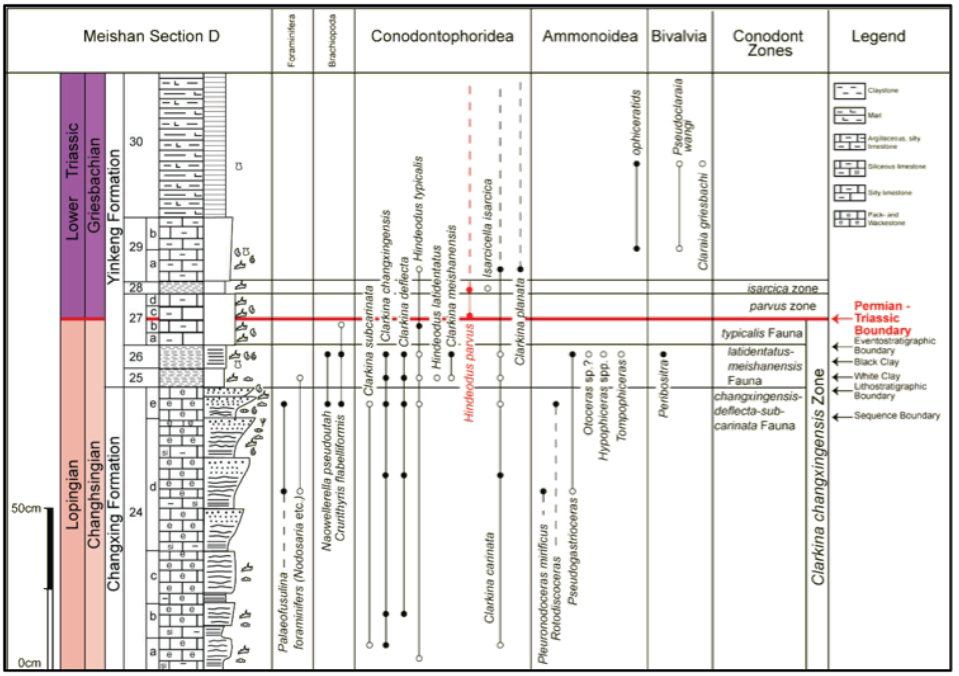

Fig. 13 – Permian-Triassic Boundary GSSP, Meishan section, South China (from Ogg 2012).

The eruption of the Siberian Traps and the Araguainha impact may directly or indirectly be responsible for the CO_2, CH_4, H_2S greenhouse gases outbursts and other halocarbon releases in the atmosphere as they hit evaporitic rocks and coal beds, increasing

the global temperature and disturbing both air and water global circulations (Renne *et al.* 1995, Kamo *et al.* 2003, Kidder & Worsley 2004, Reichow *et al.* 2009). A controversial (but somehow sexy) hypothesis suggest that the Siberian traps might have been triggered by a "gargantuan" cosmic impact at their antipodes, whose crater has been located under the Antarctic Ice sheets, know under the Wilkes Land Crater (von Frese *et al*. 2009). Rothman *et al.* (2014) have just proposed the main responsible for the End-Permian extermination to be *Methanosarcina*. This tiny bacterium feeds on the carbon and the nickel supplied by the Siberian volcanism and present in the marine water, releasing a tremendous amount of methane in the atmosphere, far more than the Siberian traps could do in the same period of time. Additional feedback effects accentuate the complexity and the regionality of these changes, fatally leading to a relatively global and shallow oceanic anoxia (Wignall & Twitchett 1996, Isozaki 1997, Gorjan & Kaiho 2007, Shen *et al.* 2007, Cao *et al.* 2009, Bond & Wignall 2010, Cao *et al.* 2010, Algeo *et al.* 2011, Kaiho *et al.* 2012, Schneebeli-Hermann *et al.* 2012, Knies *et al.* 2013, Proemse *et al.* 2013).

3.2. The Permian Triassic Boundary on Svalbard

Traditionally based on Tozer's *Otoceras* ammonoid biostratigraphic zonation (1967, 1988, 1994), the PTB on Svalbard was located at the conformable contact between the Upper Permian siliceous shales of the Kapp Starostin Fm. and the Lower Triassic Griesbachian, asiliceous shales of the

Vardebukta/Vikinghøgda fms. (Fig. 14). This lithological boundary corresponds to a major transgressive event. The ensuing Triassic sedimentary succession has been correlated with deposits from northern Alaska, the Canadian Sverdrup Basin, North and East Greenland, Bjørnøya, the Barents Shelf and the eastern Russian arctic (Embry 1989, Mørk *et al.* 1989, Weitschat & Dagys 1989, Mørk *et al.* 1993, Dagys & Weitschat 1993, Bjerager *et al*. 2006). This transgressive lithological boundary between the Kapp Starostin Fm. and the Vardebukta Fm. is notably akin to the contact between the Upper Permian Black Stripe Fm. and the Lower Triassic Blind Fjord Fm. in the Sverdrup Basin, Arctic Canada. The "black to dark grey spiculitic chert associated with siliceous shale and siltstone" (Beauchamp *et al.* 2009) are overlain by the "deep-water non-siliceous greenish-grey weathering shale" (Grasby & Beauchamp 2008).

Fig. 14 – L.B.: Lithological boundary between the Kapp Starostin Fm. on the right and the Vardebukta Fm. on the left at Festningen. Person for scale.

On Svalbard, the lowermost reported *Otoceras* ammonoid is *Otoceras boreale*. No *Otoceras concavum* has been discovered on Svalbard, but they have been found in the Sverdrup Basin and in Siberia. The first *Otoceras boreale* has been reported by Petrenko (1963) in Lusitaniadalen, even though it is not *in situ*. Buchan *et al.* (1965) in Sassendalen and Mørk *et al.* (1999a) in

Lusitaniadalen document other well-preserved *Otoceras boreale* and Nakrem *et al.* (2008) report the presence of *Neogondolella* conodonts co-occurring with *Otoceras boreale* in the lower part of the Vikinghøgda Fm.

Within the lower part of the Vardebukta/Vikinghøgda fms., ammonoids remain however fitful. Due to the restricted amount of index fossils, the accurate biochronological determination of the uppermost beds of the Kapp Starostin Fm. and the lowermost strata of the Vardebukta Fm. is still challenging.

Hindeodus parvus hasn't been documented by anyone on Svalbard so far (Nabbefeld *et al* 2010, Mørk, personal communications). However, in the correlated sedimentary succession of the Blind Fjord Fm., arctic Canada, this conodont appears a few tens of meters above the transgressive lithological boundary (Beauchamp *et al.* 2009), therefore and according to the GSSP definition of the PTB, the base of the Vardebukta/Vikinghøgda fms. is of Changhsingian age. Bjerager *et al.* (2006) suggests that the appearance of –the relatively few– *H. parvus* could be delayed in the Arctic Realm and the boreal areas. Besides, *Otoceras* has been considered as a typical Upper Permian fossil until recently, but Balini *et al.* (2010) account for the occurrence of *Otoceras boreale* below and also above *H. parvus* in the Himalayas. Consequently, one can regard *Otoceras boreale* as being of both Permian and Triassic age. Since the correlation with Tethyan conodonts is fragmentary and because the fossil

record is relatively poor nearby the contact of the Kapp Starostin Fm. and the Vardebukta/Vikinghøgda fms., one need to focuses on other methods such as sequence and magnetostratigraphy stratigraphy, isotopic analysis and palynological studies of the arctic areas.

As *Uvaesporites imperialis* palynological assemblage is defined as Changhsingian, Vigran *et al.* (2014) recommend delimiting the base of the Griesbachian within the *Reduviasporonites chalastus* palynological assemblage Zone, Tozer's (1994) *Otoceras concavum* Zone and the LT1 Magnetozone (Hounslow & Muttoni 2010) (Fig. 15). This new boundary coincides with the base of the Greenlandic *Hypophiceras martini* ammonoid Zone (Bjerager's *et al.* 2006), which corresponds to the first appearance of *H. parvus* in Greenland. It is now located in the ten first meters of both Vardebukta and Vikinghøgda fms. (see Fig. 12). It can match Wignall *et al.* (1998) $\delta^{13}C$ negative peak. Yet, the PTB issue on Svalbard is not resolved with this new Griesbachian proposition. The only undisputed conclusion is that the PTB on Svalbard is situated someplace within the *R. chalastus* assemblage Zone since the *Proprisporites pococki* palynological assemblage Zone is defined as Induan. This last Griesbachian suggestion requires to be linked to isotopes curves and to complementary stratigraphic signals in order to improve the correlation on a global level. However, palynology, micro-biostratigraphy and isotope-stratigraphy, despite their acknowledged potential for accurate stratigraphic purposes, don't help geologists in the field.

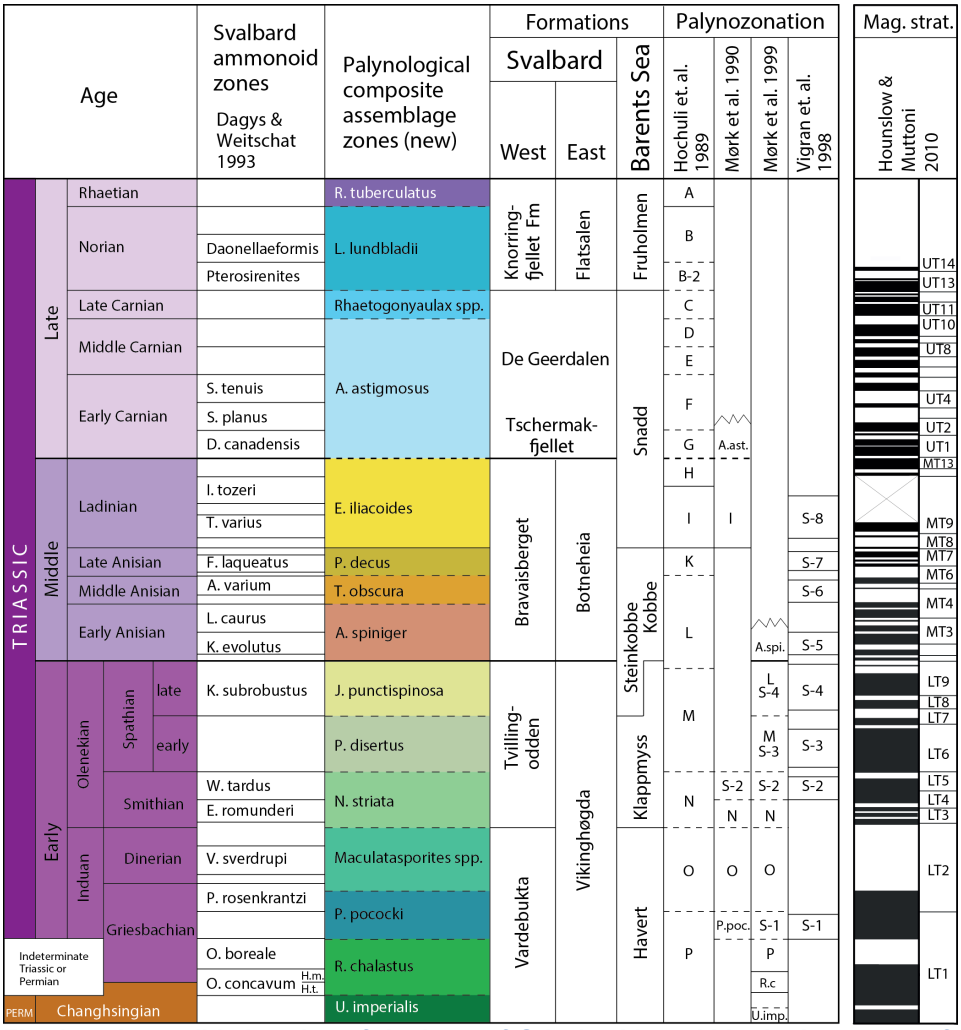

Fig. 15 – A possible location of the base of Griesbachian within the lower part of the *R. chalastus* palynological assemblage Zone, at the boundary of Bjerager *et al.*'s (2006) Greenlandic ammonoid zones *Hypophiceras triviale* (H.t.) and *Hypophiceras martini* (H.m.). This suggestion is also based on the correlation of palynological, lithological and magnetostratigraphic data (black = normal polarity, white = reverse polarity). Note that the PTB remains indeterminate (from Vigran *et al.* 2014, with the addition of Bjerager's (2006) H.t. and H.m. ammonoid zones).

Indeed, the precise correspondence of the boreal Panthalassic PTB with the Tethyan areas is relatively hard to establish with precision and remains ambiguous, even though the regional

correlation between the different arctic regions of the is commonly acknowledged (Hounslow *et al.* 2008b, Hounslow & Muttoni 2010).

The complexity of this correlation is emphasised by the dissimilar lithologies and lithological contexts that characterise these two separated provinces at that time. The Arctic Realm is typified by siliciclastic units deposited under a high sedimentation rate, while the Chinese section is a condensed carbonate succession (Grasby & Beauchamp 2008). Note that a sequence undergoing a rapid subsidence combined with a high sediment influx has a great chance to record a "continuous and gradational" $\delta^{13}C$ migration (Grasby & Beauchamp 2008).

However, the definition of the GSSP as it is now is on the edge, since Zhang *et al.* (2014) prove that first occurrence of *H. parvus* is heterochronous, as foreseen by Lucas (2010). Zhang's team point out that *H. parvus* appears in the Bed 28a of the Zhongzhai section, 18 cm below the GSSP. In other word, *H. parvus* has been found in the late Permian. Bjerager *et al.* (2006) solicit a GSSP "defined in a protracted section at a point of major environmental perturbations, marked by isotope excursions, chemical anomalies and mass extinction", rather than being centred around the heterochronous first appearance date of a single species. The use of a single and exclusive stratigraphic signal to define any GSSP can only lead to its disapprobation (Finney 2013). Lucas (2010) mentions, with reason, several additional problems associated with a dictatorial conodont-based

biostratigraphy. (i) It is impossible to identify conodonts in the field, (ii) their reworking is difficultly recognisable, (iii) like ammonoids, they suffer from provinciality, heterochroneity and facies restriction, (iv) their taxonomy is immature, hence unstable. The integration and the correlation of additional isotopes studies (Wignall *et al.* 1998, Dustira *et al.* 2013), of extra palynological, biostratigraphical and magnetostratigraphical data are essential to attain a broad and exhaustive awareness of the PTB in Svalbard and its neighbourhood.

4. Methodology

In order to complete the objectives of this thesis, data have been collected during the field campaign of July and August 2013. Two days have been spent at Marmierfjellet, three at Høgskulefjellet, one at Kongressfjellet, four at Festningen and nine in Hornsund in cooperation with SINTEF and the Norwegian Oil Directorate (NPD) (Fig. 3). Note that a preliminarily scheduled trip to Treskelen has been cancelled. This field season has been particularly rainy, with about 145% and 157% more precipitation, respectively in July and in August (weather statistic from yr.no, delivered by the Norwegian Meteorological Institute and the NRK).

Nine detailed sedimentary sections have been measured and logged. Their name refers to the location where they outcrop, accompanied by a one digit number if more than one section have been measured at the same place. They are enclosed to this thesis. Regarding the section on Lidfjellet, Hornsund, an extra two

digits number has been added to its name, which indicates the measurement year. The thickness of the different units has been measured with a standard meter stick. Logs and samples GPS coordinates have been recorded using the UTM 33x grid zone, while the height control has been piloted with a Thommen Classic TX-12 altimeters.

Systematic and intensive sampling has been conducted on each section for palynological and isotopic analysis purposes. Note that these analyses are processed at the University of Bergen[2] by Prof. Gunn Mangerud's research group. However, out of all these samples, nineteen targeted thin sections have been produced and impregnated with blue-dyed epoxy, helping quantifying the porosity of the rocks. Optical microscopes (Leica DM2500 P) have been used for the detailed study of these thin sections. Fossils and trace fossils have been determined with the assistance of Prof. Hans Arne Nakrem (University of Oslo) and Nils-Martin Hanken (University of Tromsø). Based on the field data and the thin sections analyses, sedimentary facies are identified after their sedimentary textures, structures and composition. They have been grouped into facies associations (Walker 1992), based on the vertical and lateral genetic relations of sedimentary facies, in order to determine and interpret their respective depositional environments.

[2] Note that these palynological data will not be integrated into the thesis, but will be used in further projects

5. Results and interpretation

This part of the thesis will describe (i) the different facies and facies associations identified within the different sedimentary sequences, (ii) the sedimentary logs themselves and (iii) thin sections collected in central Spitsbergen, in western Spitsbergen and on the Sørkapp-Hornsund High.

5.1. Facies description and facies association

A rock facies is defined by Reading & Levell (1996) as a “body of rock with specified characteristics […] reflecting a particular process, set of conditions, or environment”. Table 1 summarises the 17 different facies documented in this study. The observation of the rock fabric, composition, structure(s) and fossil content has been the key to interpret the processes and each of the depositional environments. However, as the interpretative value of individual facies strongly varies, facies need to be grouped in facies association based on their mutual relation in order to suggest a large-scale environmental interpretation. These facies have been organised in four main facies associations.

Table 1 – Facies description and depositional environment interpretation

Facies	Microstructures, textural characteristics and components	depositional processes	Depositional sedimentary context	Note
Cgl	Clast-supported to matrix-supported, hard, polymictic conglomerate. Matrix is orange, clasts are sub-angular to sub-rounded, up to 2 cm. Chaotic fabric, may contain some bryozoan fossil fragments	Reworking of predeposited Triassic sediments,	Shallow marine environments, trangressive cgl	Brevassfjellet Beds
Coal	Coal, with plant fragments	Rapid burrow under low-oxygen conditions, avoiding the destruction of organic matter	Flood plain *	Sergeevfjellet Fm.
F-Sand-DGy	Massive, hard cemented, dark grey fine sand bed. 50cm thick	? Rapid deposition?	?	Observed only at Kovalevskajafjellet
F-Sand-O	Massive, hardly cemented, orange fine to very fine sand bed. Scattered clast possible. 50 cm to 4 m thick	? Rapid deposition? with slight flow velocity increase to transport the bigger clasts	Shallow marine environments	Observed only at Sergeevfjellet, Brevassfjellet Beds
F-Sand-Si-DGy	Plane parallel (PPL) to wavy laminations, dark grey, inverse graded, silty fine sand beds. As hard as Sh-DGy, 4m thick	Lower part of the lower flow regime, weak oscilliary current	Transition lower-upper shoreface	Just below the dolerite, log KappStar1
F-Sand-W	Massive, hard cemented, white, fine to massive sandstone beds, up to 1 m thick	? Upper part of the lower flow regime, unidirectional current leading to subaqueous dune/transversal bar migration? Bed load (?and suspension load?)	? Proximal-distal to distal braided-stream rivers, possibly related to flash-floods *	Sergeevfjellet Fm.
Med-C-Sand-O	Massive, hard cemented, medium to coarsegrained, orange sandstone beds. Scattered calcareous nodules, sub-rounded to sub-angular clasts, ripple marks and bioturbation possible	? Hjulström diagram: current velocity of at least 30cm/s. Velocity can increase sporadically to transport the bigger clasts	Shallow marine environments	Brevassfjellet Beds
Med-Sand-LGy	Planar cross-bedding, hard cemented, light grey, medium sand beds, up to 1 m thick.	Upper part of the lower flow regime, unidirectional current leading to submarine dune/transversal bar migration, Bed load (?and suspension load?)	Proximal-distal to distal braided-stream rivers *	Hornsundneset Fm.
Mud-Blk	Thinly planar-laminated, black, sticky and cliff forming soft shale	Lowest part of the lower flow regime, settlement of suspended sediments	Moderately deep to deep shelf environments	Topmost of Marmierfjellet, Kongressfjellet, ? Lusitaniadalen Mb.
Mud-Grn	Unconsolidated green mud, up to 10 cm thick	? Lowest part of the lower flow regime, settlement of suspended sediments? Diagenesis related?	? Lower shoreface	
Nod-Bed	Calcareous nodules bed	Diagenesis		
Sh-DGy	Thinly planar/wavy laminations, dark grey, soft shale/silty shale (up to 10 % silt). Scattered calcareous nodules present, sometimes fossiliferous	Lowest part of the lower flow regime, settlement of suspended sediments	Upper offshore (ichnofacies) to lower shoreface, above Storm Base Level (SBL)	Vardebukta Fm., Selmaneset Mb.
Sh-O	Thinly planar/wavy laminated, orange, soft shale/silty shale (up to 20% silt)	Lowest part of the lower flow regime, settlement of suspended sediments	Lower shoreface, above SBL	Brevassfjellet Beds
Sh-Si-Vf-Sand-LGy	Light grey shally siltstone beds, up to 30 cm thick. Silt proportion: between 20 % and 100 %. Most of the time cross-laminated, but display PPL at the base of certain beds. A few number of beds shows clear hummocky cross-stratification (HCS). One loading structure observed in Marmierfjellet. Shell fragments observed in Kongressfjellet (52 m)	Oscilliary (storm?) current	Lower shoreface, above SBL	Slit beds in Vardebukta Fm., Vikinghøda Fm., Kapp Starostin Fm. In central Spitsbergen
Si-Sh-DGy	Hard cemented, dark grey silty shales. PPL or massive, some bioturbation observed, as well as bryozoan and brachiopods fossils	Lowest part of the lower flow regime, settlement of suspended sediments	Lower offshore (ichnofacies)	Kapp Starostin Fm., west Spisbergen
Si-Sh-Gy	Thinly planar/slightly wavy laminated, grey shally siltstone, harder than Sh-DGy but not as hard as Si-Sh-DGy Silt Proportion: up to 20 %. Scattered calcareous nodules present, sometimes fossiliferous	Lowest part of the lower flow regime, settlement of suspended sediments	? Lower offshore?	Kapp Starostin Fm., central Spitsbergen
Vf-Sand-Carb-Cem	Carbonate cemented, fossil rich (mostly bryozoans and bivalves), light grey, limestone beds. Sub-millimetric clasts may be present.	Condensed bed	shallow marine environments	*Myalina* beds

* Dallmann *et al.* 1999: Upper Paleozoic Lithostratigraphy, in: Lithostratigraphic lexicon of Svalbard, Norsk Polarinstitutt, Tromsø, 26-126

Lecture key: Cgl - conglomerate; C - Coarse; Med - Medium; F - Fine; Vf - Very fine; Si - Silt; Sh - Shales; Nod - Nodulous; Carb-cem - Carbonate cemented
DGy - Dark grey; LGy - Light grey; W - White; O - Orange; Blk - Black; Grn - Green

5.1.1. Cgl – Conglomerate

Description

This quartz-rich, poorly sorted epiclastic conglomerate has only been observed on Sergeevfjellet, Lidfjellet and Kovalevskajafjellet in Hornsund. They occur within the so-called Brevassfjellet Beds of the Kistefjellet Mb., Vardebukta Fm. (Birkenmajer 1977, Mørk *et al*. 1999b). The thickness of the conglomerate bed fluctuates between 10 cm to a metre scale. Its polymictic rock fabric varies from matrix-supported to clast-supported. These gradual variations of the matrix versus clast ratio might be seen as faint planar bedding. The sample TSK3 on Kovalevskajafjellet (Fig. 16), located at the topmost part of the conglomeratic unit (see enclosed log Kov-1,), shows a thin layer of clast-supported conglomerate to very coarse sand that distinctively carves into the sub-laying matrix-supported conglomerate. The clast-supported parts tend to be composed of grains smaller than 5 mm, while centimetre-scale grains are found in the matrix-supported horizons. Though, no sedimentary structures have been documented in this conglomeratic facies. The matrix is orange. This colour implies the presence of iron (III) (of continental origin?) in the system. Clasts are rounded to sub-angular, and their size ranges from less than 0.1 mm to 2 cm.

Fig. 16 – Cut section through TSK3 conglomeratic sample, Kovalevskajafjellet. Note the thin clast-supported layer at the top of the sample, carving through the underlying matrix-supported rock. For information, the faint curved marks crossing the sample from the lower left to the upper right are saw scars.

Thin sections TSK3, Lid-13-1-1, TSS2-3 (Appendix 2: Plates 7, 10, 15) have shown the presence of mono-crystalline and poly-crystalline quartz grains of metamorphic origin. Micas have been

reported as single crystal within the matrix, and as a preferred-oriented crystals system within poly-crystalline quartz grains, remains of the schistosity of the metamorphosed rock they are derived from. Zircons and pyrite crystals have also been documented from the thin sections. Both mono-crystalline quartz grain and micas show undulose extinction. In Lid-13-1-1, sparse calcitic cement has been spotted. The porosity is low (less than 5%, point counting measurement).

Interpretation

The roundness of the clasts indicates a substantial pre-depositional transport of the detrital material, while the heterogeneity of the variations of the matrix versus clasts ratio show changes in the flow regime. The wash out of the fines by a steady flow can explain the occurrence of these more clast concentrated horizons (Fig. 16), while the matrix-rich sections can be due to a higher sediment load in the water (Dashtgard *et al.* 2006). The presence of sub-angular grain could be explained by (i) a more proximal source or (ii) a break of the clasts during the transport. As the orange colour is due the presence of iron (III) in the system, which entails the proximity of some continental source. The oxygen level within the sediments has to be high enough to in order to oxide the iron.

It is difficult to determine the precise origin of this undulose extinction for the quartz, but it is possible to suggest that it is due to a pre-depositional deformation. On the other hand, the bent micas observed within the matrix of the conglomerate are resulting of post-depositional deformation processes.

5.1.2. Coal

Description

This coal facies has only been observed on the log Serg-2 on Sergeevfjellet in Hornsund, below the first aforementioned conglomeratic unit, as part of the Carboniferous Sergeevfjellet Fm. (Fig. 17) (Lipiarski & Čmiel 1984, Wendorff 1985, Dallmann *et al.* 1999). It consists of two dry coal seams that are about 50 cm thick each and that contain plants remains. It breaks in really small pieces, parallel to the bedding. A siltier unit overlies the second one. However, as the organic content remains high, it is therefore also assigned to the same facies. Lipiarski & Čmiel (1984) reports 18 others coal seams at lower altitude on Sergeevfjellet.

Interpretation

A rapid burrow of the plant remains leading to oxygen depletion is required to preserve the organic matter. This process is notably possible within a floodplain depositional environment.

Fig. 17 – Coal seam, Sergeevfjellet, 6 m above the start of the Serg-2 sedimentary log.

5.1.3. F-Sand-DGy – Fine sand dark grey

Description

These massive dark grey, quartz-rich, fine sand beds have only been observed on Kovalevskajafjellet in Hornsund below the first conglomeratic unit and above a white cross-bedded medium sandstone layer. According to Lipiarski & Čmiel (1984) and Birkenmajer (1990), are suggested to belong to the Carboniferous Hornsundneset Fm. However, the thin section TSK4 shares some sedimentological similarities with the facies 5.1.6. F-Sand-W – Fine sand white. The only difference between these two facies is the colour of the rock. The thickness of these hardly cemented sand beds varies between 50 cm and 75 cm. Thin section TSK4 (Appendix 2: Plate 8) has shown some faint undulose structures filled up with calcite cement and dolomite crystals probably related to post-deposition diagenetic processes.

Thin section TSK4 shows a high proportion of sub-angular mono-crystalline quartz grain of 0.1 mm and an elevated proportion of opaque minerals (pyrite?). Calcite cement is concentrated in a wavy structure, accompanied with euhedral dolomite crystal. Accessorised bended micas is also present in the rock, but is accumulated towards the top of the rock. Porosity is close to 0%.

Interpretation

It is hard to interpret this unit with certainty due to the lack of correspondence with the neighbouring areas. However, a rapid deposition could be the cause of the massiveness of these sand beds.

5.1.4. F-Sand-O – Fine sand orange

Description

This massive fine (to very fine) orange sand facies has only been observed at Sergeevfjellet. The stratigraphic position of these sands within the section suggests that they are part of the Brevassfjellet Beds. Some scattered centimetric pebbles have been reported in this sand matrix. The thickness of each beds ranges from 40 cm to approximately 2 m. Sporadic bioturbations, post-depositional calcareous nodules, and ripple cross-laminations are occasionally displayed within this sandy facies. The orange colour indicates that iron (III) is present within the rock.

TSS2-2 (Appendix 2: Plate 16) shows a moderately well sorted, grain-supported quartz-rich fine sandstone, whose pores are filled up with matrix-sized crystals of calcitic cement (Plate 16: c, c'). 80% of the quartz grains are sub-angular, while the remaining 20% tend to be more sub-rounded. Undulose extinction is common in quartz grains. Accessory minerals are zircons, micas, and opaque minerals in a lesser extent.

Interpretation

The massiveness of these sand beds could be due to, in order of probability, (i) a rapid deposition, or (ii) extensive bioturbations, as such structures have been observed at certain heights of these sand beds. The fact that some pockets of “matrix-like” calcite cement remain present in the rock suggests a rapid pore-filling of this clean sand by this matrix-like cement not too long after the deposition. However this kinematic is not an absolute truth, as the 3D arrangement of the grains is hard to visualise in thin sections. It is therefore not possible to exclude the hypothesis of a late porosity infill. The angularity of the grains suggests a proximal source of the detrital material.

5.1.5. F-Sand-Si-DGy – Fine sand silt dark grey

Description

This dark grey silty fine sand facies has only been reported from the Kapp Starostin section along the beach, just below the Cretaceous dolerite intrusion within the Triassic Vardebukta Fm. Its thickness reaches approximately 4 m. It also occurs on the Kongressfjellet section. It is characterised by plane parallel lamination (PPL) to weakly undulated laminae and a reverse grading. The transition from the underlying unit is smooth.

Interpretation

These features could have formed with the lower part of the lower flow regime, as sediments fallout, with the additional effect of a weak oscilliary current.

5.1.6. F-Sand-W – Fine sand white

Description

This massive white to grey, quartz-rich, fine to medium sand facies has been reported from Sergeevfjellet in Hornsund (?and maybe from Kovalevskajafjellet? also). These sand beds belong to the Sergeevfjellet Fm. (Lipiarski & Čmiel 1984, Wendorff 1985, Krajewski & Stempień-Salek 2003). It hasn't been observed else on Svalbard. Each bed is approximately 50cm to 1m thick.

Mono-crystalline and poly-crystalline sub-angular to sub-rounded, (moderately well to) well sorted quartz grains of metamorphic origin have been observed in thin section TSS2-0 (Appendix 2: Plate 18). Mono-crystalline quartz grains outnumber poly-crystalline quartz. Both mono-crystalline quartz grains and micas show undulose extinction. Note that contacts between grains are long, and sometimes interpenetrative when micas are involved in the system. The deformation is post depositional and related to mechanical compaction. Zircons and pyrite crystals have also been documented from the three thin sections, but are more important in TSS2-0.

Interpretation

The presence of faint planar cross-bedding suggests depositional conditions close the upper part of the lower flow regime leading to the migration of a sub-aqueous dune or a transversal bar. The massiveness of the beds can be linked to a rapid deposition process or to a high sediment concentration within the fluid in

motion. The affiliation of these beds to a precise depositional process and environment remains however uncertain.

5.1.7. Med-C-Sand-O – Medium to coarse sand orange

Description

These massive orange medium to coarse hard sand beds have only been observed on Sergeevfjellet, and belongs to the Brevassfjellet Beds. Centimetric pebbles may be present but are not homogeneously dispersed throughout the entire layer but are rather concentrated at different height. The thickness of these sand beds ranges between 50 cm and 2 m.

Thin section TSS2-1 (Appendix 2: Plate 17) shows relatively well sorted, packed, sub-angular mono-crystalline quartz grains with undulose extinction. Scattered sub-rounded, sub-centimetric lithoclasts or poly-crystalline quartz grain may be present. Several “pockets” of fine dark brown to opaque matrix material, heterogeneously distributed, have also been reported within the thin section. Post-depositional calcite cement also occurs either as sparitic crystals within one of these “pockets”, or as a 0.2 to 0.25 mm thick layer partially and irregularly encrusting the thin section.

Interpretation

The occurrence of inter-crystalline fine matrix material and the absence of sedimentary structure could be explained by the rapid deposition of the clastic material within a quiet sub-aqueous environment. The sub-angularity of the quartz grain contrasts with

the sub-roundness of the larger pebbles. However, Twenhofel (1945) reports that, for a given transport distance and energy level, clasts become more rounded than which would explain the co-occurrence of sub-angular sand-sized and sub-rounded gravel-sized clasts. The presence of scattered pebbles within this medium to coarse sandstone suggests a sporadic (but regular?) flow velocity increase within the system.

5.1.8. M-Sand-LGy – Medium sand light grey

Description

This hard, planar cross-bedded light grey, quartz-rich, medium (to coarse) sand facies has been logged on Kovalevskajafjellet and Lidfjellet in Hornsund. It hasn't been observed else on Svalbard. Each bed is approximately 50 cm thick and is thought to be affiliated to the Hornsundneset Fm. (Lipiarski & Čmiel 1984, and Birkenmajer 1990). Faint planar cross beddings been reported 2m above the base of the log in Lidfjellet.

Thin sections TSK0 at Kovalevskajafjellet (Appendix 2: Plate 9) and TSL0, TSL1, TSL min 30 and TSL min 35 at Lidfjellet (Appendix 2: Plates 12,11, 13, 14) present a grain supported, poorly sorted, medium to coarse mono- and poly-crystalline quartz-rich sandstone, whose porosity is close to nothing. Contacts between sub-rounded to sub-angular grains are long and sometimes interpenetrating, especially when (heavily bended) micas are involved in the system. Note that 15 zircon crystals have

been observed in a 2x1.25 mm area of TSL0 (Appendix 2: Plate 12)!

Interpretation

The presence of the planar cross-bedding indicates that the unidirectional current under which these sediments have been deposited belongs to the upper part of the lower flow regime, engendering the migration of a sub-aqueous dune or a transversal bar. The occurrence of amorphous silica pocket implies the establishment of pressure-dissolution processes affecting the detrital quartz grains.

5.1.9. Mud-Blk – Mud black

Description

These finely laminated, black, cliff-forming shales have been observed at the topmost part of the sections on Marmierfjellet and 8 m above the top of the Kongressfjellet sedimentary log. Yellowish scattered calcareous nodules locally occur within the shales.

Interpretation

These shales were deposited under the lowest part of the lower flow regime, from suspended sediments present within the water column. The black colour reflects the relatively high organic content compared with the other shales listed in Table 1, as a consequence of low-oxic conditions in the water- and/or sedimentary column.

5.1.10. Mud-Grn – Mud green

Description

Several layers of this green unconsolidated mud have been documented within the Triassic deposits on Kongressfjellet, at Kapp Starostin, on Sergeevfjellet and on Kovalevskajafjellet (Fig. 18). The thickness of these layers ranges from 1 cm to 10 to 12 cm. Note that on Kovalevskajafjellet, this unconsolidated green mud overlies a dark grey unconsolidated mud layer of about 20 cm.

Fig. 18 – Unconsolidated green mud horizon, Kovalevskajafjellet.

Interpretation

The non-consolidation of these fine sediments is probably a direct impact of unspecified diagenetic processes. The green colour of the mud could due to the present of Iron (II) oxide within the deposits, testifying to possible (periodic?) reductive conditions within the sediments.

5.1.11. Nod-Bed – Nodular bed

Description

Disc-shaped calcareous nodules of various diameters (5 to 30 cm) have been observed within (i) the Permian sediments in central Spitsbergen and within the (ii) Triassic mudstones of the Vardebukta and Vikinghøgda fms. in central, western and southern Spitsbergen. These concretions usually grow around some kind of a nucleus, which might be a fossil (Fig. 19a). Note that on Kongressfjellet and on Marmierfjellet sections, a higher nodule concentration is reported from particular heights of the sections interpreted as Permian age, to a point where they form almost continuous beds. *A contrario*, in the Kapp Starostin area and on Sergeevfjellet in Hornsund, their density increases drastically in certain specific horizons in the lower part of the Vardebukta Fm., before becoming more and more infrequent towards younger deposits. None of these nodules have been observed in the hard shales of the Kapp Starostin Fm. or other older formations.

Fig. 19 – a. Fragment of a calcareous nodule, which had been growing around an unidentified ammonoid remain, Marmierfjellet. The black contour outlines the outer rim of the fossil. b. Deformed sediments due to the growth of the nodule, Marmierfjellet.

Interpretation

These calcareous nodules beds are interpreted as a consequence of post-depositional diagenetic processes, as they deformed the surrounding sediments (Fig. 19b). Köhler-Lopez & Lehmann

(1984) suggest that they start developing “close to the sediment surface of a nearly anaerobic putrid calcareous mud”, as their eventual fossil nucleus is relatively uncrushed. The reason for the concentration of these beds at specific heights of the different succession remains, however, poorly understood.

5.1.12. Sh-DGy – Shales dark grey

Description

These soft, non-siliceous dark grey shales have been observed at every studied section throughout central, western and southern Spitsbergen. This facies correspond to the shales of the Vardebukta and Vikinghøgda fms. These shales, often heavily altered at the surface, form gently dipping slopes in the Svalbardian landscape or embayments when beds are sub-vertical. Fresh sections are necessary to observe their laminated to undulated (to rippled?) structures. Good exposures are found in stream gullies or shovelled out using a potato-digger. Silt content is variable, but do not exceed 25% of the rock. Silt content tends to be higher in the shales of Hornsund than anywhere else on the archipelago, so the colour of these shales is a little bit lighter on the Sørkapp-Hornsund High than in western and central Spitsbergen.

Scattered fossiliferous nodules and nodular beds have been reported from several localities in Spitsbergen (see 5.1.10. Nod-bed – Nodular bed). Also, the higher the silt content, the more undulated the beds seem to become. Bioturbations are really

scarce within these shales. Extremely sparse fossils have been documented within these shales. In this study, two ammonoids have been found (within a calcareous nodule) at Marmierfjellet, but their degree of preservation couldn't allow any identification.

Interpretation

The planar laminations of these shales, as well as their (yet poor) fossil content suggest that they have been deposited from really fine suspended sediments present in the marine water column. The undulations of certain layers have been induced by a factor of weak oscilliary motion, which implies the depositional environment to be located above the Storm Weather Base Level (SWBL), but below the Fair Weather Base Level (FWBL). The extremely low number of fossils and bioturbations in these shales suggests a really limited amount of individual living at that time.

5.1.13. Sh-O – Shales orange

Description

Sergeevfjellet is the only locality where these orange, planar laminated soft shales have been observed. They are related to the other Brevassfjellet Beds deposits. The thickness of their sequences ranges from 10 cm to 2 m. They interlay massive, very fine to fine orange sand beds. Silt content varies between 0 and 25%. The orange colour is related to the presence of iron (III) in the system.

Interpretation

These shales have been deposited from suspended sediments within the water column in a low energetic environment. The orange colour of the shales (and each of the beds below and above them) comes from the oxidation of the iron present within the rocks. However, the origin of the iron, as well as the timing of its oxidation are difficult to assess with precision and are not treated within this work.

5.1.14. Sh-Si-Vf-Sand-LGy – Shally silt to very fine sand light grey

Description

These light grey, hardly cemented shally siltstone beds have been observed at every studied location within the shales of the Vardebukta Fm. and the Kapp Starostin Fm. in central Spitsbergen. Their thickness varies between 2 to 30 cm. The sand content is variable, but isn't lower than 20%. A few beds display unmistakable Hummocky Cross-Stratification (HCS). Most of these beds display smaller scale cross-lamination (Fig. 20a), with some possible plane parallel lamination at their base. However, most of these beds present a sharp erosion surface at their base. Note that some of these beds present a massive inner structure, and more occasionally some plane parallel laminations at their base. One loading structure has been observed at Marmierfjellet (Fig. 20b), while some fossils of shell fragments have been reported at Kongressfjellet, 52 m above the start of the section. In central

Spitsbergen, some of the beds adorn themselves with some light greenish reflects.

Fig. 20 – a. Small scale cross-stratification, Lidfjellet. b. Loading structure in a storm-influenced sand bed, Marmierfjellet.

Interpretation

The presence of HCS, as well as smaller scale cross-laminations suggest that these sediments have been deposited by periodic (weak) and chronic oscilliary storm currents. This implies the depositional environment to be located above the SWBL.

5.1.15. Si-Sh-DGy – Silty shales dark grey

Description

These dark grey, hard, cherty-silicified and/or spiculitic, finely laminated silty shales have been observed within the Kapp Starostin Fm. at the Kapp-Star-1 and Vard-1 sections. They are found all along western Spitsbergen. Several fossil-rich horizons have been reported, with the presence of bryozoans, brachiopods, and unidentified fossils or ichnofossils (?). The top of the strata, at the contact with the soft shales of the Vardebukta Fm., displays planar substrate-feeder *Zoophycos* bioturbations (Uchman *et al.* in prep., Mørk, personal information). Note that the fossil content drastically diminishes towards the contact with the Vardebukta shales. However, with the fossil-rich layers becoming sparser, a few yellowish to light brown lenses (Fig. 21) have been spotted, which may also contain fossil remains. Note that the sub-horizontal laminations disappear towards the top of the formation, while the spicule content increases (extensive bioturbations?).

Thin section TS0 (Appendix 2: Plate 1) shows a matrix-supported rock with sub-rounded microcrystals of quartz, micas, pyrite clusters, rare zircons and glauconite. The biggest crystals reach

0.05 mm. The thin section also displays boring marks (Hanken personal information) among other fossils remains of brachiopods, corals (?) and one specimen of gastropod. The matrix is composed of micro-granular quartz or chert. The brownish tone of the matrix could be due to some calcareous trace in it. TS3 (Appendix 2: Plate 2) shows sponges spicules “pockets” within a cherty matrix. Note that the spicules tend to orient sub-horizontally, and that (sub-horizontal) fractures are concentrated within these spiculitic “pockets”. Possible echinoderm remains might also be present. Glauconite, micas and rare zircons can also be observed in this thin section.

Fig. 21 – Example of one of these yellowish fossiliferous lenses, Kapp Starostin Fm., Festningen.

Interpretation

The presence of sponge spicules, brachiopods and bryozoans fossils suggests a cold-water, nutrient-rich and well oxygenated marine environment. The fine material has been deposited from

suspended detrital particles present within the water column. The fine planar laminations imply the energy level of the milieu to be low, being part of the lower part of the lower flow regime. The diminution of the fossil content towards the top of these shales suggests a degradation of the living conditions. The absence of any storm generated or rippled beds implies a depositional environment located below the SWBL. Also, the increase of the massiveness of the beds towards the topmost strata, if due to an increase in bioturbation activity, suggests better-oxygenated waters, as well as a shallowing-up trend (Blomeier *et al.* 2013).

5.1.16. Si-Sh-Gy – Silty shales grey

Description

These grey, finely planar laminated silty shales occur in central Spitsbergen and belong to the Kapp Starostin Fm. as well. They are the pendants of the facies 5.1.15. Si-Sh-DGy. They are a little bit softer than their correlated spiculitic deposits and a their silt content is a little lower as well. Ripple cross-laminated siltstone beds and nodular layers are interlaid within the silty shales. Scattered nodules (sometimes fossiliferous: one ammonoid remains found at Marmierfjellet) and ripple marks have been reported within the silty shales themselves. No bioturbations have been observed in the field, but Uchman *et al.* (in prep.) report *Zoophycos*, *Nereites* and *Phycosiphon* ichnofossils from the top of the Hovtinden Mb. in central Spitsbergen.

Interpretation

Suspended sediments settling down from the water column have been forming these laminated rocks in a low energy context. However, the energy of the system can increase periodically in order to undulate the silty shales laminations and to depose the storm siltstone beds.

5.1.17. Vf-Sand-Carb-Cem – Very fine sand carbonate cemented

Description

These condensed carbonate cemented, fossil-rich beds, have been observed from Kovalevskajafjellet and Sergeevfjellet in Hornsund (Fig. 22a, b). They haven't been spotted on Lidfjellet or anywhere else on Svalbard. They are capped by the soft, dark grey shales of Triassic age, and overlie the orange polymictic conglomerate. The literature refers to these beds as the *Myalina* Beds (Worsley & Mørk 1978, Mørk *et al.* 1999b). On Kovalevskajafjellet, three beds are superposed on top of each other, reaching a total thickness of approximately 1.20 m. On Sergeevfjellet tough, only the Serg-3 section displays these three condensed beds and their thickness extents only to roughly 50 cm.

Thin sections TSK2, TSK1, TSS3-0 and TSS3-2 (Appendix 2: Plates 3, 4, 5, 6, 21, 19) show the highest fossil content observed in this study. TSS3-1 (Appendix 2: Plate 20) shows a high calcitic cement content, but no fossil. Sparitic calcite cement fills up the inter- and intra-particle porosity. The twinning of the calcite is a

consequence of the stress induced during the formation of the WSFTB. Centimetric bivalves shells (*Myalina*) have been replaced by calcite cement during the diagenesis. Lower Triassic (Dienerian-Smithian) trepostome bryozoans of the *Arcticopora* genus are also present (Nakrem & Ernst 2008, Nakrem personal information), albeit most of them are fragmented. Echinoderm remains also occur within these beds, showing several degrees of alteration. Some polychaete-tubes of type microconchidae have also been reported from the thin sections TSK1 and TSK2 (Nakrem, personal information). In TSK2, an unidentified shell fragment of approximately 1cm has been observed (gastropod?).

Thin sections from Sergeevfjellet show a higher clastic content than the ones on Kovalevskajafjellet, with sub-rounded mono-crystalline and poly-crystalline quartz grain (up to 1cm) and sparse micas. However, TSS3-0 displays the biggest inter-particle sparitic cement crystals, compared to the cement occurring in TSS3-1. The uppermost thin section at Sergeevfjellet, TSS3-2, shows a high pyrite content filling up macro-pores, concentrated at the top of the thin section. It is also the only thin section that shows a clear sub-horizontal internal structure, although the inner architecture TSK1 from Kovalevskajafjellet leans towards sub-horizontality as well, while the other thin sections show no internal structures.

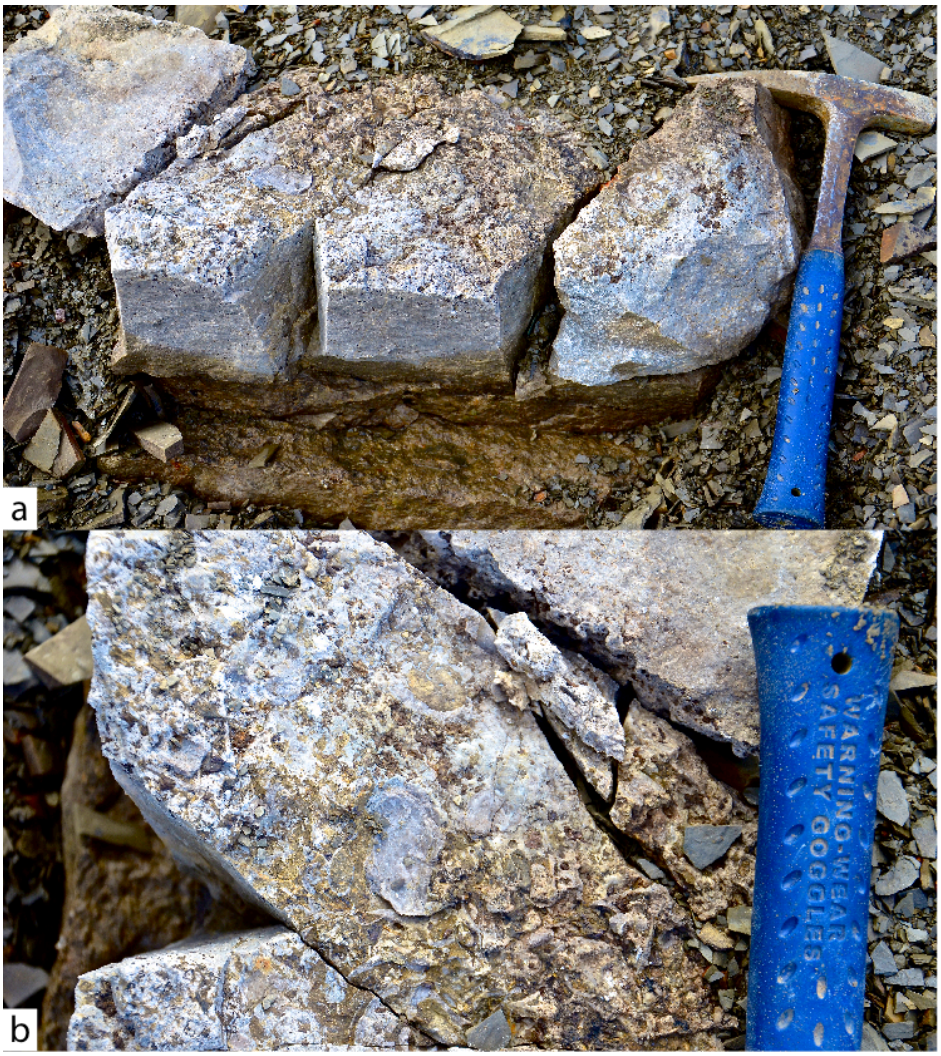

Fig. 22 – a. Photograph of the *Myalina* bed on Kovalevskajafjellet. b. Picture of the top surface of these condensed limestone beds.

Interpretation

The occurrence of this condensed carbonate cemented fossiliferous beds of shallow marine origin suggests a sediment starvation and a high level of energy after a possible transgression of the Hornsund High, and before a new increase in fine clastic material input with the deposition of the soft and finely laminated

dark grey shales of the Vardebukta Fm. The presence of *Myalina* shell remains and of eroded trepostome bryozoan fragments of the *Arcticopora* genus implies that the rock from out of which these debris derived from is of Dienerian-Smithian age. However, as the overlying unit consist of soft shales of the Vardebukta Fm., it is possible to suggest that this bed has to be of Dienerian age. Indeed, if these bryozoan debris were of Smithian age, then the overlying shales would have to belong to the Tvillingodden Fm. instead of the Vardebukta Fm., which would be in contradiction with the defined lithostratigraphy (Mørk *et al.* 1999b).

The unidentified shell fragment observed in TSK2 is most probably a gastropod. Since the gastropods shell is made of aragonite, it is unstable and more prone to dissolution than the brachiopods one, which is composed of Mg-calcite. This shell fragment reveals a three steps history of its diagenesis, with a first geopetal, intraskeletal, micritic-bioclastic, partial infill of its chamber with microconchidae fragments, “which records the water level in the cavity at the time of deposition of the internal sediment” (Flügel 2004). It is followed by the sparitic cementation of the remaining primary porosity, and an eventual replacement of the shell by calcite spar. The transition from micritic-bioclastic infill to sparitic calcite cement implies (i) the drowning of the rock into a phreatic environment, (ii) an increase of the energy within the system, (iii) a change of the fluid chemistry and (iv) the presence an actual flow running through the rock.

5.2. Facies associations

These 17 facies have been grouped into four main facies associations (Table 2): (i) Braided river, (ii) “Cold” offshore transition, (iii) Upper shoreface, shallow marine and (iv) “Warm” offshore transition. These associations are displayed in the correlation chart enclosed with this thesis. It is important to note that both “braided river” and “Upper shoreface shallow marine” associations only appear on the Sørkapp-Hornsund High. The “cold offshore transition” facies association hasn’t been reported from the High itself, but is present further to the East, on the Treskelen Peninsula (Birkenmajer 1977, Worsley & Mørk 1978, Mørk 1978, Winsnes et al. 1993, Mørk et al. 1999b). The “warm offshore” facies association appears at every location visited on Spitsbergen.

Table 2 – Facies associations

Facies association	Depositional environment	facies
Braided river	flood plain, subaqueous bar	Coal; ?F-Sand-Dgy; F-Sand-W; Med-Sand-Lgy;
Cold offshore transition	Marine, cold water environments: (i) western Spitsbergen: offshore, moderaly deep shelf, below the SBL; (ii) central Spitsbergen: uppermost offshore transition, above the SBL	Mud-Grn; Nod-Bed; Sh-Si-Vf-Sand-Lgy; Si-Sh-Dgy; Si-Sh-Gy
Upper shoreface shallow marine		Cgl; F-Sand-O; Med-C-Sand-O; Sh-O; Vf-Sand-Carb-Cem
Warm offshore transition	Marine, warmer water environment, upper offshore transition, above the SBL	F-Sand-Si-Dgy; Mud-Grn; Nod-Bed; Sh-Dgy; Sh-Si-Vf-Sand-Lgy

*Mud-Blk, as being the only facies of its association, hasn't been implemented in this table. Please refer to Table 1.

The facies in blue belong to different facies associations.

5.3. Sedimentary sections

5.3.1. Marmierfjellet

The Marm-1 sedimentary log (Fig. 23 and enclosed sedimentary log) is a 62 m section investigated in a water brook running down the north-eastern face of Marmierfjellet, in Lusitaniadalen (idea to call it: Patronbekk) (33x coordinates: 0538449 – 8692946). Note that meteorological conditions were clement during the day spent at that location. Ammonoid remains have been reported at 29, 33, 37.2 m above the start of the section, but their poor condition has made their interpretation impossible (Fig. 24).

It consists of three main units. The lowermost 14 m consist of soft, grey, finely laminated silty shales frequently interbedded with some storm-influenced silty sand, sand or nodular layers. From 14 m to 37 m, the colour changes slightly towards darker tones, albeit they remain as soft their silt content linger similar. They represent a certain intermediate facies change between the underlying grey, silty shales, and the overlying dark grey mudstone. The recurrence of storm-beds diminishes as well. Note that a unique loading structure has been observed at 23.5 m above the start of the section in one of these storm beds (Fig. 20b).

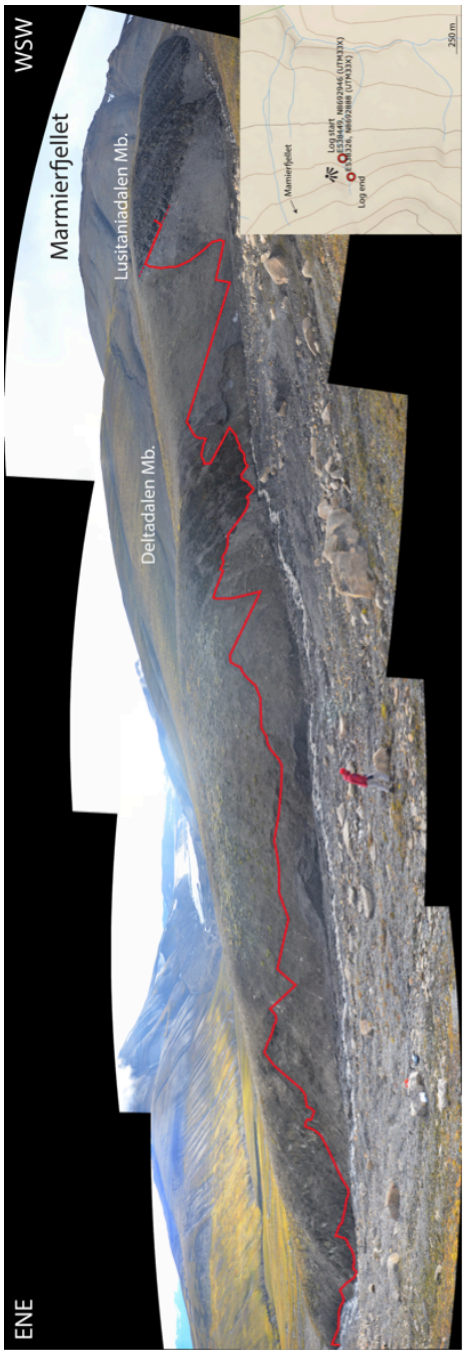

Fig. 23 – Panoramic picture of the section measured on Marmierfjellet (thick red line). The red dashed line marks the boundary between the Deltadalen Mb. and the Lusitaniadalen Mb. Note that the Kapp Starostin Fm. is probably missing (topographical map from Kart over Svalbard, GPS coordinates and picture location added).

Fig. 24 – Unidentified ammonoid remain, Marmierfjellet. The white line enhances the contour of the fossil.

Between 37 and 56.5 m, the silt content sharply diminishes, and the laminated shales become darker. They remain soft and as altered/alterable as the underlying silty shales. A fewer number of storm-influenced beds interpose the mudstone deposits. Post-depositional nodules also occur within these shales. The topmost part of the sedimentary log starts just above a thick (50 cm), rippled, silty sandstone bed. It consists of black, finely laminated, soft mudstone. Yellow-coloured nodules are either scattered sparsely within the black mudstone, or concentrated within several, common, well-defined nodular beds. The loss of silt towards the top of the section suggests a deepening of the

depositional environment throughout the succession. However, this section is to take with great caution, as its localisation on a precise stratigraphic scheme remains problematic. Another visit at that particular location would greatly help to analyse this issue and to re-evaluate the stratigraphy of this section.

5.3.2. Høgskulefjellet

The data regarding the Høg-2 sedimentary log (Fig. 25 and enclosed sedimentary log) have been collected in a narrow water stream (idea to call it: Gravbekk) on the east slope of Høgskulefjellet, just north of a small melting glacier (idea to call it: Døendebreen) (33x coordinates: 0520884 – 8716924). A shoulder sticks out of the relief about 50m below the start of the log. After long discussions, it has been decided not to investigate this part of the succession, as a non-negligible number of gradually disappearing, silicified rock fragments have been observed above this level. The meteorological conditions during the time spent at that location have been cloudy with no precipitations. The log starts at 337 masl, and consists of 17m of altered, soft, finely laminated silty shales and shales, interbedded with thin rippled siltstone beds (up to 10 cm thick). The boundary between the Kapp Starostin and the Vikinghøgda fms. has been place at approximately 9.80 m above the start of the log, where the silt content decreases, along with a change in colour towards darker tinges.

Fig. 25 – Picture of Høgskulefjellet, wit the measured section in red. The purple line demarcates the lithological boundary between the Kapp Starostin Fm. and the Vikinghøgda Fm.

5.3.3. Kongressfjellet

The 56 m of sedimentary succession presented in log Kong-1 have been carefully examined in a water stream on the eastern slopes of Kongressfjellet (idea to call it: Kongressbekk) (Fig. 26 and enclosed sedimentary log) (33x coordinates: 0506209 – 8719590). It resembles the Marm-1 log in the way that, it starts with approximately 27.5 m of soft, altered, finely laminated, grey, silty shales, interbedded with hummocky cross-stratified and rippled sand layers. One unconsolidated layer of green mud occur 8m above the start of the log.

The following 34.5 m of the log consist of dark grey, soft and altered, finely laminated shales. Storm beds also occur within

these shales. Note that, the sediments between 28 and 38 m are characterized by a coarsening upwards trend, leading to a two metres thick, undulated, silty sand to very fine sand unit. A poorly preserved ammonoid specimen have been found in a calcareous nodule 35 m above the start of the log, accompanied with undifferentiated shell fragments, which also occur at 52 m. *A l'instar de* Marmierfjellet, the uppermost unit consist of black, soft, finely laminated cliff forming shales, with well-defined yellowish nodular beds intercalations.

The boundary between the older deposits of the Kapp Starostin Fm. and the younger sediments of the Vikinghøgda Fm. is to take with great caution as well, as the only difference between these two units observed in the field was a change in colour and a decrease of the silt content, as their hardness remains relatively similar. Note that, the measured section Kong-1 is quite different than the one presented by Dustira *et al.* (2013), as no phosphatic lag or spiculitic shales have been documented.

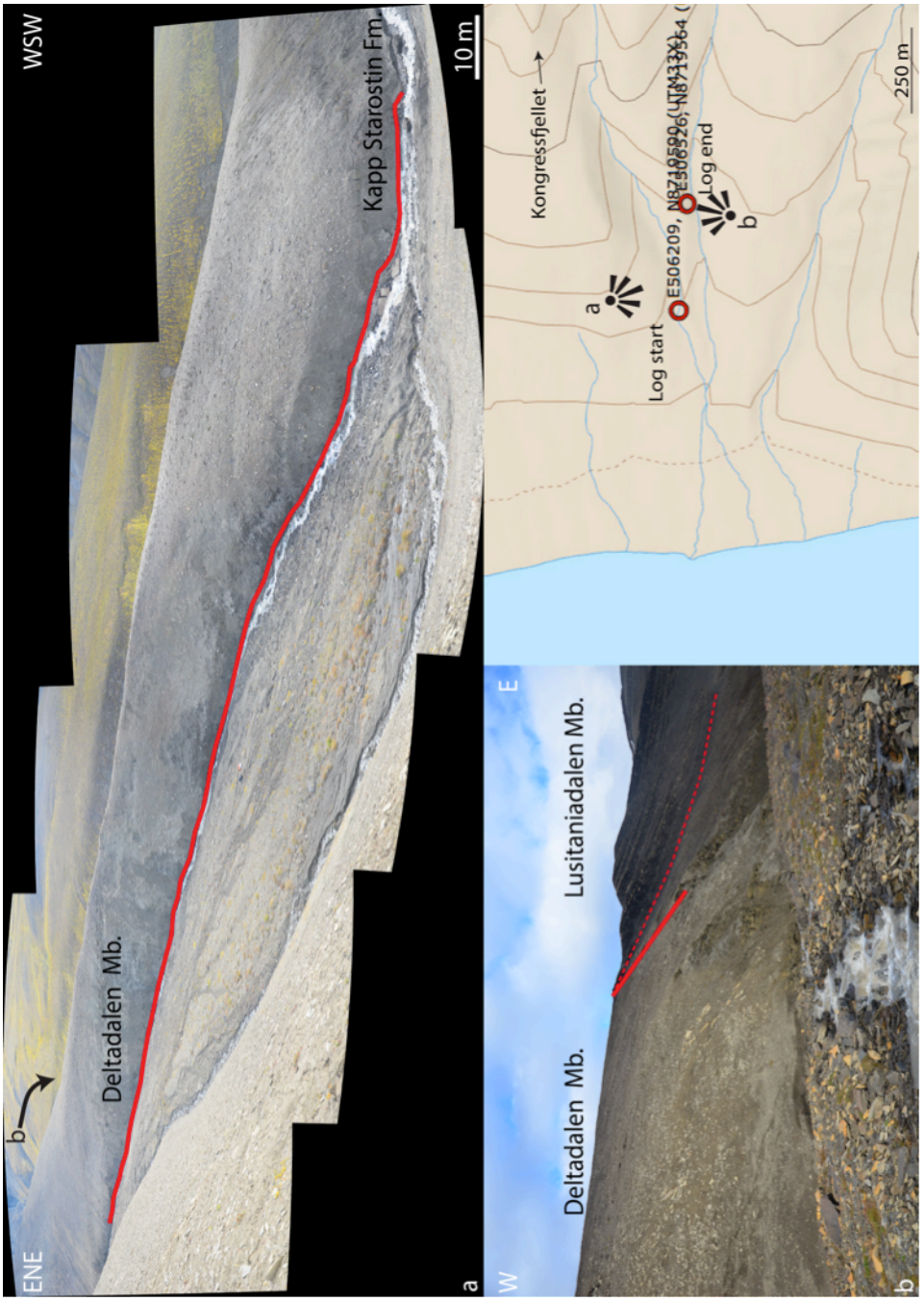

Fig. 26 – The thick red line indicates the measured section on Kongressfjellet, while the dashed streak represents the boundary between the Deltadalen Mb. and the Lusitaniadalen Mb. Note that the precise location of the lithological boundary between the Kapp Starostin Fm. and the overlying Deltadalen Mb. remains uncertain.

5.3.3. Festningen

Two sedimentary logs have been produced at Festningen, after the careful study of strata belonging the Kapp Starostin and Vardebukta fms. (direction and dip: 047/40).

The first one, Kapp Star-1 (Fig. 27 and enclosed sedimentary log) (33x coordinates: 0473002 – 8669280), corresponds to the beach section at Vardebukta. The second one, Vard-1 (enclosed log), is located in a narrow water stream SE of the Kapp Star-1 log (idea to call it: Vardebekk). During the four days spent at Festningen, the rain has been showering most of the time, before allowing the sun to pierce through its clouds on the last day.

Kapp Star 1 sedimentary log is 37 m long, and comprises 16m of dark grey, hard-silicified shales of the Permian Kapp Starostin Fm., which are overlain by 20 m of dark grey, soft shales of the Triassic Vardebukta Fm., before reaching a dolerite intrusion. Fossils of brachiopods, undifferentiated shells and shell fragments, bryozoans, as well as another unidentified, networked (?)fossil/trace fossil(?) (TS0 and TS1, Appendix 2: Plates 1, 2) have been reported between 1 m and 3 m, where the rocks are more lithified than at the top of the formation. The fossil content and the lithification diminish toward the top of the formation (extensive bioturbations?), while the proportion of sponge spicules increases.

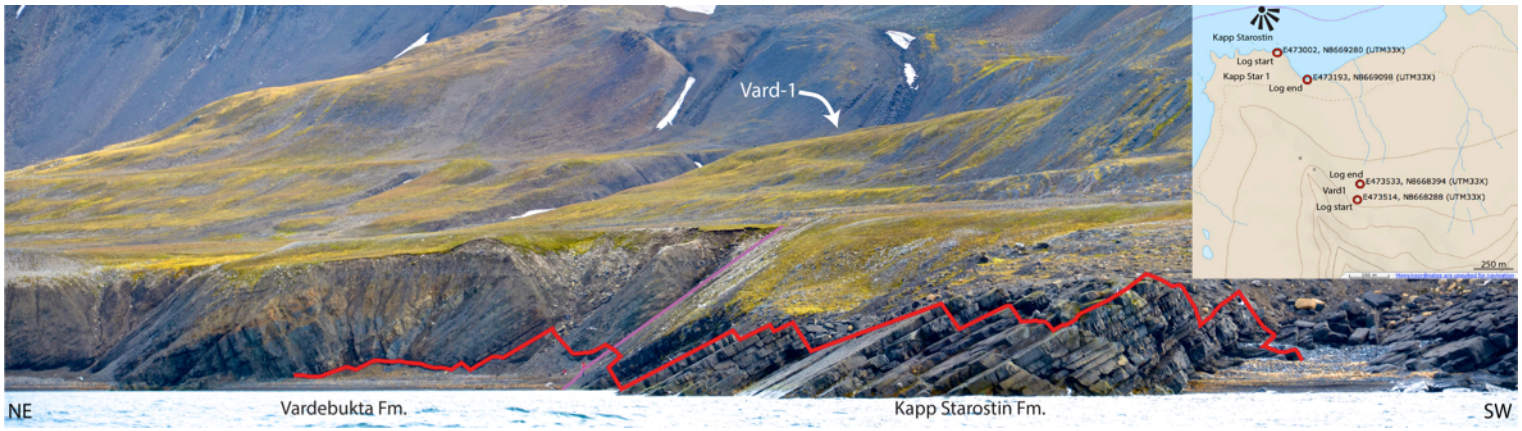

Fig. 27 – Kapp-Star-1 section, Festningen. View width: 200 m.

The thin section TS0, at 1.15 m, displays boring marks within the unidentified fossil, remains of brachiopod shells and one unique specimen of gastropod. Thin section TS3 at 12.5 m shows a high number of spicules, which tend to be concentrated dense in “pockets”, separated by chert-rich zones. Their size is most of the time sub-millimetric (*microspiculae)*, but can reach one millimetre in exceptional cases (*megaspiculae*). Both longitudinal and transversal cross sections through these spicules show the occurrence of a central canal. Note that the spicules orientation leans towards sub-horizontality. Also, the density of sub-horizontal fractures increases within these spicules “pockets”. Planar substrate-feeder *Zoophycos* bioturbations have been reported from the topmost strata of the formation (Uchman *et al.*, in prep., Mørk, personal information).

No evidences of erosional or non-depositional event have been observed in the field at the lithological boundary between the Kapp Starostin and the Vardebukta fms., as the soft shales of the Vardebukta Fm. rest conformably on the Permian Kapp Starostin Fm. The drastic softening of the sediments occurs within centimetres. No fossils or ichnofacies have been reported from these altered dark grey shales, at all. However, Korčinskaja (1986) and Mørk (personal communications) report the occurrence of *Otoceras boreale* within the first meters of the formation. Interbedded storm-generated and/or rippled beds increase in number and thickness towards the dolerite intrusion, while nodular beds decreases. A reverse grading, plane parallel laminated

sequence occurs in the four last metres, right below the dolerite. Note that the grain size increases from silt so very fine sand between 32 to 33 m, before remaining constant until the magmatic intrusion. Several thrusted horizons have been observed at approximately 19 m and just bellow 26 m. Their order of magnitude doesn't overwhelm scale of the centimetre, while a normal fault has been observed 5 m bellow the magmatic sill, whose displacement is proposed to reach several metres (no precise measurements of its displacement have been conducted though).

The 31 m long Vard-1 sedimentary log (coordinates: 0473514 – 8668288) crosses the same lithological boundary between the Kapp Starostin Fm. and the Vardebukta Fm., approximately 750m inland. However, only 4 m of the hard, cherty, dark grey shales of the Kapp Starostin Fm. have been investigated. No fossils have been reported from these strata. The base of these beds tends to be more laminated than the more massive upper part. The boundary itself is missing, covered by the narrow Vardebekk water stream and its rocky bed. The overlying 27 m of sediments consist soft, planar laminated, dark grey shales of the Vardebukta Fm. interbedded with nodular beds and storm-generated silt beds, following the same trend than in the neighboured beach section: the number of nodular beds diminishes, while rippled and hummocky cross-stratified beds occur more and more often towards the top of the section. No fossils have been documented

in these soft shales neither, but thin, unconsolidated green mud occurs at 6.40, 8.50, 9 and 14.50 m above the start of the log.

5.3.3. Hornsund

In Hornsund, only three mountains have been targeted to look at the lowermost Triassic deposits of the Kistefjellet Mb. and their underlying units, as a consequence of the really rough and rainy weather conditions occurring 6 out 9 days spent on the Sørkapp-Hornsund High.

Kovalevskajafjellet

The first section to be considered is Kovalevskajafjellet, located on the western side of Lisbetdalen (coordinates: 0521222 – 8534596) (Fig. 28 and enclosed log Kov-1). The 29 m sedimentary log Kov-1 starts at 440 masl. The lowermost bed consists of 1m of hard, light grey, planar cross-stratified, medium-sized, quartz-rich sandstone, whose grains are sub-angular (TSK0, Appendix 2: Plate 9). The porosity is non-existent. It is overlain by a thin layer of approximately 10 cm of dark-grey, medium to coarse, hard sandstone. This bed, as well as the three following one, are characterised by the absence of any sedimentary structure in them. These three hard, massive, dark grey, quartz-rich, fine sandstones are respectively 50, 70 and 75 cm thick. TSK4 (Appendix 2: Plate 8) shows the occurrence of a normal grading towards the top of the thin section, as well as a high proportion of opaque minerals among the other sub-angular quartz grains. Pore-filling calcitic cement is also present in the thin section,

preserving one unique undulated structure. According to Lipiarski & Čmiel (1984), these rocks belong to the Hornsundneset Fm.

Fig. 28 – Location of the Kov-1 sedimentary log, Kovalevskajafjellet. The red dashed line marks the upper boundary of the Brevassfjellet Beds.

The next orange, fine sandstone bed outcrops 4 m above the start of the log, but as the section being partly covered by screes, the exact boundary between these dark sandstones and the overlying orange units remain unclear. The following 10 m consist of hard, orange sand beds, which sometimes display scattered clasts, grading upward to more conglomeratic deposits (Fig. 29). This changes in the sediments towards coarser material suggests an increase of the flow energy. These polymictic conglomerates display an alternation of matrix- and clast-supported horizons. As detailed in subchapter 5.1.1., the establishment of steady flow conditions could remove the fine material of these deposits, whose sub-roundness to sub-angularity grain shape (TSK3) attests to a

certain transport from the source area they have derived from. In the literature, these strata are interpreted as the Brevassfjellet Beds (Mørk *et al.* 1999b).

Fig. 29 – Conglomeratic bed, Kovalevskajafjellet, 8.5 m above the start of the sedimentary log.

The overlying 1.20 m of the section consists of a condensed fossil-rich limestone, whose top surface is karstified, interpreted in the literature as the *Myalina* beds (Birkenmajer 1977, Worsley & Mørk 1978, Birkenmajer 1990, Mørk 1999b). The presence of this hardground necessitates a slow sedimentation rate, and the absence of nearly every detrital material requires a high-energy environment (Nicolaides & Wallace 1997). Transported bryozoan fragments have been dated to be of Triassic age by Prof. Hans Arne Nakrem (University of Oslo). No Permian fossils have been documented within the collected samples. The karstification of the upper surface would traditionally imply sub-aerial exposure of the rock. However, this isn't an absolute truth, as karstification

processes can also appear in marine conditions (Land & Paull 2000, Surić 2005). The occurrence of calcite spar involves fresh water running through the system.

The Following 18 m consist of planar laminated, dark grey, soft shales of the Vardebukta Fm., interbedded with hummocky cross-laminated and rippled beds. Note that these storm-generated strata appear more often between up to 18 m above the start of the sedimentary log. Two main differences exist between the shales of the Vardebukta Fm. on the Sørkapp-Hornsund High and elsewhere on Svalbard. First of all, their silt content is higher than on western and central Spitsbergen, and secondly, bioturbations have been reported from the High. The occurrence of Triassic bryozoan fragments as well as these bioturbations entail that the lowermost part of the Vardebukta Fm. is missing.

Lidfjellet

The sedimentary log Lid-13-1 is located on the NW ridge of Lidfjellet (Fig. 30 and enclosed log) (33x coordinates: 0518357 – 8533176). 47 m of sediments have been investigated. The 11 first meters consist of white to light grey, hard, massive, quartz-rich medium sandstone beds. TSL0 shows sub-angular quartz grain, and a high proportion of sub-rounded zircons. Each bed can reach approximately 1 m, and can display some faint planar cross-stratification, notably visible 2 m above the start of the log. Above these strata, towards the west, an 8 m thick succession of dark grey, medium-grained quartz-rich sandstone (Fig. 31a) is present,

but it is completely missing towards the investigated ridge. The thin section TSL1 shows, however, a composition relatively similar to TSL0, with a extremely high sub-angular quartz content, bended micas and other accessory minerals. At this particular location, screes cover 10m of the overlying Brevassfjellet Beds, since they are situated at the foot of the ridge (Fig. 31b). Therefore, only one clast-supported conglomeratic layer has been excavated 13 m above the start of the log (Fig. 32). Thin section Lid-13-1-1 displays sub-rounded to sub-angular, centimetric poly-crystalline quartz grains, separated by smaller mono-crystalline quartz and calcite cement. The next rock unit outcrops 21 m above the start of the log. It consists of the shales of the Vardebukta Fm., interbedded with storm-influenced deposits. Note that screes bury the section between 24 and 26 m, as well as 27 to 38 m.

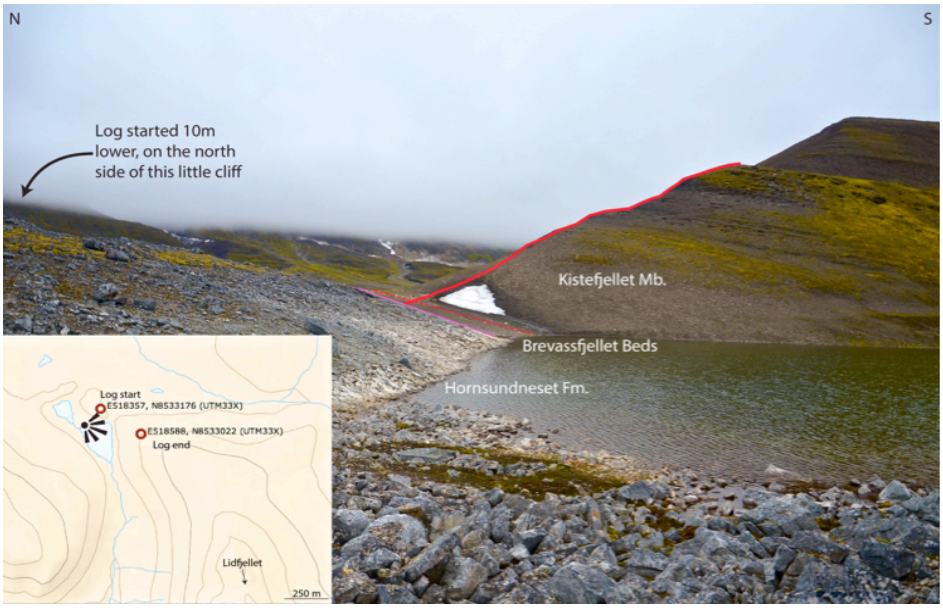

Fig. 30 – Location of the Lid-13-1 sedimentary log on Lidfjellet. As screes cover the Brevassfjellet Beds, the boundary between the Carboniferous strata and the Triassic rocks, as well as the upper limit of the Brevassfjellet Beds remain uncertain.

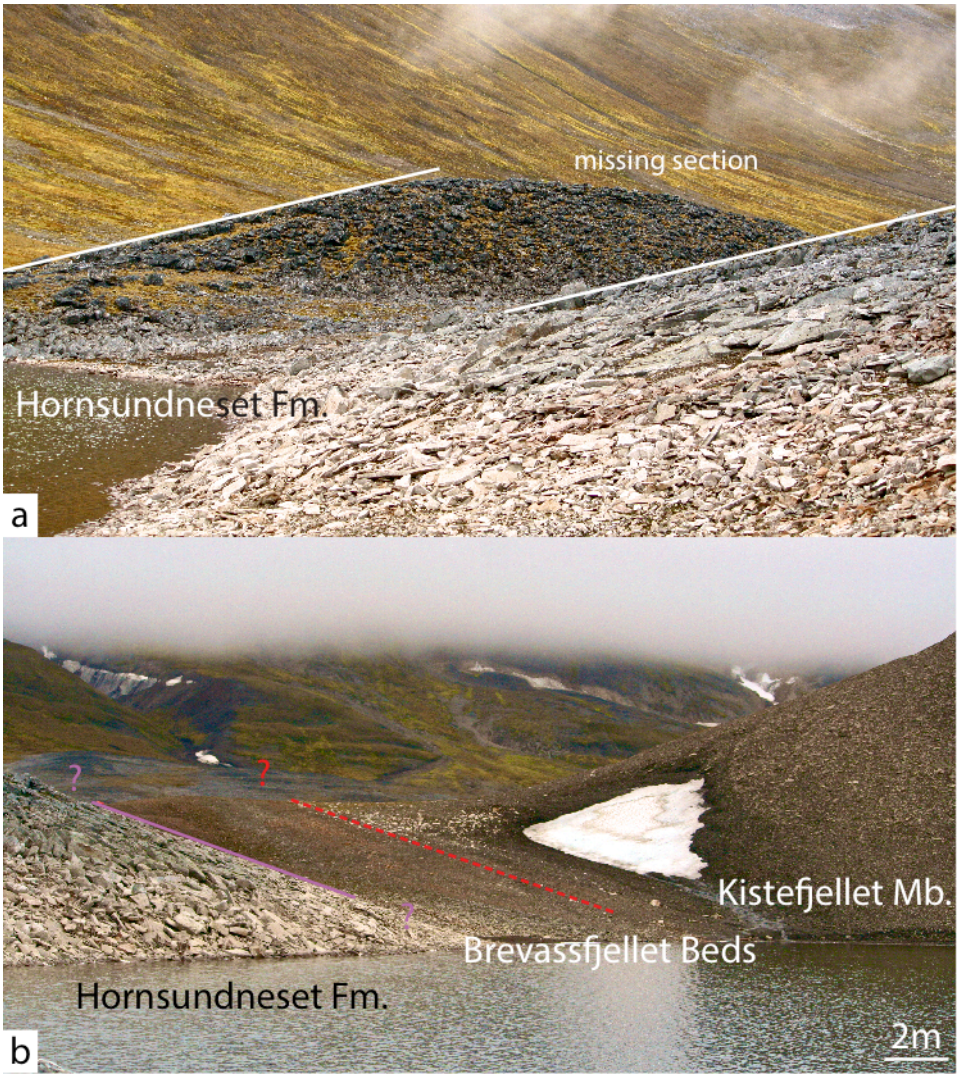

Fig. 31 – a. Photograph of the 8 m thick missing sequence of dark grey sandstone. b. The purple line delimitates the boundary between the Carboniferous strata of the Hornsundneset Fm. and the Triassic rocks of the Vardebukta Fm., while the upper limit of the Brevassfjellet Beds is marked by the red dashed line. Yet the true position of the member boundary remains uncertain.

Fig. 32 – Conglomeratic strata of the Brevassfjellet Mb., Lidfjellet, 13 m above the start of the sedimentary log.

Sergeevfjellet

On Sergeevfjellet, two sedimentary logs have been produced out of three visited locations on the NW face of the mountain. The log Serg-2 synthesises a 29 m thick section (Fig. 33 and enclosed log) (33x coordinates: 0516652 – 8534044) studied on the N ridge. The orientation and the dip values of these strata are 133-30. It starts with 2 m of light grey, hard, quartz-rich hard sandstone. TSS2-0 (Appendix 2: Plate 18) is the only thin section that displays a clear orientation of the micas crystals within the angular to sub-angular quartz grain. Two different orientations are visible, and they change throughout the thin section. In the lower part, the overall orientation of the crystals dips 60° to the right of the image, with some minor crystals dipping with the same angle towards the left of the picture. Further up, the dip of the crystal flattens up, with a value closer to 30°. Also, the majority of the minerals are oriented

towards the left of the image, which contrasts with the lower part of the thin section. The overlying 6 m are an alternation of soft mudstone and coal seam. The lowermost mudstone reaches a thickness of 1m, and is overlain by a first 50 cm thick coal seam. Two metres of finely laminated shales separate the next coal seam. Note that plant fragments have been reported from both coal beds. The next two metres consist of organic rich finely laminated mudstone, before reaching a thin layer of green unconsolidated mud 8 m above the start of the log. In the literature, these sandy, muddy and coaly sediments are interpreted as part of the Sergeevfjellet Fm.

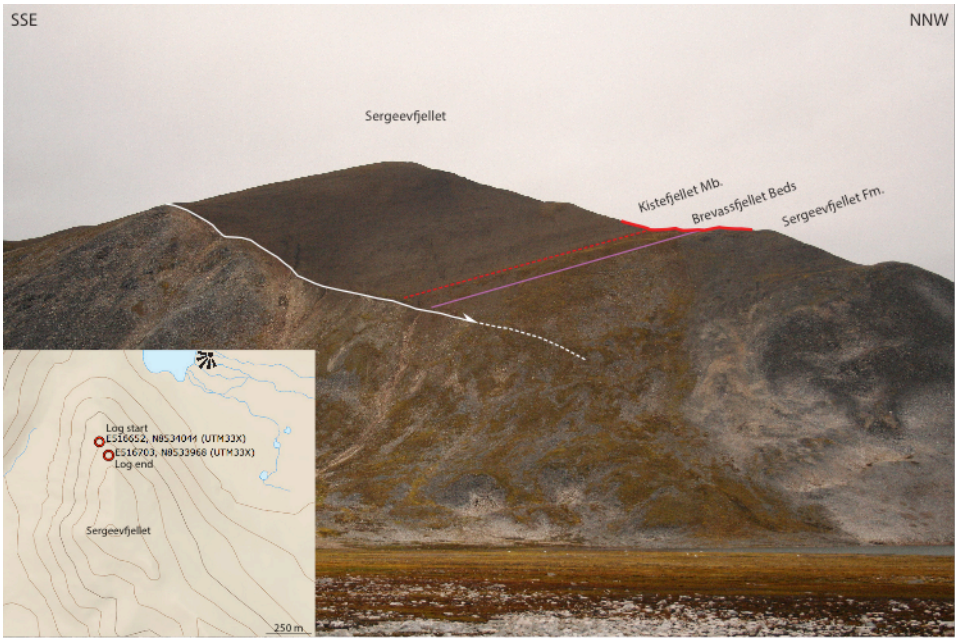

Fig. 33 – Picture of Sergeevfjellet, with the location of the sedimentary log Serg-2. Note the occurrence of a major normal fault, whose displacement reaches several hundred meters.

The orange conglomerate and sandstone layers of the Brevassfjellet Beds outcrop between 8 and 15 m above the start of the log. The lowest 2.2 m consist of an alternation of clast supported and matrix-supported conglomeratic horizons, with a high proportion of medium-sized sand grains, as displayed in TSS2-1 (Appendix 2: Plate 17). Screes cover the rocks between 10.2 and 11.2 m. A hard, orange, fine, sub-angular to sub-rounded sandstone is deposited on top of the conglomerate, until 14.9 m above the start of the log. The number of pebbly clasts varies, as well as the matrix content, as visible in TSS2-2 (Appendix 2: Plate 16). The topmost layer of this Brevassfjellet beds consists of 30 cm thick conglomerate. The proportion of centimetric sub-rounded clast is relatively high. These pebbles are surrounded by a matrix of mixed fine quartz grains and finer material (TSS2-3, Appendix 2: Plate 15). Note that shell fragments, which were thought to have been observed in the field, haven't been reported from the thin sections study. Also, no *Myalina* Beds have been documented at that location. The finely laminated shales and the storm beds of the Vardebukta Fm. cap this conglomeratic bed located approximately at 15 m above the start of the log. Note that the density of the storm-generated beds is diminishing above 20 m. Minor bioturbations have been reported from both storm beds and shales.

The sedimentary log Serg-3 is located 200 m to the south from the top of Serg-2 (Fig. 34 and enclosed log) (33x coordinates: 0516680 – 8533800). The log is 17 m long, and starts with a 1 m

thick, white, hard, planar cross-bedded fine sandstone. No coal seams occur in this section. The overlying 16 m are characterized by orange tones, the exception made of three unconsolidated mud horizons at 1.5, 10 and 12.5 m above the start of the log, and correspond to the Brevassfjellet Beds. The lowermost of these orange units is a 40 cm thick layer of massive coarse sand, whose separated from the overlying grey unit by a distinctive erosive surface, which hasn't been observed anywhere else on the Sørkapp-Hornsund High, since the boundary is covered on Kovalevskajafjellet and Lidfjellet, and is overlying soft shales lower down on the Serg-2 log. Between 1.6 and 6.5 m high, the succession goes as follow: 1m of hard sandstone, whose grains are grading from fine to very fine. Note the occurrence of a 10 cm horizon of coarse sand with scattered gravel in it at 1.8m, while bioturbations are reported from its top part. Between 2.6 and 4 m, two successive reverse-graded beds have been observed. Their grain size ranges from silt to very fine sand.

At the high of 4 m, a first conglomeratic layer occurs. This 10 cm thick conglomerate is matrix supported and most of the observed pebbles are sub-rounded. The rock layer between 4.1 and 6.5 m above the start of the log consists of an alternation of shales and massive very fine sand beds, with scattered nodules and bioturbations also present. Note that the last 1.25 m displays a normal grading, from fine to very fine sand. Soft, finely laminated shales have been deposited between 6.5 and 8 m.

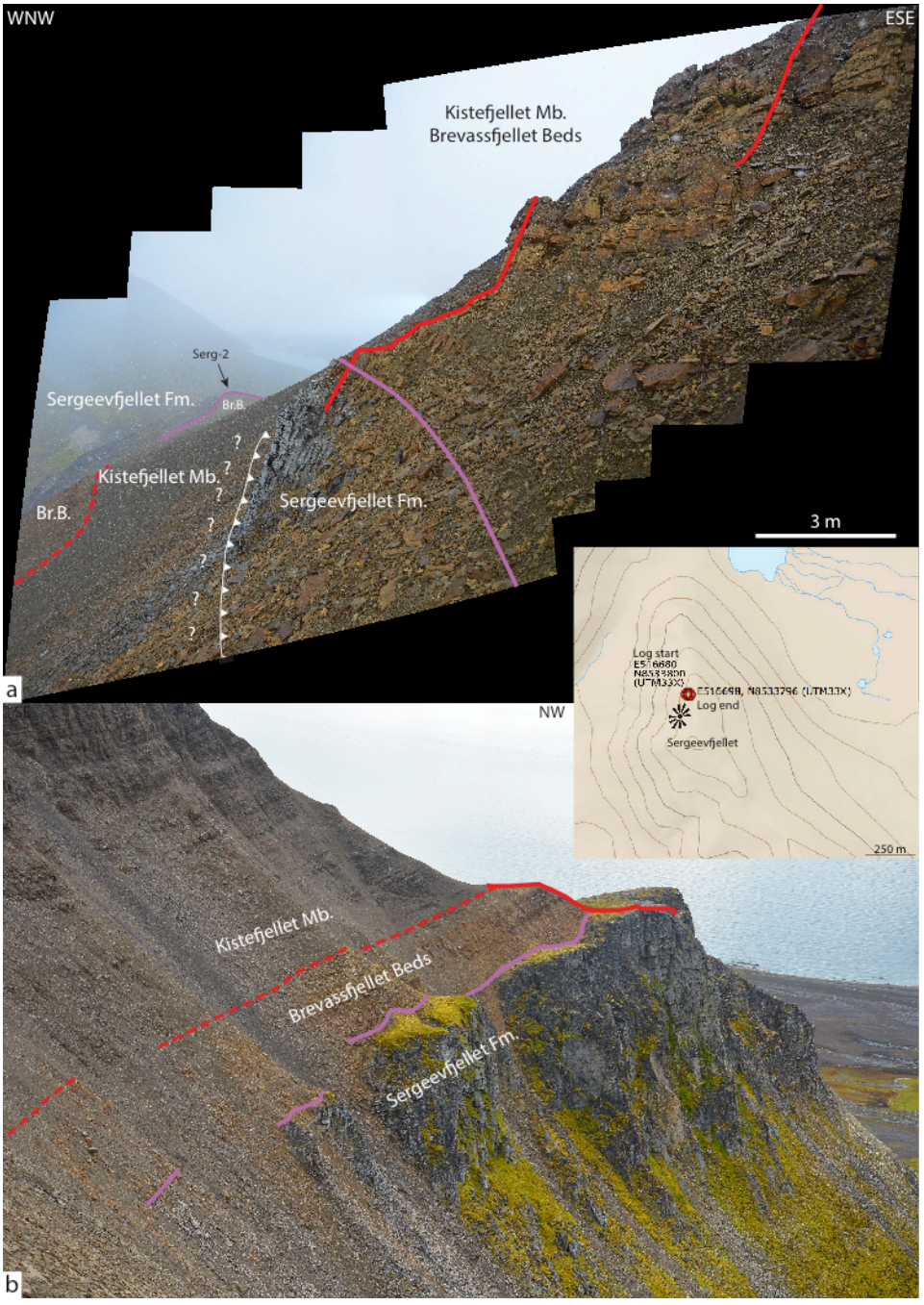

Fig. 34 – a. the actual measured section Serg-3. Note the repetition of the Carbo-Triassic boundary three different altitudes, which suggests the existence of a major thrusting system within the Triassic shales. b. more extensive view of the section towards the SW (unmeasured). Br.B: Brevassfjellet Beds.

A second conglomeratic layer caps these shales. It is clast-supported, and these clasts are sub-angular, though. A massive, fine sand bed occurs on top of it, up to 10 m above the start of the log. It is characterised by the presence of calcareous nodules and scattered pebbles in it lower parts, and a level grading up to medium sand between 9 and 9.5 m. Scattered pebbles reappear in the last 50 cm of this bed. A thin layer of unconsolidated green mud underlies the next massive, 1.8 m thick, fine to medium-grained sandstone bed, which reaches a high of nearly 12 m above the start of the section. The succession between 12 and 13 m comprises three different units. It starts with a 40 cm thick, matrix-supported conglomerate, whose pebble roundness ranges from sub-angular to sub-rounded. It is followed by a 30 cm thick green mud deposit, and another conglomeratic layer, which grades upwards to a clast-free fine sand. The overlying 2.2 m are made of fine sandstone, grading to very fine sandstone at 14.5 m above the start of the log. Pebbles are scattered throughout the entire bed, while bioturbations have been reported within the lowermost 50 cm. Note that ripple marks do also occur at several horizons within this sandstone interval. The last conglomeratic bed occurs at approximately 15.25 m above the start of the log.

The last 50cm overlying this conglomerate bed and below the dark shales of the Vardebukta Fm. correspond to the same condensed calcareous deposits observed at Kovalevskajafjellet, also just below the same dark shales. It consists of three distinct limestone beds, characterised by the reduction of the clastic component

towards the upper limit, together with an increase of opaque minerals, both in number and in size. The thin section TSS3-0 (Appendix 2: Plate 21) has been produced from the lowermost of them. It displays the biggest calcite spars of all collected sample. Note that the cement crystals are remarkably twinned, due to the tectonic stress endured during the WSFTB orogeny. The mono- and poly-crystalline quartz grains are sub-angular to sub-rounded, and can reach a size of 0.5mm. Their fossil content is relatively rich, but poorly diversified, as only bryozoan remains have been documented. Thin section TSS3-1 (Appendix 2: Plate 20) is taken from the second and middle layer, which is characterised by ripple marks at the top of it. It is basically made of microscopic calcitic crystals (approximately 0.05 mm). Rare sub-rounded clastic grains also occur within these calcareous crystals. No fossils have been found in this thin section. The thin section TSS3-2 (Appendix 2: Plate 19) taken from the uppermost limestone layer shows the occurrence of echinoderm remains and macroscopic recrystallized bivalve shells within a matrix of microscopic calcitic cement. Note that the shells have replaced by (twinned) calcite spar. The proportion of opaque minerals is high in comparison with the other samples taken from this condensed section, both on Kovalevskajafjellet and on Sergeevfjellet. They can reach a size of several millimetres. The occurrence of macroscopic opaque minerals is correlated with the existence of porosity in the rock, while microscopic ones are dispersed within the matrix.

A repeated sequence involving the Carboniferous Sergeevfjellet Fm., and the Triassic Brevassfjellet Beds and the overlying shales of the Vardebukta Fm. has been observed only on the western slopes of the mountain. The recurrence of these units implies a post-deposition tectonic event. This will be discussed in greater detail in the next chapter.

6. Discussion

6.1. Central Spitsbergen and western Spitsbergen

All three sections, Marm-1, Høg-2 and Kong-1 measured in central Spitsbergen are on the mountains of Marmierfjellet, Høgskulefjellet and Kongressfjellet, respectively. Each section has been investigated within semi-exposed, narrow water streams. All of which display soft, altered shales, interbedded with silty storm layers. The silt content of the shales diminishes vertically within in the succession. The boundary between the Kapp Starostin Fm. and the overlaying Vikinghøgda Fm. is therefore delicate to identify with precision, on these partially scree-covered slopes. The present geological maps are not ideally suited to detailed fieldwork due to their resolution being too poor for practical applications. The stratigraphy provides more of an order-of-magnitude of the thickness of the strata rather than a precise measurement. Since no identifiable index fossils have been collected, the main criteria to differentiate the different units in the field have been based on sharp (but also somewhat subtle) colour changes.

Mørk *et al.* (1999a, b) place this lithological boundary at the topmost part of a Permian, greenish, glauconitic sandstone bed (Fig. 35). The Vikinghøgda Fm., as mentioned in the subchapter "2.1.3. Triassic units", is 250 m thick at the type section, located in Deltadalen, a valley adjacent to Lusitaniadalen. The lowermost Deltadalen Mb. is 68 m at the type section, while the two overlaying Lusitaniadalen Mb. and Vendomalen Mb. are respectively 88 and 94 m thick (Mørk *et al.* 1999a, b). The Billefjorden (Dallmann *et al.* 2009) and Sassendalen (Major *et al.* 1992) geological maps suggest a thinning of the Vikinghøgda Fm. towards the west, down to approximately 150 m in the region around Høgskulefjellet and Kongressfjellet.

Fig. 35 – The red glove marks the position of the lithological boundary between the Kapp Starostin Fm. and the Vikinghøgda Fm. in Lusitaniadalen (from Mørk *et al.* 1999b).

The common point between the Marm-1 and Kong-1 sedimentary logs is the occurrence of the black, soft, cliff-forming shales at the top of each measured section (see enclosed logs Marm-1 and Kong-1). Note that they have neither been measured nor observed on Høgskulefjellet.

Even though the geological maps are not precise enough for field application, the GPS coordinates of these black shales appear within the Vikinghøgda Fm. (Fig. 36). Yet, their stratigraphic association remains uncertain without biostratigraphical and/or palynological data. However, after carefully reviewing the available literature (Mørk *et al.* 1999a, b), they are thought to belong to the Lusitaniadalen Mb. This interpretation implies that the underlying sediments correspond to the Deltadalen Mb. Once again, palynological results would have provided accuracy as well as a relative certainty to this analysis, as Vigran *et al.* (2014) place this member boundary at the palynological turnover between *Maculatasporites* spp.-*Naumovaspaura striata* palynological assemblage zone.

Therefore, if this analysis and the GPS coordinates are accurate, and “based” on the Billefjorden (Dallmann *et al.* 2009) and Sassendalen (Major *et al.* 1992) geological maps, the thickness of the underlaying Deltadalen Mb. has to range between 100 and 150 m on Marmierfjellet and reaches approximately 50-60 m on Kongressfjellet, considering the dip of the strata. This eventual thickness difference of the Deltadalen Mb. between the type

section in Deltadalen, and the measured sections on Marmierfjellet and Kongressfjellet certainly implicates a few topographical troughs and highs as the cause, which would slightly influence the depositional pattern of these fine sediments unmapped low angle(?) faulting or *décollement niveau(x)* within these Triassic shales as a consequence of the formation of the WSFTB. These structures could indeed lead to the overpacking and subsequent repetition of the different sequences. Blinova *et al*. (2013) have interpreted thrust structures notably in Carboniferous, Permian and Triassic sediments in Isfjorden and Sassenfjorden. However, the seismic resolution doesn't allow for the interpretation of any eventual smaller scale structures.

The boundary with the Kapp Starostin Fm. and the Vikinghøgda Fm. is missing in Lusitaniadalen, as the sedimentary log Marm-1 does not extend deep enough to reach the mapped boundary. However, this lithological boundary has most probably been crossed both on Kongressfjellet and on Høgskulefjellet (Fig. 37). The similar silty shales facies occurs in the lowermost part of both measured sections, as expected. However, this facies also seems to correspond to the lowermost beds of the Marm-1 sedimentary log. Yet, without any bio- and/or palynostratigraphical calibration, any attempt to theorise this eventual facies correlation remains, of course, hypothetical, and the eventuality of mispositionning oneself throughout these shale dominant sequences persists.

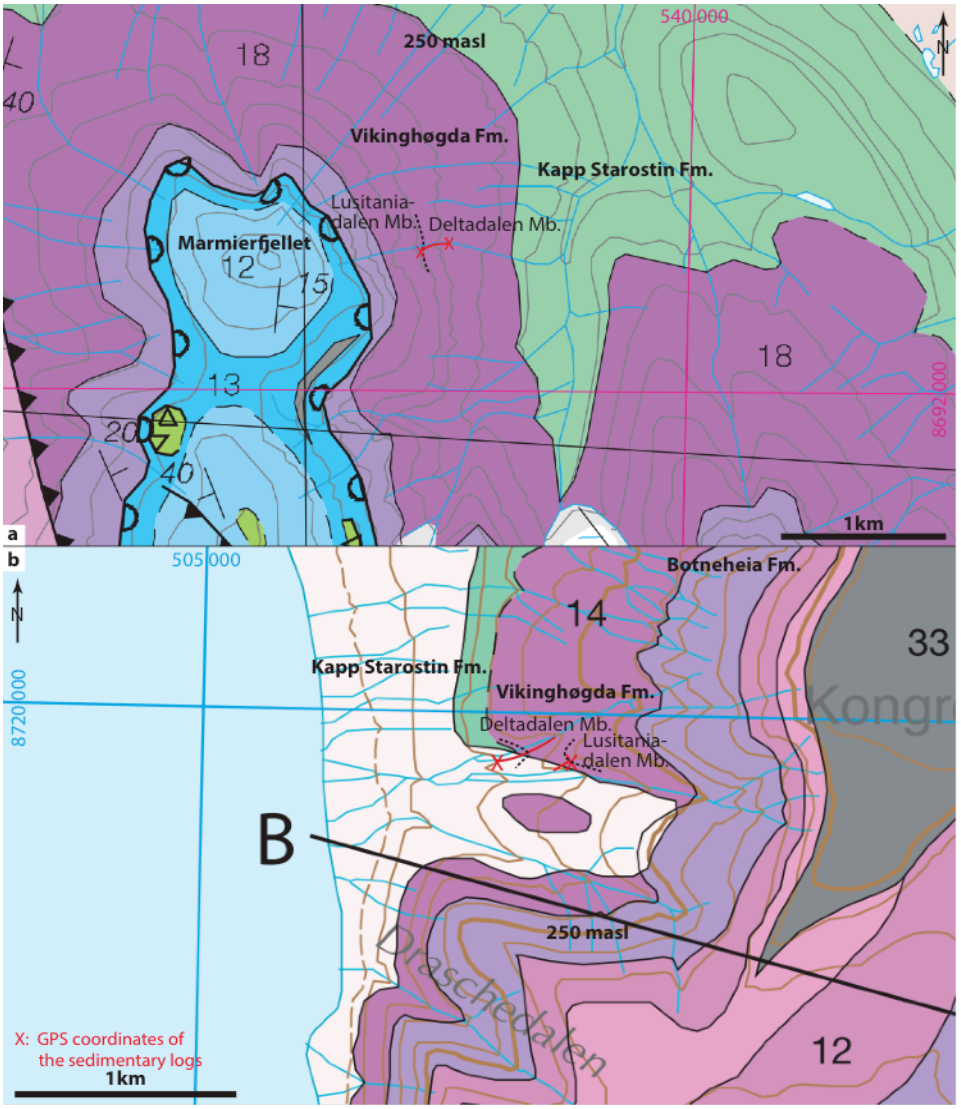

Fig. 36 – a. Geological map from the Marmierfjellet area, with the two red "X" indicating the Marm-1 measured section (from Major *et al.* 1992, with the addition of the measured log, the stratigraphy and UTM 33x coordinates). b. Geological map from Kongressfjellet and its neighbourhood, with the indication of the Kong-1 sedimentary log location (from Dallmann *et al.* 2009, with the addition of the measured log, the stratigraphy and UTM 33x coordinates).

Nevertheless, if this facies correlation is proven to be correct and accepting the mapped position of the boundary between the Kapp Starostin as well as the Vikinghøgda fms., potential uncharted

thrusts could conceivably wedge trapped Permian sediments into Triassic shales. It is also necessary to consider the thickness similarities of the overlying Lusitaniadalen Mb. and Vendomalen Mb. between Marmierfjellet and Kongressfjellet. In both locations, accepting once again that the GPS coordinates are correct, and do correspond to the base of the Lusitaniadalen Mb., it seems that together these two members reach a thickness of approximately 100 m. This thickness (order-of-magnitude), doesn't match with the type section, where they represent ca. 180 m. Further detailed biostratigraphical and geochemical researches are needed in order to accept, or to reject, each of these hypothesises, as well as a special, high-resolution focus on the lateral architecture of these formations.

A notable difference regarding (i) the silt content, (ii) the storm influence and (iii) the hardness of the topmost layers of the Kapp Starostin Fm. can be observed between the two sections at Høg-1 and Kong-1 in central Spitsbergen, and those at Festningen. While the silt content, together with the impact of storms, diminish towards the west. The hardness, *a contrario*, increases drastically, as well as the spiculitic content. These observations suggest depositional environment to be more oxygenated, trough-shaped, lower in energy and deeper than the SWBL, towards the west. The additional effect of a higher sediment influx in the eastern areas, along with an eventual sediment bypass in the west, can't be excluded, but appears less obvious, given paleogeography of the

area at that time, where shorelines were situated W-SW of what is called Svalbard today.

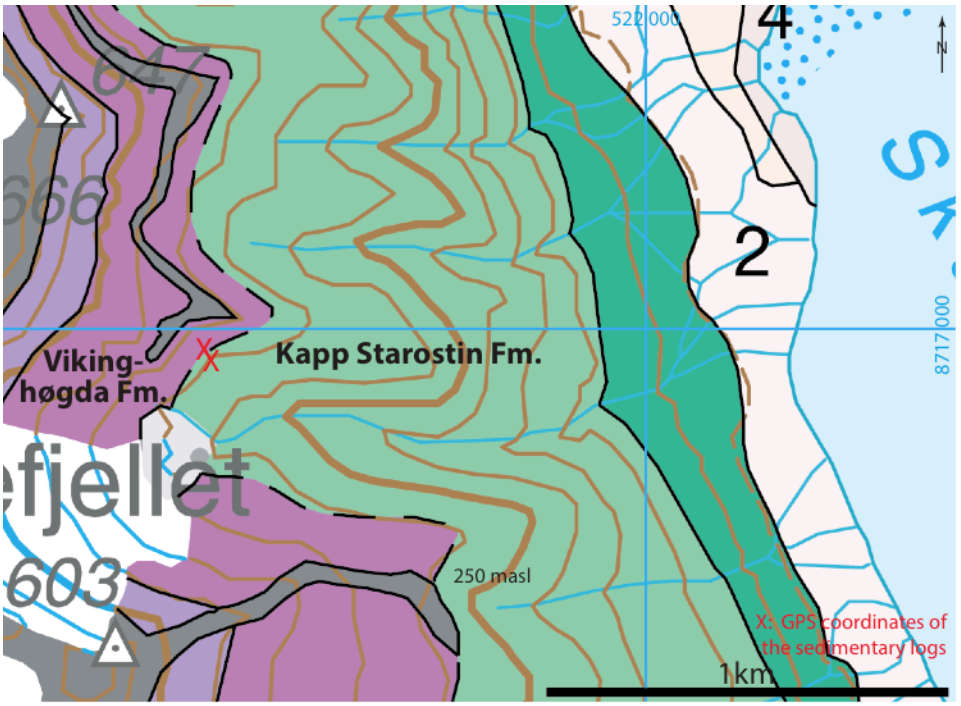

Fig. 37 – Geological map from eastern slopes of Høgskulefjellet. The red "X"s represent the GPS coordinates of the Høg-1 sedimentary log (from Dallmann *et al.* 2009, with the addition of the measured log, the stratigraphy and UTM 33x coordinates).

The transition between Kapp Starostin Fm. and the Vikinghøgda/ Vardebukta fms., and the collapse of the silica factories have been interpreted as a major transgressional episode, with the return of warmer climatic conditions both on land and in the water column (Embry 1989, Mørk *et al.* 1989, Weitschat & Dagys 1989, Mørk *et al.* 1993, Dagys & Weitschat 1993, Beauchamp & Baud 2002, Bjerager *et al*. 2006, Grasby & Beauchamp 2008). This lithological boundary corresponds to a Maximum Regressive Surface (MFS) and is therefore, interpreted as a major sequence boundary.

Nevertheless, this transgression is not as evident and obvious as it may seem, especially in region of western Spitsbergen. Textbook transgressional deposits usually display a deepening-up succession (Boggs 1995). However, within the sections at Vard-1 and Kapp Star-1, storm-generated and rippled beds are absent in the Permian strata. They do, however, occur in the shales of the Vardebukta Fm., suggesting these have therefore been deposited within a shallower depositional environment. In central Spitsbergen, where storm-beds occur in both Kapp Starostin and Vikinghøgda fms., Ichnofossils also suggest the same energy increase through the lithological boundary, as well as a shallower depositional environment. Uchman *et al*. (in prep) suggest transition from a lower offshore energy zone, to an upper offshore energy zone. The occurrence of a really fast transgression at the base of the Vardebukta/Vikinghøgda fms., followed by regression and its sets of shallower deposits, could be the reason for the existence of such deposits.

6.2. Hornsund

As already mentioned in this thesis, no Upper Carboniferous or Permian deposits have been reported from the three localities visited on the Sørkapp-Hornsund High. Nevertheless, Birkenmajer (1977, 1990), Worsley & Mørk (1978), Dallmann (1992), Winsnes *et al.* (1993), Dallmann *et al.* (1999), Błażejowski (2009), Chwieduk (2009) and Hellem & Worsley (unpublished), among other authors, have documented the occurrence of folded and sub-vertical rock units belonging to the Gipsdalen and

Tempelfjorden Groups. Most notably these occur on; the peninsula of Treskelen, on Austjøkultinden, at the SW point of Øyrlandet and also the neighbouring islands of Tokrossøya, Stjernøya and Sørkappøya. On Kovalevskajafjellet, Lidfjellet and Sergeevfjellet, the basal conglomeratic Brevassfjellet Beds, capped by the marine *Myalina* limestone of Triassic age, overlie the Visean/Serpukhovian continental and fluvial deposits of the Hornsundneset or Sergeevfjellet fms., as Winsnes *et al.* (1993) display on their geological map. This lithological boundary corresponds *de facto* to a major sequence boundary.

The oldest units observed on the Sørkapp-Hornsund High were the Carboniferous aged Hornsundneset and Sergeevfjellet fms. However, the fine quartz arenite (TSS2-0, Appendix 2: Plate 18) of the Sergeevfjellet Fm. has only been reported from Sergeevfjellet. This sandstone, overlain by the Triassic Brevassfjellet beds, doesn't correspond to the units underlying the same Triassic basal conglomerate on Kovalevskajafjellet and Lidfjellet. In addition, no flood plain deposits, such as coal seems, root beds or palaeosols, have been reported from the sections at Kov-1 and Lid-13-1. Analysis of thin sections TSK0, TSL1, TSL0, TSL min 30 and TSL min 35 (Appendix 2: Plates 9, 11, 12, 13, 12) shows a coarser quartz arenite than TSS2-0 (Appendix 2: Plate 18), belonging to the Sergeevfjellet Fm. on Sergeevfjellet, which suggests the depositional environment of these rocks to have undergone a higher level of energy, which better corresponds to braided river depositional environment of the Hornsundneset Fm. Winsnes *et al.*

(1993) mapped potential deposits belonging to the Sergeevfjellet Fm. at the foot of Lidfjellet. Both field observation and thin section analysis suggest extending the Hornsundneset Fm. to base of the Brevassfjellet Beds at Lidfjellet. However, the precise assignation of these rock units to the Hornsundneset Fm. would require further investigations, such as stable isotope, palynological and magnetostratigraphic analyses. Yet, TSK4 on Kovalevskajafjellet displays a fine-grained, well-sorted quartz arenite, which has some resemblance with the Sergeevfjellet Fm.

The non-depositional or erosional essence of this hiatus is still a topic of discussion among researchers. Yet, no evidences of the eventual deposition, subsequent erosion and re-deposition of rocks belonging to the Gipsdalen and Tempelfjorden Groups have been reported thus far. The geometry of the formations belonging to the Gipsdalen and Tempelfjorden Groups, outcropping in west and central Spitsbergen, do pitch out towards the High (Birkenmajer 1977, Worsley & Mørk 1978, Mørk 1978, Winsnes *et al.* 1993, Mørk *et al.* 1999b). This wedge architecture advocates for a non-depositional event, rather than a depositional-erosional episode. However, this conceivable non-depositional event has to end no later than the Lower Triassic, with the transgression of the Sørkapp-Hornsund High and the settlement of Dienerian or ?Smithian? sediments, as implied by the occurrence of trepostome bryozoans of the *Arcticopora* genus. These Dienerian or ?Smithian? rocks have then been entirely eroded (together with part of their (?pre-)Triassic *substratum*?) with detrital material

being transported over a short distance, documented by the presence of bryozoan fragments and the sub-angularity of clasts. These re-worked sediments now represent the Brevassfjellet conglomerate. The broad orange colour of these units indicates a relative proximity to a continental iron input. Birkenmajer (1977) and Vigran *et al.* (2014) provide sedimentary logs of the Treskelen Peninsula, where the same conglomeratic units of the Brevassfjellet Beds and the *Myalina* limestone occur 26 m above the Upper Permian Kapp Starostin Fm., reaching a thickness of approximately 6.1 m. The shales of the Vardebukta Fm. conformably overlay these conglomeratic and fossiliferous limestone beds. The occurrence of the Vardebukta Fm. shales above the fossiliferous limestone, notably on the Treskelen Peninsula, therefore suggests the reported bryozoans to be of Dienerian age. If these bryozoans are of Smithian age, the mapped stratigraphy is consequently wrong, and the overlying shales would essentially belong to the Tvillingodden Fm., which doesn't correspond to the field observations. Buchan *et al.* (1965) and Vigran *et al.* (2014) also report *Myalina*-rich beds within the Vardebukta Fm. (i) at Festningen, approximately 110 m, and between 150 and 220 m above the boundary with the Kapp Starostin Fm., and (ii) at Bravaisberget, between circa 110 and 120 m. They don't report any conglomeratic units at these two locations. Further investigation is required in order to provide an accurate correlation of these *Myalina* limestone beds in the Lower Triassic of Svalbard.

Focusing on the Brevassfjellet and the *Myalina* beds on the High itself, it is noticeable that a major difference of thickness is present at the various field locations. On Kovalevskajafjellet, the thickness ranges between approximately 7 and 7.5 m. The imprecision is explained by the presence of thick scree cover atop the lower boundary of the Triassic deposits. On Lidfjellet, only one single conglomeratic bed has been exhumed, but is it possible to propose a maximum thickness of 10 m. This value represents the height difference between the top of the Hornsundneset Fm. and the lowermost sample of Triassic shales. The greatest difference in thickness has been observed on Sergeevfjellet, where the Brevassfjellet Beds measure 6 m at the Serg-2 location, while they reach 15.7 m on the neighboured section Serg-3! This difference of thickness is accompanied by a variation of the stacking pattern between the four measured sections, whose complexity increases westwards. In Serg-3, several shale horizons interbedded with coarser sand layers are present. A higher proportion of coarser sand and pebbles is observed first on Serg-2, before migrating towards Kovalevskajafjellet. However, on a broader scale, the occurrence of coarser units towards the east indicates a laterally increasing energy gradient between Sergeevfjellet and Kovalevskajafjellet, while the uncluttered stacking architecture attests of steadier energy level.

It can also be observed that the finest material of each section is located around the middle of it. The presence of relative finer material halfway up the Brevassfjellet Beds implies a relative

energy decrease over the entire area, before rising again towards the *Myalina* limestone. Smaller scale intra-bed flow variations also occur, as attested by the changes of the matrix-clasts ratio. Note that it is not known whether the shales occurring within these sections (in particular Serg-3) could (partially) correspond to the shales underlying the Brevassfjellet Beds on the Treskelen Peninsula. A detail study of the lateral evolution of the Brevassfjellet Beds is suggested in order to obtain an extensive understanding of the development of these conglomeratic units.

The thickness of the *Myalina* calcareous beds is seen to thin from 1 m at Kovalevskajafjellet, to 40 cm on the Serg-3 log. Note that the *Myalina* limestone is absent from Serg-2, and hasn't been observed at Lidfjellet, due to scree cover. A high energy is required in order to wash away the fine detrital material and to precipitate the cement crystals (Morse 2003). No references have been reported from the literature, which would demonstrate whether the thickness of the condensed section is a direct consequence of the energy of the system. However, the detrital content within these fossiliferous limestone beds decreases towards Kovalevskajafjellet, which entails a higher level of energy towards the east, in the continuation of the thick conglomeratic deposits.

No cement stratigraphy has been carried out systematically, however, no trace of marine aragonitic cement has been observed in thin sections. Only calcite cement is seen to occur, sometimes

in sparitic form. Calcitic cement denotes a cementation under fresh water condition, and the size of the calcite spars is a direct consequence of the rapidity of the meteoritic cementation (Land 1970). The geopetal infill of the gastropod(?) shell indicates that the rock has undergone vadose cementation, at least for a certain period of time, prior to voids being entirely cemented by calcite spar under phreatic conditions. Finally, shells have been dissolved and recrystallized by a second generation of calcite spars.

Suggestions for amendments to the C13G geological map

The Sørkapp-Hornsund High has undergone a complex tectonic development, extending through different periods of geological time, as demonstrated by Dallmann (1992) and Krajewski (2003). On Sergeevfjellet, a normal fault that appears on the geological map (Winsnes *et al.* 1993) north of the summit requires relocation to the south side, as visible in Fig. 32, and the geology should be adapted accordingly. On the mountain of Savičtoppen, although no detailed sedimentary or structural analyses have been conducted, a normal fault has been identified in the field, during a reconnaissance of the area and is seen to be traceable down the western slopes. Further investigations are necessary in order to (i) confirm the existence of this normal fault on Savičtoppen, and (ii) if present, precise GPS coordinate are required in order to place it accurately on the geological map.

On Lidfjellet, Krajewski (2003) shows that part of the Lower Carboniferous Sergeevfjellet Fm. has been thrusted atop the

Upper Jurassic shales of the Agardhfjellet Fm. The sedimentary section measured on this mountain didn't reach the thrust. However, a complex and repeated sequence has been observed on the western slopes of Sergeevfjellet (Fig. 38), where the dip of the geological strata follows the same SE orientation, even though they dip angle has been measured at approximately 30°. The Sergeevfjellet Fm.-Brevassfjellet Beds boundary occurs at three different heights of the mountains.

Such a recurrent sequence could be explained by the presence of (i) two (?duplex*?*) thrusts or (ii) two normal faults (Fig. 39). Further investigations are necessary to answer this question with confidence. However, the hypothesis of compressive structures developing in the sedimentary rocks of Sergeevfjellet seems more probable given (i) the thrust on Lidfjellet, (ii) the lamination of the shales are parallel to the bedding and do not display any mark of normal faulting, and (iii) the rheology of the shales, are prone to develop *décollement niveau* within their sediments. This hypothesis implies that only appendages of the topmost Carboniferous sandstone beds have been trapped by these compressive tectonic event(s). The presence of a normal fault instead, would also entail the Sergeevfjellet, in its completeness, to appear in the landscape and notably on the eastern face of the mountain. However, this particular style of lateral architecture has not been observed in the field.

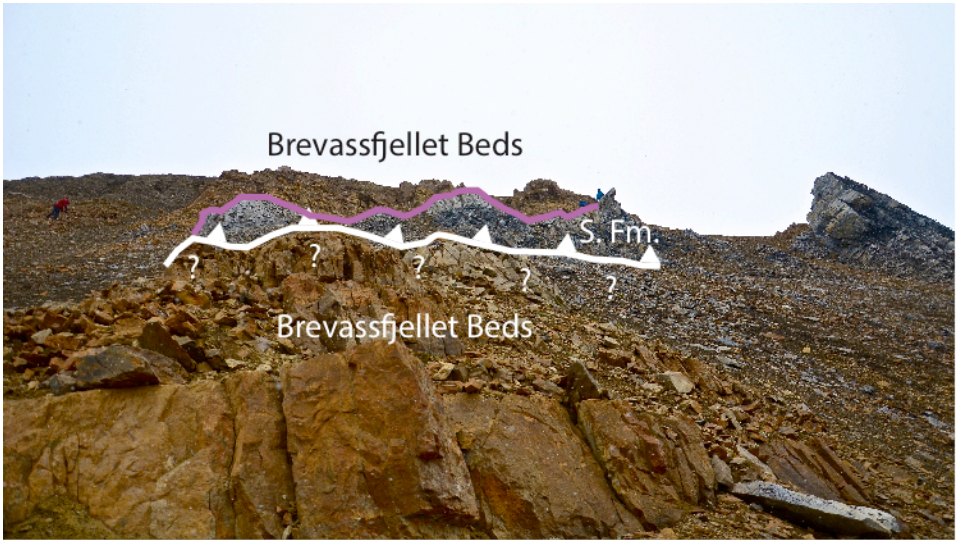

Fig. 38 – Picture of top of the western slopes of Sergeevfjellet. The Triassic Brevassfjellet Beds occurs both below and above the Carboniferous Sergeevfjellet Fm. (S. Fm.). Note that the soft shales of the Kistefjellet Mb. have also been observed below the Sergeevfjellet Fm., but isn't visible due to the effect of the perspective. The thrusts symbol is hypothetical. Geologists for scale.

Much dissimilarity subsists between the mountain of Lidfjellet and Sergeevfjellet, regarding this compressive hypothesis. The first difference regards the location of the eventual thrust(s) within the stratigraphy. As no Jurassic units are present on Sergeevfjellet, the thrusts would be located within the Triassic shales of the Vardebukta Fm. This leads to the second issue, which concerns the stratigraphy of the units overlaying the thrust. Krajewski (2003) places the Tvillingodden Fm. on top of the Brevassfjellet Beds, while the shales occurring above basal Triassic conglomerate on Sergeevfjellet belong to the Vardebukta Fm. The doubts raised about the presence of the Tvillingodden Fm. above the Brevassfjellet Beds are due to (i) the occurrence of the *Myalina* Beds within the shales of the Vardebukta elsewhere on Spitsbergen and (ii) the absence of any evidence for deposition-

erosion of the Vardebukta Fm. on the Sørkapp-Hornsund High. If the Vardebukta Fm. had been deposited and eroded on the High before the deposition of the Tvillingodden Fm., it would imply (i) a break in sedimentation between the Dienerian *Myalina* beds and the overlaying Tvillingodden Fm., or (ii) the *Myalina* limestone beds are of Smithian age. In this case the correlation with the Treskelen Peninsula would need to be re-evaluated. Further investigation could help answering this question, particularly the processing and the analysis the samples collected for palynological purposes during the field season in the summer of 2013.

The geological map provided by Winsnes *et al.* (1993) needs to be consequently updated, at the light of these new results. Fig. 40 presents the blueprint for the revision that this thesis would bring to Winsnes *et al.*'s (1993) geological map:

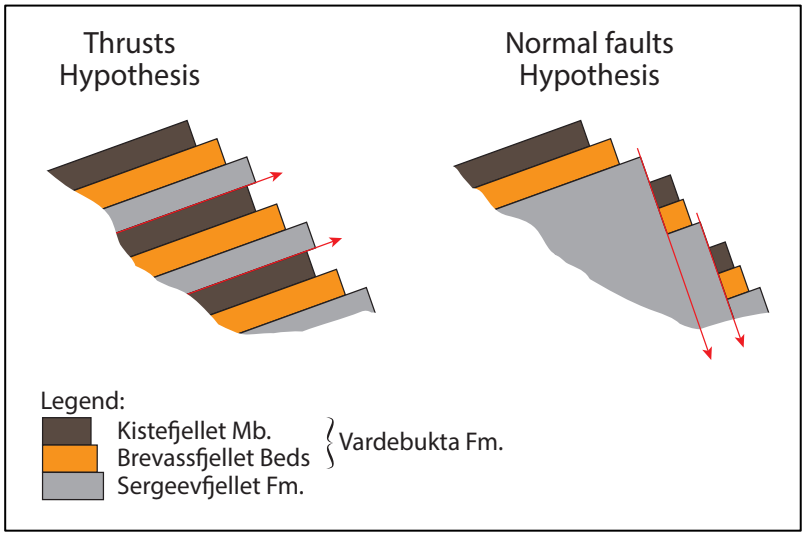

Fig. 39 – Structural scheme, which could explain the repetition of the different geological units on the western slopes of Sergeevfjellet.

1. At the foot of Lidfjellet, where the sedimentary log Lid-13-1 has been measured, the unit underlying the Triassic Brevassfjellet Beds should be moved to the Hornsundneset Fm., and not the Sergeevfjellet Fm. This is due to (i) the reported coarse quartz arenite, which displays more similarities to the one is documented on the lowermost strata of Kovalevskajafjellet, and (ii) no coal seems, or any other low energy marginal fluvial deposits have been reported, down to 35 m below the start of the sedimentary log. It is not known if the rock in the upper part of Lisbetdalen, between Skiferpasset and Lidfjellet, belong to the Hornsundneset Fm. or to the Sergeevfjellet Fm.
2. Nevertheless, on Kovalevskajafjellet, a 3 m thick sequence could belong the Sergeevfjellet Fm. just below the Brevassfjellet Bed.
3. The normal fault mapped on the northern ridge of Sergeevfjellet should be redrawn, such as its apex reaches the surface south of the summit.
4. Further investigation are requested in order to confirm this hypothesis, but preliminary field observation point at the existence of a normal fault on the western slopes/northern ridge of Savičtoppen, which might actually be connected to the normal fault observed on Sergeevfjellet.
5. The triple repetition of the lithological boundary between the Carboniferous Sergeevfjellet Fm. and the Triassic basal conglomerate of the Brevassfjellet beds has been only observed on the western flanks of Sergeevfjellet. This

entails that either (i) two thrusts of limbs of the topmost beds of the Sergeevfjellet Fm., together with the Triassic conglomeratic strata and the part of the overlaying Triassic shales or (ii) two normal faults are present. A double thrust (?*en duplex*?) seems the more probable cause, due to (i) the proximity with other thrusts in the direct neighbouring area, whose geometry seems to be a consequence of the same stress conditions, and (ii) the laminations of the shales parallel to the bedding as well as their rheology, which is prone to develop thrusts and *décollement niveaux*. These suggestions remain highly hypothetical and would need further analyses to be confirmed or rejected.

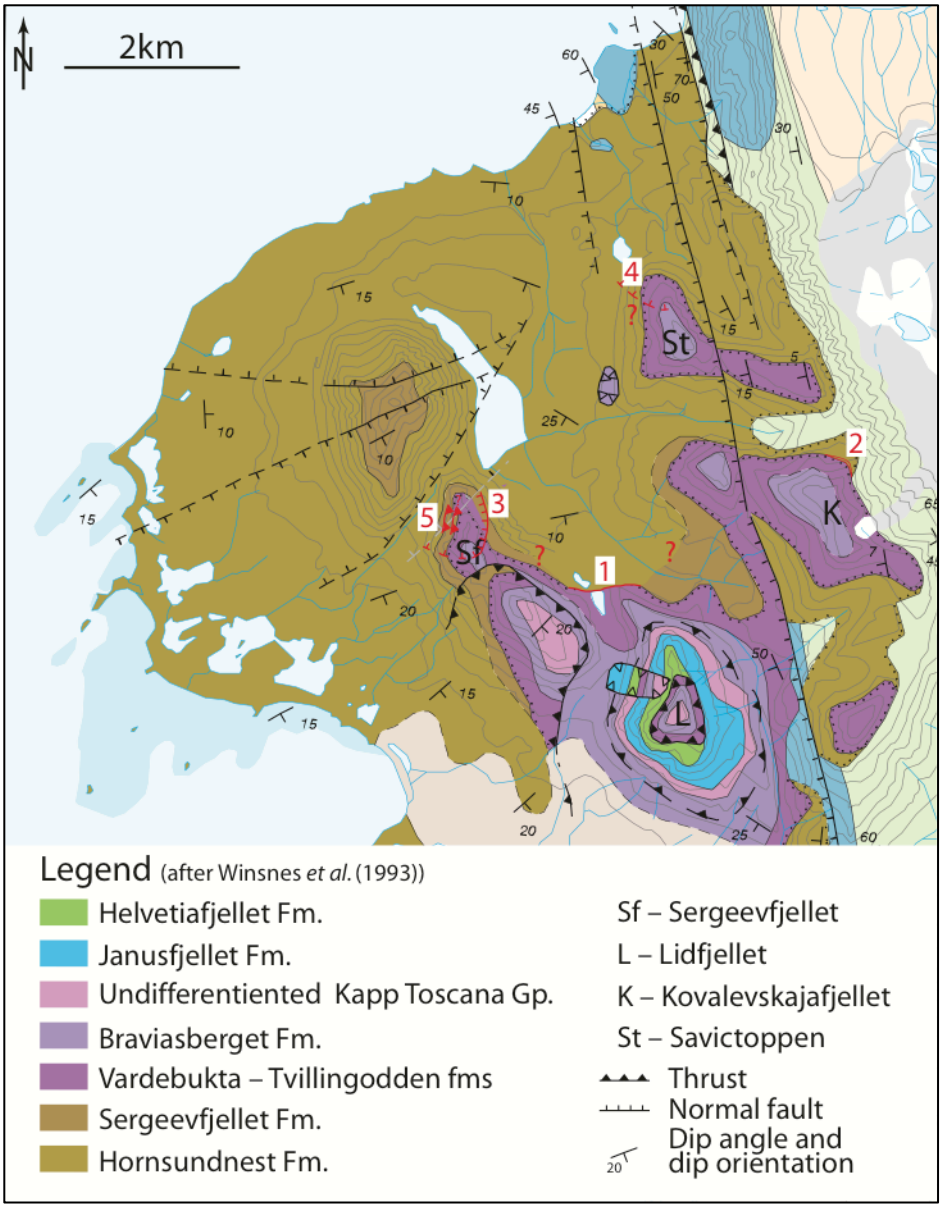

Fig. 40 – Geological map from the Hornsundneset area (Winsnes *et al.* (1993)). The numbers 1 to 5 represent the suggested modifications that the map requires. They refer to the explanations in pages 105-106. Note that these modifications are approximately mapped, and give an idea on where to investigate in further field campaign.

7. Conclusion

The Permian-Triassic Boundary on Svalbard is undefined, as the conodont *Hindeodus parvus* has not been documented on Svalbard. Nevertheless, Vigran *et al.* (2014) suggest the PTB to be located within the *Reduviasporonites chalastus* palynological Assemblage Zone, since the underlying *Uvaesporites imperialis* and the overlying *Proprisporites pococki* Assemblage Zones are respectively defined as Permian and Triassic. They propose a re-location of the base of the Griesbachian within Tozer's (1994) *Otoceras concavum* Zone, at the base of the Greenlandic *Hypophiceras martini* ammonoid Zone (Bjerager's *et al.* 2006), which coincides with the first appearance of *H. parvus* in Greenland. The PTB, as well as the base of the Griesbachian, are therefore located within the first meters of the Vikinghøgda and Vardebukta fms.

The Kapp Starostin Fm. outcropping in central Spitsbergen displays shallower sedimentary features than its correlated, undisturbed and spicule-rich sequence in western Spitsbergen. The latter is marked by the absence of storm-influenced beds, a higher spiculitic content, as well as a lower silt to clay ration. This lateral facies variation at the topmost of the Permian strata suggests the existence of a trough-shaped depositional environment, deeper than the SWBL, in the area known today as western Spitsbergen. The lithological boundary between the hard Kapp Starostin Fm. and the soft Vardebukta Fm., as observed in the two sedimentary sections measured at Festningen, displays no

evidence of any break in sedimentation. The collapse of the silica factories at the transition between these two formations, despite the brutal and obvious change in the landscape geometry, seems to be gradual on a centimetric scale.

Also, in western Spitsbergen, the boundary between the undisturbed Kapp Starostin Fm. and the storm-influenced Vardebukta Fm. is characterized by a shallowing-up sequence, or by the lack of a typical “text-book-like”, deepening-up, transgressive sequence, even though it is interpreted as a major transgressive event correlated throughout the neighbouring arctic areas (Embry 1989, Mørk *et al.* 1989, Weitschat & Dagys 1989, Mørk *et al.* 1993, Dagys & Weitschat 1993, Bjerager *et al*. 2006, Grasby & Beauchamp 2008, Beauchamp *et al.* 2009). In central Spitsbergen, ichnofossils also suggest the same energy increase through the lithological boundary, as well as a shallower depositional environment. The occurrence of a really fast transgression at the base of the Vardebukta/Vikinghøgda fms., followed by regression and its sets of shallower, storm-influenced deposits, could be the reason for the existence of the actual sedimentary sequence.

The boundary between the Kapp Starostin Fm. and the Vikinghøgda Fm. has been crossed on Kongressfjellet and Høgskulefjellet. This contact has not been traversed on Marmierfjellet, despite the fact that both Marm-1 and Kong-1 sedimentary logs do display what is interpreted as the same

Deltadalen-Lusitaniadalen member boundary. The thickness variations of the Deltadalen Mb. between the two sections (100-150 m at Marmierfjellet and 50-60 m at Kongressfjellet) is thought to be partly due to the eventual existence of low angle thrusts or *décollement niveaux* in the Triassic shales, which would lead to the overpacking of Triassic sedimentary sequences.

On the Sørkapp-Hornsund High itself, the Kapp Starostin Fm. is missing, as well as the lowermost part of the Vardebukta Fm., but both have notably been reported from the Treskelen Peninsula and Austjøkultinden (Birkenmajer 1977, 1990, Worsley & Mørk 1978, Dallmann 1992, Winsnes *et al.* 1993, Dallmann *et al.* 1999, Błażejowski 2009, Chwieduk 2009, Hellem & Worsley unpublished). The Triassic basal conglomerate of the Brevassfjellet Beds overlies the Carboniferous Hornsundneset Fm. and Sergeevfjellet Fm. The latter has only been reported from the two sedimentary logs measured on Sergeevfjellet. The non-depositional or erosive nature of this hiatus is a question, which remains unanswered. The Triassic conglomeratic units display lateral variations of their internal sedimentary architecture, and their stacking pattern becomes more complex towards the west. The occurrence of finer and more intricate units towards the west indicates a laterally decreasing energy gradient between Kovalevskajafjellet and Sergeevfjellet, while the more disturbed stacking architecture attests of a relative higher amplitude and a higher frequency of energy variation within the flow.

The fossiliferous Myalina limestone overlies the Brevassfjellet Beds. Bryozoan remains documented in these calcareous beds indicate a Dienerian or Smithian age. The stratigraphical position of these Brevassfjellet Beds and *Myalina* limestones 26m above the base of the Vardebukta Fm. in the neighboured section of Treskelen (Birkenmajer 1977, Worsley & Mørk, 1978, Mørk 1978) suggests these units to be of Dienerian age. If they were of Smithian age, the overlying shales couldn't belong to the Vardebukta Fm., but would belong to the Tvillingodden Fm. This hypothesis would render the defined stratigraphy as well as their demonstrated correlation with the Treskelen Peninsula obsolete, which does not seem highly probable.

Also, this study suggests five potential amendments to the C13G geological map (Winsnes *et al.* 1993): (i) The Hornsundneset Fm. should be extended to the foot of the northern ridge of Lidfjellet and (ii) a limb of the Sergeevfjellet Fm. should be mapped on Kovalevskajafjellet; (iii) a normal fault mapped on the northern ridge of Sergeevfjellet should be relocated on the south side of the summit; (iv) an eventual fault has been observed on the western slopes /northern ridge of Savičtoppen, which could actually be connected to the normal fault on Sergeevfjellet; and (v) two thrusts (or two less probable normal faults) have to be mapped on the western slopes of Sergeevfjellet, in order to explain the triple Carboniferous-Triassic repetition observed at that particular location.

This thesis doesn't pretentiously claim for any outstanding outcomes. However, it does raise interesting questions that definitely require further detailed investigation, especially since biostratigraphical and palynological calibrations are simply lacking in this study. Their scientific contribution would have been non-negligible, as they would have helped accurately placing the different measured section on a high-resolution chronostratigraphical scale. It is suggested to prioritise the investigation and the study of the following research axes: (i) the processing and the analysis of the palynological samples collected during the field season in the summer of 2013. These results would allow the accurate placement of the sedimentary logs on a chronostratigraphical scale and would therefore support or reject the different hypotheses formulated in this thesis. (ii) A large scale and high-resolution study of the lateral architecture of the Vikinghøgda Fm. is required to understand and to explain the lateral thickness variations observed between Marmierfjellet and Kongressfjellet. (iii) The Sørkapp-Hornsund area necessitates tremendous efforts in order to provide an updated and accurate geological map. (iv) Detailed research should also be conducted in order to comprehend the provenance as well as the detail vertical and lateral development of the Hornsundneset and Sergeevfjellet fms., the Brevassfjellet Beds and the *Myalina* limestone.

References

Algeo, T.J., Kuwahara, K., Hiroyoshi, S., Bates S., Lyons, T., Elswick, E., Hinnov, L., Brooks, E., Moser, J., Maynard, J.B., 2011: Spatial variation in sediment fluxes, redox conditions, and productivity in the Permian–Triassic Panthalassic Ocean, *Paleogeography, Paleoclimatology, Paleoecology 308*, 65-83

Balini, M., Lucas, S.G., Jenks, J.F., Speilmann, J.A., 2010: Triassic ammonoid biostratigraphy: an overview, in: *The Triassic Timescale*, Geological Society, London, Special Publications 334, 221-262

Baud, A., Magaritz, M., Holser, W.T., 1989: Permian-Triassic of the Tethys: Carbon isotopes studies, *Gelogische Rundschau 78/2*, 649-677

Bergh, S.G., Braathen, A., Andersen, A., 1997: Interaction of basement-involved and thin-skinned tectonism in the Tertiary fold-thrust belt of central Spitsbergen, Svalbard, *AAPG bulletin 81*, 637-661

Bergh, S.G., Maher, H.D.jr, Braathen, A., 2011: Late Devonian transpressional tectonics in Spitsbergen, Svalbard, and implications for basement uplift of the Sørkapp-Hornsund High, *Journal of the Geological Society 168*, 441-456

Bernard-Griffiths, J., 1993: Age and nature of some protoliths is a Caledonian blueschist-eclogite complex in Spitsbergen: a combined approach from U-Pb, Sm-Nd and REE geochemistries. *Lithos 30*, 81-90

Beauchamp, B. & Baud, A., 2002: Growth and demise of Permian biogenic chert along northwest Pangea: evidence for end-Permian collapse of thermohaline circulation, *Paleogeography, Paleoclimatology, Paleoecology 184*, 37-63

Beauchamp, B., Henderson, C.M., Grasby, S.E., Gates, L.T., Beatty, T.W., Utting, J., James, N.P., 2009: Late Permian sedimentation in the Sverdrup Basin, Canadian Arctic: the Lindström and Black Stripe formations, *Bulletin of Canadian Petroleum Geology 57*, 167-191

Birkenmajer, K., 1977: Triassic sedimentary formations of the Hornsund area, *Studia Geologica Polonica 51*, 7-74

Birkenmajer, K., 1990: Geology of the Hornsund area, Spitsbergen. Explanations to the map 1:75,000 scale, *Uniwersytet Śląski, Katowice*, 3-42

Bjerager, M., Seidler, L., Stemmerik, L., Surlyk, F., 2006: Ammonoid stratigraphy and sedimentary evolution across the Permian-Triassic boundary in East Greenland, *Geological Magazine 143*, 635-656

Błażejowski, B., 2009: Foraminifers from the Treskelodden Formation (Carboniferous-Permian) of south Spitsbergen, *Polish Polar Research 30*, 1993-230

Blinova, M., Faleide, J.I., Gabrielsen, R.H., Mjelde, R., 2013: Analysis of structural trends of sub-sea-floor strata in the Isfjorden area of the West Spitsbergen Fold-and-Thrust Belt based on multichannel seismic data, *Journal of the Geological Society 170*, 657-668.

Blomeier, D., Dustira, A., Forke, H., Scheibner, C., 2011: Environmental change in the Early Permian of NE Svalbard: from a warm-water carbonate platform (Gipshuken Formation) to a temperate, mixed siliciclastic-carbonate ramp (Kapp Starostin Formation), *Facies 57*, 493-523

Blomeier, D., Dustira, A.M., Forke, H., Scheibner, C., 2013: Facies analysis and depositional environments of a storm-dominated, temperate to cold, mixed siliceous–

carbonate ramp: the Permian Kapp Starostin Formation in NE Svalbard, *Norwegian Journal of Geology 93*, 75-93

Boggs, S.Jr., 2006: *Principles of Sedimentology and Stratigraphy*, 4th edition, Prentice Hall

Bond, P.G. & Wignall, P.B., 2010: Pyrite framboid study of marine Permian–Triassic boundary sections: A complex anoxic event and its relationship to contemporaneous mass extinction, *Geological Society of America Bulletin 122*, 1265-1279

Braathen, A., Bergh, S.G., & Maher, H.D., 1999: Application of a critical wedge taper model to the Tertiary transpressional fold-thrust belt on Spitsbergen, Svalbard. *Geological Society of America Bulletin 111,* 1468-1485

Buchan, S.H., Challinor A., Harland W.B., Parker J.R., 1965: The Triassic stratigraphy of Svalbard, *Norsk Polarinstitutt Skrifter 135*

Cao, C.Q., Love, G.D., Hays, L.E., Wang, W., Shen, S., Summons, R.E., 2009: Biogeochemical evidence for euxinic oceans and ecological disturbance presaging the end-Permian mass extinction event, *Earth and Planetary Science Letters 281*, 188-201

Cao, C.Q., Yang, Y.C., Shen, S.Z., Wang, W., Zheng, Q.F., Summons, R.E., 2010: Pattern of $\delta^{13}C_{carb}$ and implications for geological events during the Permian-Triassic transition in South China, *Geological Journal 45*, 186-194

Chwieduk, E., 2009: Early Permian solitary rugose corals from Kruseryggen (Treskelodden Fm., Hornsund area, southern Spitsbergen), *Geologos 15*, 57-75

Clarkson, M.O., Richoz, S., Wood, R.A., Maurer, F., Krystyn, L., McGurty, D.J., Astratti, D., 2013: A new high-resolution $\delta^{13}C$ record for the Early Triassic: Insights from the Arabian Platform, *Gondwana Research 24*, 233-242

Dagys A. & Weitschat W., 1993: Correlation of the Boreal Triassic, *Mitteilungen Geologisch-Paläontologisches Institut Universität Hamburg 75*, 249-256

Dallmann, W.K., 1992: Multiphase tectonic evolution of the Sørkapp-Hornsund mobile zone (Devonian, Carboniferous, Tertiary), Svalbard, *Norsk Geologisk Tidsskrift 72*, 49-66

Dallmann, W.K. (ed.), 1999: *Lithostratigraphic lexicon of Svalbard*, Norsk Polarinstitutt, Tromsø, 17-24

Dallmann, W.K., Gjelberg, J.G., Harland, W.B., Johannessen, E.P., Keilen, H.B., Lønøy, A., Nilsson, I., Worsley, D., 1999: Upper Paleozoic Lithostratigraphy, in: *Lithostratigraphic lexicon of Svalbard*, Norsk Polarinstitutt, Tromsø, 26-126

Dallmann, W.K., Piepjohn, K., Blomeier, D., Elvevold, S., 2009: Geological Map Svalbard 1:100 000 sheet C8G, Billefjorden, revised edition, *Nork Polarinstitutt Temakart 43*

Dashtgard, S.E., Gingras, M.K., Butler, K.E., 2006: Sedimentology and stratigraphy of a transgressive, muddy gravel beach: Waterside Beach, Bay of Fundy, Canada, *Sedimentology 53*, 279-296

Dörr, N., Clift, P.D., Lisker, F., Spiegel, C., 2013: Why is Svalbard an island? Evidence for two-stage uplift, magmatic underplating, and mantle thermal anomalies, *Tectonics 32,* 473-486

Dustira, A.M., Wignall, P.B., Joachimski, M., Blomeier, D., Hartkopf-Fröder, C., Bond, D.P.G., 2013: Gradual onset of anoxia across the Permian-Triassic Bondary in Svalbard, Norway, *Paleogeography, Paleoclimatology, Paleoecology 374*, 303-313

Ehrenberg, S.N., Pickard, N.A.H., Henriksen, L.B., Svånå, T.A., Gutteridge, P., Macdonald, D., 2010: strontium isotope dating of spiculitic Permian strata from

Spitsbergen outcrops and Barents Sea well-cores, *Journal of Petroleum Geology 33*, 247-254

Elvevold, S. (ed.), Dallmann, W.K., Blomeier, D., 2007: *Geology of Svalbard*, Norsk Polarinstitutt, Tromsø, 1-36

Embry A.F., 1989: Correlation of Upper Paleozoic and Mesozoic sequences between Svalbard, Canadian Arctic Archipelago, and northern Alaska, in: *Correlation in Hydrocarbon Exploration*, Norwegian Petroleum Society, Graham and Trotman, 89-98

Engen, Ø., Faleide, J.I., Dyreng, T.K., 2008: Opening of the Fram Strait gateway: A review of plate tectonic constraints, *Tectonophysics 450,* 51-69

Erwin, D.H., 1989: The End-Permian Mass Exctinction: What Really Happened and Did It Matter?, *TREE 4, n°8*, 225-229

Faleide, J.I, Tsikalas, F., Asbjørn, J.B., Mjelde, R., Ritzmann, O., Engen., Ø., Wilson, J., Eldholm, O., 2008: Structure and evolution of the continental margin off Norway and the Barents Sea, *Episodes 31*, 82-91

Finney, S.C., 2010: The reality of GSSPs, *Ciências da Terra 18*, 9-12

Flügel, E., 2004: *Microfacies of carbonate rocks: analysis, interpretation and application*, Springer,

Foster, W.J. & Twitchett, R.J., 2014: Functional diversity of marine ecosystems after the Late Permian mass extinction event, *Nature Geoscience 7*, 233-238

v.Frese, R.R.B., Potts, L.V., Wells, S.B., Leftwich, T.E., Kim, H.R., Kim, J.W., Golynsky, A.V., Hernandez, O., Gaya-Piqué, L.R., 2009: GRACE gravity evidence for an impact basin in Wilkes Land, Antarctica, *Geochemistry, Geophysics, Geosystems 10*,

Friend, P.F., Williams, B.P.J., Ford, M., Williams, E.A., 2000: Kinematics and dynamics of Old Red Sandstone basins, in: *New Perspectives on the Old Red Sandstone*, Geological Society, London, Special Publications 180, 29-60

Gabrielsen, R.H., Færseth, R.B., Jensen, L.N., Kalheim, J.E. & Riis. F., 1990: Structural elements of the Norwegian continental shelf Part 1: The Barents Sea Region. *NPD-Bulletin 6*, 3-33

Gee, D.G., 1991: Caledonian terranes on Svalbard: New evidence of basement in Ny Friesland, Geonytt 18, 24

Gee, D.G., Schouenborg, B., Peucat, J.J., Abakumov, S.A., Krasil'schikov, A.A., Tebenkov, A., 1992: New evidence of basement in the Svalbard Caledonides: Early Proterozoic zircon age from Ny Friesland granites. Norsk Geologisk Tidskrift 72, 81-190

Gee, D.G. Björklund, L., Stølen, L.-K., 1994: Early Proterozoic basement in Ny Friesland-implications for the Caledonian tectonics of Svalbard, Tectonophysics 231, 171-182

Gee, D.G., Johansson, Å., Ohta, Y., Tebenkov, A.M., Krasil'schikov, A.A., Balashov, Y.A., Larionov, A.N., Gannibal, L.F., Ryungenen, G.I., 1995: Grenvillian basement and a major unconformity within the Caledonides of Nordaustlandet, Svalbard, *Precambrian Research 70,* 215-234

Gee, D.G. & Pease, V., 2004: The Neoproterozoic Timanide Orogen of eastern Baltica: introduction, in: *The Neoproterozoic Timanide Orogen of eastern Baltica*, Geological Society, London, Memoirs 30, 1-3.

Gjelberg, J.G. & Steel, R.J., 1981: An outline of Lower-Middle Carboniferous sedimentation on Svalbard: Effects of tectonic, climatic and sea level changes in rift basin sequences, *Canadian Society of Petroleum Geologists Memoir 7*, 543-561

Golonka, J., 2011: Phanerozoic paleoenvironment and paleolithofacies maps of the Arctic region, in: *Arctic Petroleum Geology*, Geological Society, London, Memoirs 35, 79-129

Gorjan, P. & Kaiho, K., 2007: Correlation and comparison of seawater δ34Ssulfate records at the permian-triassic transition, *Chemical Geology 243*, 275-285

Grasby, S.E. & Beauchamp, B., 2008: Interbasin variability of the carbon-isotope record across the Permian-Triassic transition, Sverdrup basin, Arctic Canada, *Chemical Geology 253*, 141-150

Hallam, A. & Wignall P.B., 1997: *Mass Extinctions and Their Aftermath*, Oxford University Press

Hellem, T. & Worsley D., unpublished: *Permian Depositional Environments of Svalbard*

Hounslow, M.W., Peters, C., Mørk, A., Weitschat, W., Vigran, J.O., 2008a: Biomagnetostratigraphy of the Vikinghøgda Formation, Svalbard (Arctic Norway), and the geomagnetic polarity timescale for the Lower Triassic, *Geological Society of America 120*, 1305-1325

Hounslow, M.W., Hu, M., Mørk, A., Weitschat, W., Vigran, J.O., Kaloukovski, V., Orchard, M.J., 2008b: Intercalibration of Boreal and Tethyan time scales: the magnetobiostratigraphy of the Middle Triassic and the latest Early Triassic from Spitsbergen, Arctic Norway, *Polar Research 27*, 469-490

Honuslow, M.B. & Muttoni, G., 2010: The geomagnetic polarity timescale for the Triassic: linkage to stage boundary definitions, in: *The Triassic Timescale*, Geological Society, London, Special Publications 334, 61-102

Ingólfsson, O., 2008: home page, available at: https://notendur.hi.is/oi/svalbard_photos.htm (accessed: 29/01/2014)

Isozaki, Y., 1997: Permo-Triassic Boundary Superanoxia and Stratified Superocean: Records from Lost Deep Sea, *Science 276*, 235-238

Joachimski, M.M., Lai, X., Shen, S., Jiang, H., Luo, G., Chen, B., Chen, J., Sun, Y., 2012: Climate warming in the latest Permian and the Permian–Triassic mass extinction, *Geology 40*, 195-198

Johansson, Å., Gee, D.G., Larionov, A.N., Ohta, Y., Tebenkov, A.M., 2005: Grenvillian and Caledonian evolution of eastern Svalbard – a tale of two orogenies, *Terra Nova 17*, 317-325

Kaiho, K., Oba, M., Fukuda, Y., Ito, K., Ariyoshi, S., Gorjan, P., Riu, Y., Takahashi, S., Chen, Z.-Q., Tong, J., Yamakita, S., 2012: Changes in depth-transect redox conditions spanning the end-Permian mass extinction and their impact on the marine extinction: Evidence from biomarkers and sulfur isotopes, *Global and Planetary Change 94-95*, 20-32

Kart over Svalbard, available at: toposvalbard.npolar.no (accessed: 02/05/2014)

Kamo, S.L., Czamanske, G., Amelin, Y., Fedorenko, V.A., Davis, D.W., Trofimov, V.R., 2003: Rapid eruption of Siberian £ood-volcanic rocks and evidence for coincidence with the Permian-Triassic boundary and mass extinction at 251Ma, *Earth and Planetary Science Letters 214*, 75-91

Khomentovsky, V.V., 2002: Baikalian of Siberia (850-650 Ma), *Russian Geology and Geophysics 43*, 313-333

Kidder, D.L. & Worsley, T.R., 2004: Causes and consequences of extreme Permo-Triassic warming to globally equable climate and relation to the Permo-Triassic extinction and recovery, *Paleogeography, Paleoclimatology, Paleoecology 203*, 207-237

Knies, J. Grasby, S.E., Beauchamp, B., Schubert, C.J., 2013: Water mass denitrification during the latest Permian extinction in the Sverdrup Basin, Arctic Canada, *Geology 41*, 167-170

Köhler-Lopez, M. & Lehmann, U., 1984: The Triassic ammonite *Arisroptychites kolymensis* (Kiparisova) from Botneheia, Spitsbergen, *Polar Research 2*, 61-75

Korčinskaja, M.V., 1986: Biostratigrafija indskogo jarusa Spicbergena, (Induan biostratigraphy of Spitsbergen), in: *Geologija osadočnogo čehla Spicbergena*, (*Geology of the sedimentary cover of Spitsbgeren*), PGO "Sevmorgeologija", 77-93 (in Russian)

Korte, C., Kozur, H.W., Joachimski, M.M., Strauss, H., Veizer, J., Schwark, L., 2004a: Carbon, sulfur, oxygen and strontium isotope records, organic geochemistry and biostratigraphy across the Permian/Triassic boundary in Abadeh, Iran, *International Journal of Earth Science 93*, 565-581

Korte, C., Kozur, H.W., Mohtat-Aghai, P., 2004b: Dzhulfian to lowermost Triassic $\delta^{13}C$ record at the Permian/Triassic boundary, *Hallesches Jahrbuch für Geowissenschaften B Beiheft 18*, 73-78

Korte, C. & Kozur, H.W., 2010: Carbon-isotope stratigraphy across the Permian-Triassic boundary: A review, *Journal of Asian Earth Sciences 39*, 215-235

Krajewski, K.P. & Stempień-Salek, M., 2003: Overthrust Carboniferous strata (Sergeijevfjellet Formation) at Lidfjellet, NW Sørkapp Land, Spitsbergen, *Polish Polar Research 24*, 61-72

Krajewski, K.P., 2008: The Botneheia Formation (Middle Triassic) in Edgeøya and Barentsøya, Svalbard: lithostratigraphy, facies, phosphogenesis, paleoenvironment, *Polish Polar Research 29*, 319-364

Land, L.A. & Paull, C.K., 2000: Submarine karst belt rimming the continental slope in the Straits of Florida, *Geo-Marine Letters 20*, 123-132

Land, L. S., 1970: Phreatic versus vadose meteoric diagenesis of limestones: evidence from a fossil water table. *Sedimentology 14*, 175-185.

Leever, K.A., Gabrielsen, R.H., Faleide, J.I., Braathen, A., 2011: A transpressional origin for the West Spitsbergen fold-and-thrust belt: Insight from analog modelling, *Tectonics 30*, 1-24

Lipiarski, I. & Čmiel, S., 1984: The geological conditions of the occurrence of Carboniferous coal in the northwestern part of Sörkap Land in West Spitsbergen, *Polish Polar Research 5*, 255-266

Lord, G.S., 2013: *Steep Fracture Patterns And Their Characteristics Within The Triassic De Geerdalen Formation On Svalbard, An emphasis on regional trends, local variations and lithological controls*, master thesis, Norwegian Institute of Science and Technology, Department of Geology and Mineral Resources Engineering

Lord, G.S., Solvi, K.H., Klausen, T.G., Mørk, Al., in prep.: Channels on Hopen, Svalbard: Their spatial distribution and paralic setting within the Triassic De Geerdalen Formation, *Norwegian Petroleum Directorate Bulletin*

Lucas, S.G., 2010: The Triassic Chronostratigraphic scale: history and status, in: *The Triassic Timescale*, Geological Society, London, Special Publications 334, 17-39

Maher, H.D., Craddock, H.D., Maher, K.A., 1986: Kinematics of Tertiary structures in Upper Paleozoic and Mesozoic strata on Midterhuken, West Spitsbergen, *Geological Society of America Bulletin 97*, 1411-1421

Major, H., Nagy, J., Haremo, P., Dallmann, W.K., Andresen, A., Salvigsen, O., 1992: Geological Map of Svalbard 1:100 000, sheet C9G, Adventdalen, revised preliminary edition, *Nork Polarinstitutt Temakart 31*

Malkowski, K., 1982: Development and Stratigraphy of the Kapp Starostin Formation (Permian) of Spitsbergen**,** *Palaeontologia Polonica 43*, 69-81

Martin, E.E. & MacDougall, J.D., 1995: Sr and Nd isotopes at the Permian/Triassic boundary: A record of climate change, *Chemical Geology 125*, 73-99

Mørk, A., 1978: Observations on the stratigraphy and structure of the inner Hornsund area, *Norsk Polarinstitutt Årebok 1977*, 61-70

Mørk, A., Knarud, R., Worsley, D., 1982: Depositional and diagenetic environments of the Triassic and Lower Jurassic succession of Svalbard, *Canadian Society od Petroleum Geologists Memoir 8*, 371-398

Mørk, A., Embry, A.F., Weitschat, W., 1989: Triassic transgressive-regressive cycles in the Sverdrup Basin, Svalbard and the Barents Shelf, in: *Correlation in Hydrocarbon Exploration*, Norwegian Petroleum Society, Graham and Trotman, 113-130

Mørk, A., Vigran, J.O., Korchinskaya, M.V., Pcelina, T.M., Fefilova, L.A., Vavilov, M.N., Weitschat, W., 1993: Triassic rocks in Svalbard, the Arctic Soviet islands and the Barents Shelf: bearing on their correlations, in: *Arctic Geology and Petroleum Potential*, NPF Special publication 2, 457-479

Mørk, A., Elvebakk, G., Forsberg, A.W., Hounslow, M.W., Nakrem, H.A., Vigran, J.O., Weitschat, W., 1999a: The type section of the Vikinghggda Formation: a new Lower Triassic unit in central and eastern Svalbard, *Polar Research 18*, 51-82

Mørk, A., Dallmann, W.K., Dypvik, H., Johannessen, E.P., Larsen, G.B., Nagy, J., Nøttvedt, A., Olaussen, S., Pcelina, T.M., Worsley, D., 1999b: Mesozoic Lithostratigraphy, in: *Lithostratigraphic lexicon of Svalbard*, Norsk Polarinstitutt, Tromsø, 127-214

Mørk, A., Lord, G.S., Solvi, K.H., Dallmann, W.K., 2013: Geological Map of Svalbard 1:100 000, sheet G14G Hopen, *Norsk Polarinstitutt Temakart 50*

Morse, J. W., 2003: Formation and diagenesis of carbonate sediments, *Treatise on geochemistry 7*, 67-85

Müller, R.D. & Speilhagen, R.F., 1990: Evolution of the Central Tertiary Basin of Spitsbergen: towards synthesis of sediment and plate tectonic history, *Paleogeography, Paleoclimatology, Paleoecology 80*, 153-172

Mundil, R., Pálfy, J., Renne, P.R., Brack, P., 2010: The Triassic timescale: new constraints and a review of geochronological data, in: *The Triassic Timescale*, Geological Society, London, Special Publications 334, 41-59

Myhre, A.M. & Eldholm, O., 1988: The western Svalbard Margin (74°-80°N). *Marine and Petroleum Geology 5*, 134-156

Nabbefeld, B., Grice, K., Twitchett, R.J., Summons, R.E., Hays, L., Böttcher, M.E., Asif, M., 2010: An integrated biomarker, isotopic and palaeoenvironmental study through the Late Permian event at Lusitaniadalen, Spitsbergen, *Earth and Planetary Science Letters 291*, 84-96

Nakrem, H.A., 1994: Bryozoans fomr the Lower Permian Vøringen Member (Kapp Starostin Formation), Spitsbergen, Svalbard, *Norsk Polarinstitutt 196*

Nakrem, H.A. & Ernst, E., 2008: Arcticoporidae Fam. Nov. (Bryozoa, Trepostomata) from the Lower Triassic of Ellesmere Island (Canada) with Remarks on some other Triassic Bryozoans, in: *14th Internation Bryozoology Association Conference Volume*,

Special Publication Series of the Virginia Museum of Natural History Press, Martinsville, 143-152

Nakrem, H.A & Mørk, A., 1991: New early Triassic Bryozoa (Trepostomata) from Spitsbergen, with some remarks on the Stratigraphy of investigated horizons, *Geological Magazine 128*, 129-140

Nakrem, H.A., Orchard, M.J., Weitschat, W., Hounslow, M.W., Beatty, T.W., Mørk, A., 2008: Triassic conodonts from Svalbard and their Boreal correlations, *Polar Research 27*, 523-539

Newton, R.J., Pevitt, E.L., Wignall, P.B., Bottrell, S.H., 2004: Large shifts in the isotopic composition of seawater sulphate across the Permo–Triassic boundary in northern Italy, *Earth and Planetary Science Letters 218*, 331-345

Nicolaides, S. & Wallace, M. W., 1997: Submarine cementation and subaerial exposure in Oligo-Miocene temperate carbonates, Torquay Basin, Australia, *Journal of Sedimentary Research 67*, 397-410

Ohta, Y., 1994: Caledonian and precambrian history in Svalbard: a review, and an implication of escape tectonics, *Tectonophysics 231*, 183-194

Petrenko, V.M., 1963: Some important finds of Lower Triassic fossils from Spitsbergen, NIIGA, Leningrad, *Sci. Notes 3*, 50-54

Peucat, J.J., Ohta, Y., Gee D.G., Bernard-Griffiths, J., 1989: U-Pb, Sr and Nd evidence for Grenvillian and latest Proterozoic tectonothermal activity in the Spitsbergen Caledonides, Arctic Ocean, *Lithos 22*, 275-285

Piepjohn, K., Brinkmann, L., Grewing, A., Kerp, H., 2000: New data on the age of the uppermost ORS and the lowermost post-ORS strata in Dickson Land (Spitsbergen) and implications for the age of the Svalbardian deformation, in: *New Perspectives on the Old Red Sandstone*, Geological Scociety, London, Special Publications 180, 603-609

Proemse, B.C., Grasby, S.E., Wieser, M.E., Mayer, B., Beauchamp, B., 2013: Molybdenum isotopic evidence for oxic marine conditions during the latest Permian extinction, *Geology 41*, 967-970

Raup, D.M., 1979: Size of the Permo-Triassic Bottleneck and Its Evolutionary Implications, *Science 206,* 217-218

Reading, H. G. & Levell, B. K., 1996: Controls on the sedimentary rock record, in *Sedimentary Environments: Processes, Facies and Stratigraphy*, Oxford, Blackwell Science Ltd, 5-35

Reichow, M.K., Pringle, M.S., Al'Mukhamedov, A.I., Allen, M.B., Andreichev, V.L., Buslov, M.M., Davies, C.E., Fedoseev, G.S., Fitton, J.G., Inger, S., Medvedev, A.Y., Mitchell, C., Puchkov, V.N., Safonava, I.Y., Scott, R.A., Saunders, A.D., 2009: The timing and extent of the eruption of the Siberian Traps large igneous province: Implications for the end-Permian environmental crisis, *Earth and Planetary Science Letters 277*, 9-20

Reid, C.M., James, N.P., Beauchamp, B., Kyser, T.K., 2007: Faunal turnover and changing oceanography: Late Paleozoic warm-to-cool water carbonates, Sverdrup basin, Canadian Arctic Archipelago, *Paleogeography, Paleoclimatology, Paleoecology 249*, 128-159

Renne, P.R., Zichao, Z., Richards, M.A., Black, M.T., Basu, A.R., 1995: Synchrony and Causal Relations between Permian-Triassic Boundary Crises and Siberian Flood Volcanism, *Science 269*, 1413-1416

Riis, F., Lundschien, B.A., Høy ,T., Mørk, A., Mørk, M.B.E., 2008: Evolution of the Triassic shelf in the northern Barents Sea region, *Polar Research 27*, 318-338

Rothman, D.H., Fournier, G.P., French, K.L., Alm, E.J., Boyle, E.A., Cao, C., Summons, R.E., 2014: Methanogenic burst in the end-Permian carbon cycle, *Proceedings of the National Academy of Sciences of the United Statds of America*, early edition, available at: www.pnas.org (accessed: 01/04/2014)

Scheibner, C., Hartkopf-Fröder, C., Blomeier, D., Forke, H., 2012: The Mississippian (Lower Carboniferous) in northeast Spitsbergen (Svalbard) and a re-evaluation of the Billefjorden Group, *Zeitschrift der Deutschen Gesellschaft für Geowissenschaften 163*, 293-308

Schneebeli-Hermann, E., Kürschner, W., Hochuli, P.A., Bucher, H., Ware, D., Goudemand, N., Ghazala, R., 2012: Palynofacies analysis of the Permian–Triassic transition in the Amb section (Salt Range, Pakistan): Implications for the anoxia on the South Tethyan Margin, *Journal of Earth Sciences 60*, 225-234

Schneebeli-Hermann, E., Kürschner, W.M., Hochuli, P.A., Ware, D., Weissert, H., Bernasconi, S.M., Roohi, G., ur-Rehman, K., Goudemand, N., Bucher, H., 2013: Evidence for atmospheric carbon injection during the end-Permian extinction, *Geology 41*, 579-582

Shen, W., Lin, Y., Xu, L., Li, J., Wu, Y., Sun, Y., 2007: Pyrite framboids in the Permian–Triassic boundary section at Meishan, China: Evidence for dysoxic deposition, *Paleogeography, Paleoclimatology, Paleoecology 253*, 323-331

Shen, S.-Z., Cao, C.-Q., Zhang, H., Bowring, S.A., Henderson, C.M., Payne, J.L., Davydov, V.I., Chen, B., Yuan, D.-X.Y., Zhang, Y.-C., Wang, W., Zheng, Q.-F., 2013: High-Resolution $\delta^{13}C_{carb}$ Chemostratigraphy from Latest Guadalupian Through Earliest Triassic in South China and Iran, *Earth and Planetary Science Letters 375*, 156-165

Sepkoski, J.J.J., 1989: Mass exctinctions, Concept of, *Encyclopedia of Biodiversity 4*, 97-110

Sun, Y., Joachimski, M.M., Wignall, P.B., Yan, C., Chen, Y., Jiang, H., Wang, L., Lai, X., 2012: Lethally Hot Temperatures During the Early Triassic Greenhouse, *Science 338*, 366-370

Surić, M., 2005: Submerged karst–dead or alive? Examples from the Eastern Adriatic coast (Croatia), *Geoadria 10*, 5-19

Sysselmannen, 2008: Geology, available at: http://oldweb.sysselmannen.no/hovedEnkel.aspx?m=45298 (accessed: 17/10/2013)

Szuriles, M., 2007: Latest Permian to Middle Triassic cyclo-magnetostratigraphy from the Central European Basin, Germany: Implications for the geomagnetic polarity timescale, *Earth and Planetary Science 261*, 602-619

Takahashi, S., Kaiho, K., Hori, R.S., Gorjan, P., Watanabe, T., Yamakita, S., Aita, Y., Takemura, A., Spörli, K.B., Kakegawa, T., Oba, M., 2013: Sulfur isotope profiles in the pelagic Panthalassic deep sea during the Permian–Triassic transition, *Global and Planetary Change 105*, 68-78

Torsvik, T.H.**,** Van der Voo, R., Meert, J.G., Mosar, J., Walderhaug, H.J., 2001: Reconstructions of the continents around the North Atlantic at about the 60th parallel, *Earth and Planetary Science Letters 187,* 55-69

Tozer, E.T., 1967: A standard for Triassic time, *Geological Survey of Canada Bulletin 156*

Tozer, E.T., 1988: Towards a definition of the Permian-Triassic Boundary, *Episodes 11*, 251-255

Tozer, E.T., 1994: Canadian Triassic ammonoid faunas, *Geological Survey of Canada Bulletin 467*

Twenhofel, W.H., 1945: The Rounding of Sand Grains, *Journal of Sedimentary Petrology 15*, 51-71

Uchman, A., Hanken, N.-M., Nielsen, J.K., Grundvåg, S.-A., Piasecki, S., in prep.: Depositional environment, ichological features and anoxicity of Permian to earliest Triassic marine sediments in central Spitsbergen

Veizer, J., Ala, D., Azmy, K., Bruckschen, P., Buhl, D., Bruhn, F., Carden, G.A.F., Diener, A., Ebneth, S., Godderis, Y., Jasper, T., Korte, C., Pawellek, F., Podlaha, O.G., Strauss, H., 1999: $^{87}Sr/^{86}Sr$, $\delta^{13}C$ and $\delta^{18}O$ evolution of Phanerozoic seawater, *Chemical Geology 161*, 59-88

Vigran, J.O., Mangerud, G., Mørk, A., Worsley, D. and Hochuli, P.A., 2014: Palynology and geology of the Triassic succession of Svalbard and the Barents Sea, *Geological Survey of Norway Special Publication 14*, 1-270

Walker, R.G., 1992. Facies, facies models and modern stratigraphic concepts, in: Facies Models, Response to Sea Level Change, Geological Association of Canada, 1-14

Weather statistic from yr.no, delivered by the Norwegian Meteorological Institute and the NRK, available at: http://www.yr.no/place/Norway/Svalbard/Longyearbyen/statistics.html (accessed: 08/03/2014)

Weitschat, W. & Dagys, A.S., 1989: Triassic biostratigraphy of Svalbard and a comparison with NE-Siberia, *Mitteilungen Geologisch-Paläontologisches Institut Universität Hamburg 68*, 179-213

Wendorff, M., 1985: Geology of the Palffyodden area (NW Sorkappland, Spitsbergen): course and some results of investigations in 1982, *Zeszyty Naukowe UJ, Prace Geograficz ne 63*, 33-55

Wignall, P.B. & Twitchett, R.J., 1996: Oceanic Anoxia and the End Permian Mass Extinction, *Science 272*, 1155-1158

Wignall, P.B., Morante, R., Newton, R., 1998: The Permo-Triassic transition in Spitsbergen: $\delta^{13}C_{org}$ chemostratigraphy, Fe and S geochemistry, facies, fauna and trace fossils, *Geological Magazine 135*, 47-62

Winsnes, T. S., Birkenmajer, K., Dallmann, W.K., Hjelle; A., Salvigsen, O., 1993: Geological map of Svalbard 1:100 000 sheet C13G, *Nork Polarinstitutt Temakart 17*

Worsley, D. & Mørk, A., 1978: The Triassic stratigraphy of southern Spitsbergen, *Norsk Polarinstitutt Årebok 1977*, 43-60

Worsley, D., 2008: Post-Caledonian Svalbard-Barents Sea, *Polar Research 27*, 298-317

Yin, H., Zhang, K., Tong, J., Yang, Z., Wu, S., 2001: The Global Stratotype Section and Point (GSSP) of the Permian-Triassic Boundary, *Episodes 24*, 102-114

Zhang, Y., Zhang, K.-X., Shi, G.R., He, W.-H., Yuan, D.-X., Yue, M.-L. Yang, T.-L., 2014: Restudy of conodont biostratigraphy of the Permian—Triassic boundary section in Zhongzhai, southwestern Guizhou Province, South China, *Journal of Asian Earth Sciences 80*, 75-83

Ziegler, P.A., 1988: Laurussia – The old Red Continent, in: *The Devonian of the World. Volume 1.,* Canadian Society of Petroleum Geologists*,* Memoirs 14, 15-48

Appendix

Appendix 1 – Legend use for the measured sections

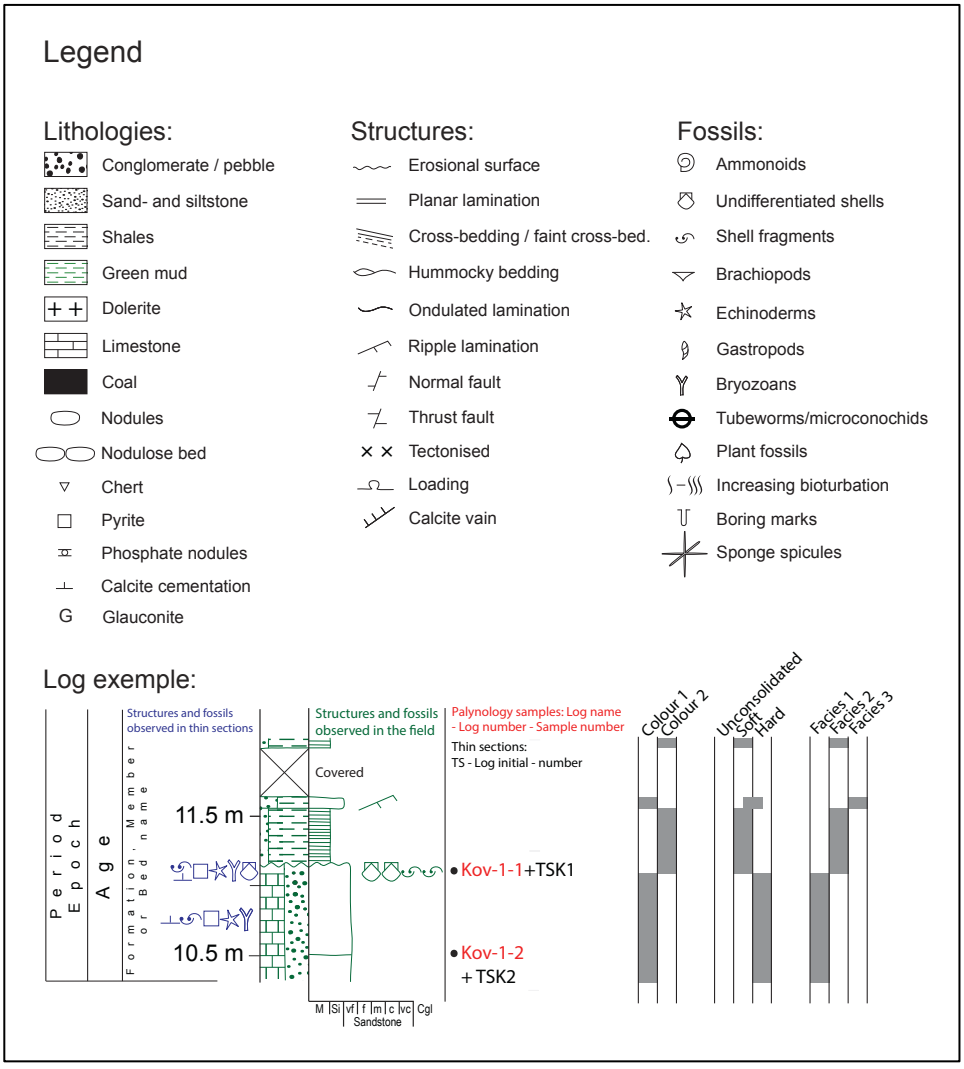

Appendix 2 – Thin sections

Note that the thin sections are listed under their corresponding location, and they are displayed from the youngest to the oldest deposits. Please, refer to their respective enclosed sedimentary log for detailed information about their accurate position in the stratigraphy. If no particular note is provided, microphotographs on the left column have been captured under Transmitted Plane-Polarized Light (TPPL), while the right column show Cross-Polarized Light.

List of Abbreviations

as	Amorphous silica	mi	Micas
acm	Accessory mineral	ph	Phosphate
bi	Bivalve shell fragment	po	Porosity
br	Bryozoan fragment	py	Pyrite
cc	Calcite cement	q1	Mono-crystalline quartz
d?	Dolomite crystal?	q2	Poly-crystalline quartz
ec	Echinoderm	Qmcg	Quartz micro-granules
gl?	Glauconite?	sid?	Siderite
lit	Lithoclast	zi	Zircon
mc	Microconchidae		

Festningen, Kapp Star-1

Plate 1 – TS3: **a-c'**: Microphotographs of spiculitic shales taken at different magnification, displaying both *micro*- and *megaspiculae*. Kapp Starostin Fm., 12.5 m above the start of the sedimentary section.

Plate 2 – TS0: **a-a'**: These two microphotographs expose an unidentified, macroscopic, concentric fossil or ichnofossil(?), surrounded by a chert-rich matrix. Note that the outer rim of the fossil is characterised by boring marks (Hanken personal information, indicated "bor") filled up with matrix. **b-b'**: Fragmented brachiopod shell in a chert-rich matrix. **c-c'**: Gastropod shell, whose voids are partly filled with calcitic cement. Kapp Starostin Fm., 1.25 m above the start of the sedimentary section.

Plate 1 – TS3

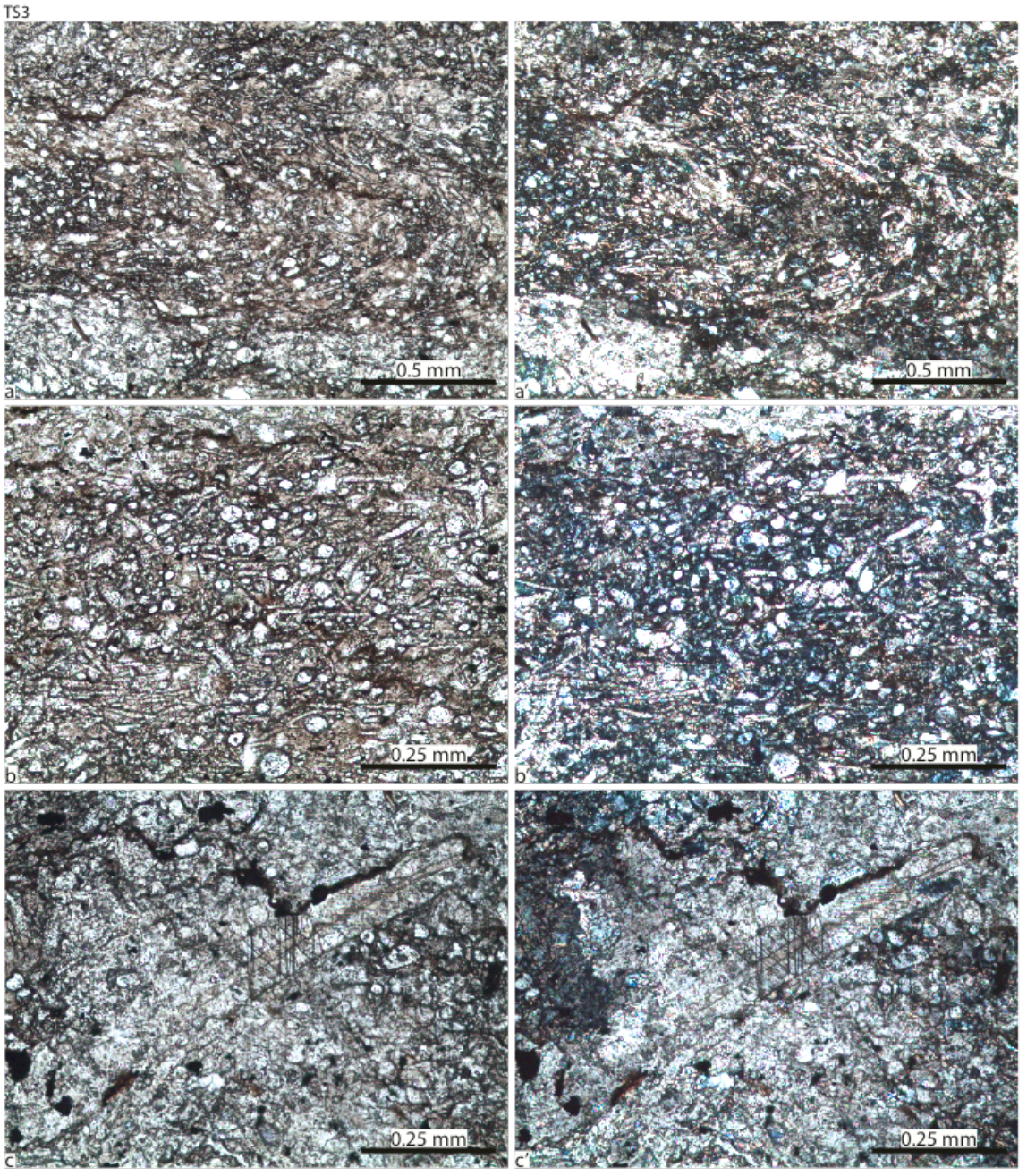

Plate 2 – TS0

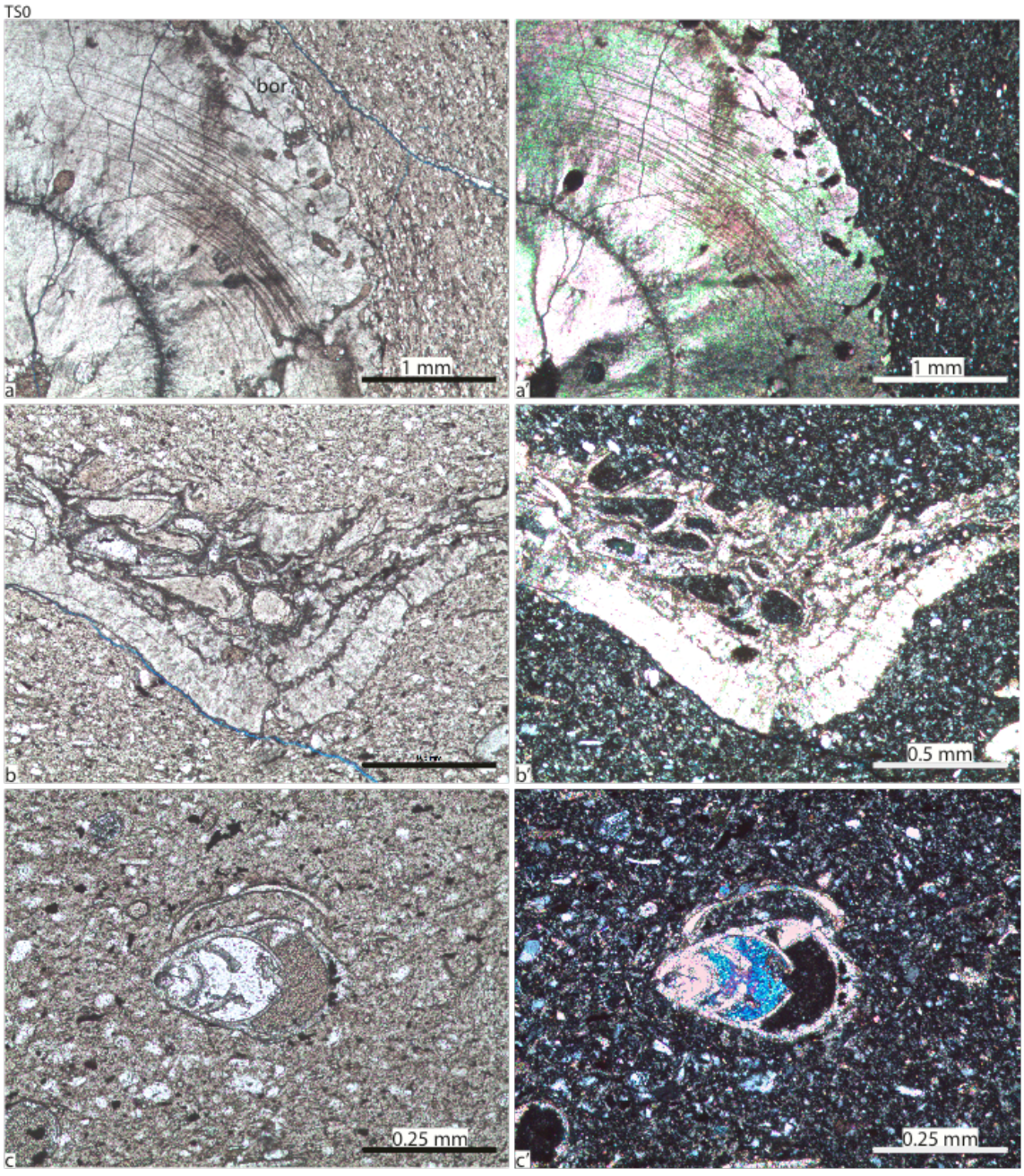

Hornsund, Kovalevskajafjellet, Kov-1

Plate 3 – TSK2: a: Microphotograph presenting an echinoid spine (ec), polychaete-tubes of type microconchidae (mc) and a recrystallized bivalve shell fragment (bi). The calcitic spars occurring as inter-particle cement and as replacive crystals testify to a complex diagenetic history, but indicate the indubitable involvement of fresh water. **b:** Microphotograph taken by Prof. Hans Arne Nakrem, University of Oslo, under TPPL. It displays a transversal section through a microconchidae, whose inner void is filled up with calcite spars. **b-b':** Weathered twinned mono-crystal of calcite as the last remain of an echinoderm. **c-c':** sub-horizontal section through a trepostome bryozoans (br) of the *Arcticopora* genus above a recrystallized bivalve shell fragment. *Myalina* limestone beds, 11.1 m above the start of the sedimentary section.

Plate 4 – TSK2: a-a': Microphotographs displaying two fragments of recrystallized bivalve shell. The calcite spars have first appeared as inter-particle cement, before filling the mold of the dissolved shell fragments. **b-c':** These microphotographs exhibit the recrystallized remain of a shell, which is thought to be of gastropod origin. The geopetal infill of the inner void attests of the vadose environment in which the shell was deposited, before being drown below the water table, as shown by the subsequent pore-filling calcite spars. Finally, the last generation of calcite cement occupies the space created by the dissolution of the shell itself. *Myalina* limestone beds, 11.1 m above the start of the sedimentary section.

Plate 5 – TSK1: a-a': Microphotographs of polychaete-tubes of type microconchidae, occurring together with fragmented and recrystallized bivalve shells (bi) and one echinoderm. Pore-filling, sparitic calcite cement is also visible. **b-c'**: Oblique to longitudinal section through fragments of trepostome bryozoans of the *Arcticopora* genus, surrounded by microconchidae and pore-filling calcitic cement. Note that the calcite spars occur both as inter- and intra-particle cement. *Myalina* limestone beds, 10.5 m above the start of the sedimentary section.

Plate 6 – TSK1: a-b': Microphotographs of another oblique to longitudinal section through a fragment of trepostome bryozoans of the *Arcticopora* genus, occurring together with microconchidae. Pictures b and b' exhibit the same bryozoan fragment, but its higher magnification offers a better close-up of the *autozooechia* being filled up by calcitic cement and phosphate (ph). Diaphragm remains are sometimes visible within the *auto*- and *mesozooechia*. **c-c'**: Twinned mono-crystal of calcite as the last remain of an echinoderm. *Myalina* limestone beds, 10.5 m above the start of the sedimentary section.

Plate 7 – TSK3: a-a': These microphotographs exhibit an example of a polymictic, matrix supported conglomerate, which displays sub-angular to sub-rounded mono- (q1) and poly-crystalline quartz grains (q2), lithoclasts (lit). **b-c':** The micas (mi) occurring within the poly-crystalline quartz present a common orientation upper left corner-lower right corner. This particular orientation of these phyllosilicates is the reminiscence of the metamorphic schistosity of their source rock. Zircons (zi) can also be trapped in a poly-crystalline quartz grains. Brevassfjellet Beds, 9.8 m above the start of the sedimentary section.

Plate 8 – TSK4: a-c': These microphotographs show a fine-grained, well sorted, quartz arenite, with a high opaque minerals content and rare supersized quartz grains. Inter-crystalline porosity is filled up by calcitic cement. The occurrence of a cemented wavy structure in this thin section is surprising, and not completely understood, in the way that it is the only potential sedimentary structure present in the thin section and in the rock sample. A discrete normal grading is observed towards the uppermost 0.5 mm of the thin section. Sergeevfjellet Fm.(?), 2.5 m above the start of the sedimentary section. Eventual spare crystals of dolomite (d?) might also occur.

Plate 9 – TSK0: a-c': Microphotographs of a medium mono- (q1) and poly-crystalline (q2) quartz arenite, with rare accessory bended micas (mi) present between the quartz grains. Note the sub-angularity and the moderately poor sorting of the clasts. Amorphous silica (as) may occupy the inter-crystalline voids. Hornsundneset Fm., 80 cm above the start of the sedimentary section. The porosity is inexistent.

Plate 3 – TSK2

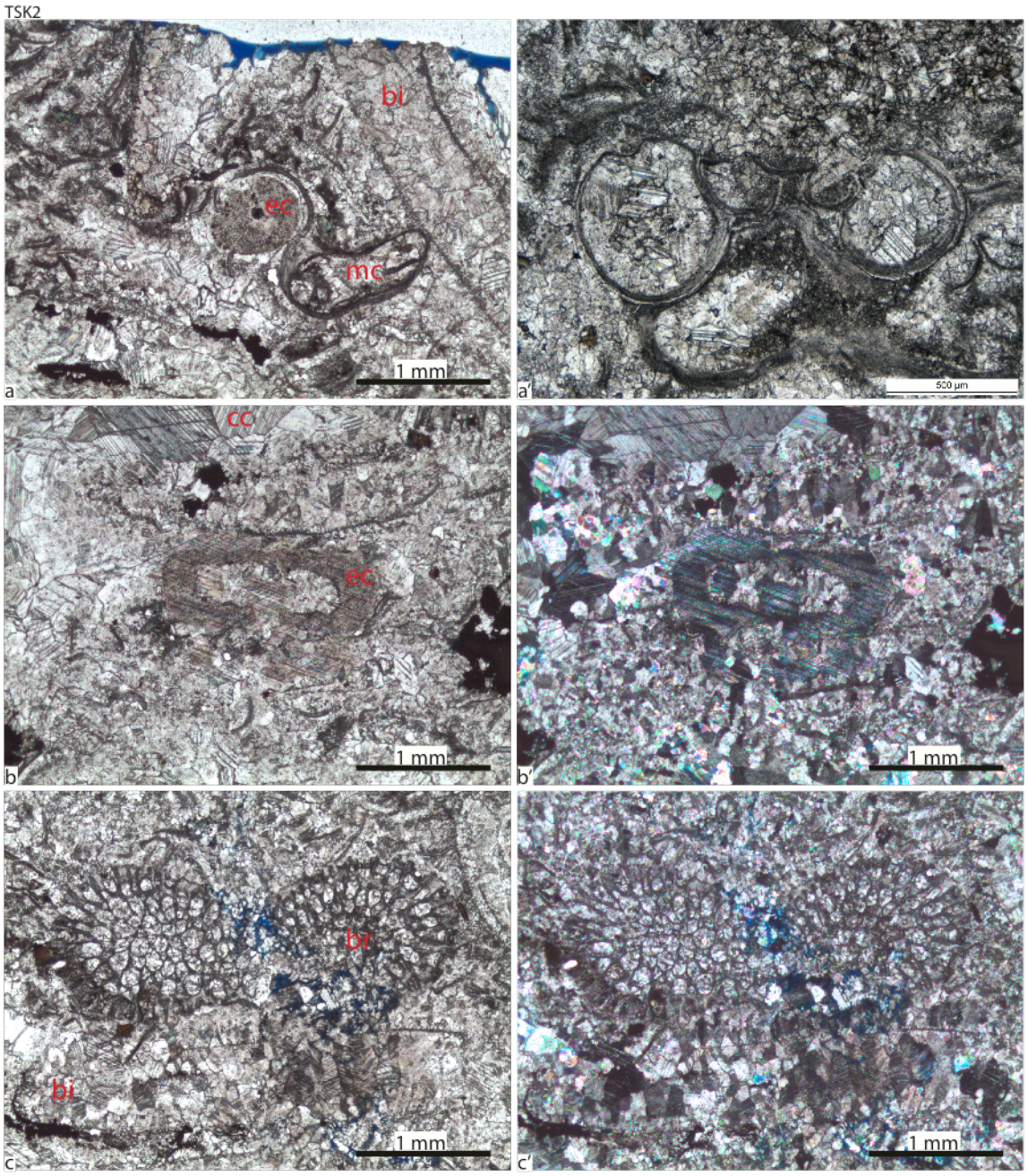

Plate 4 – TSK2

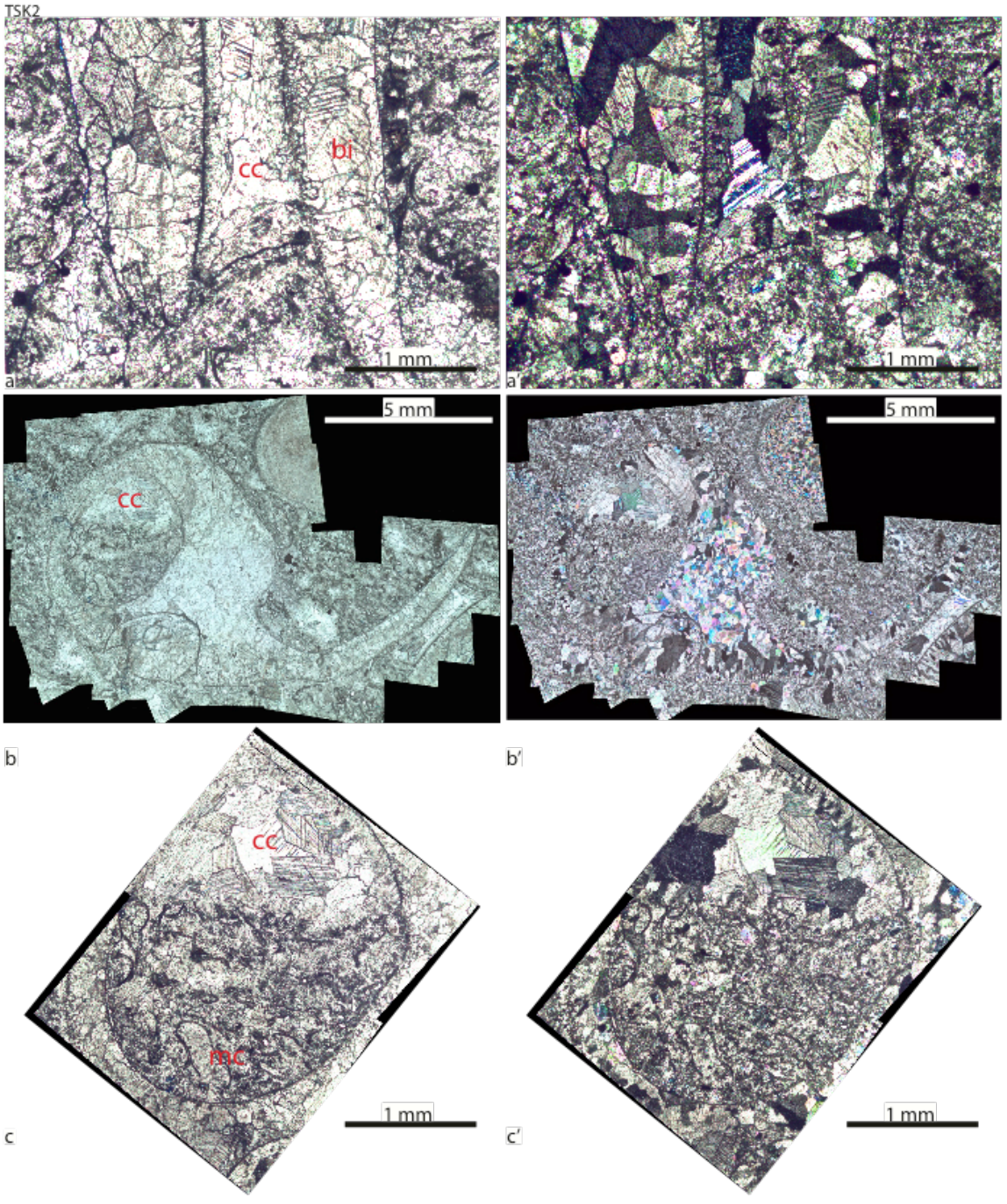

Plate 5 – TSK1

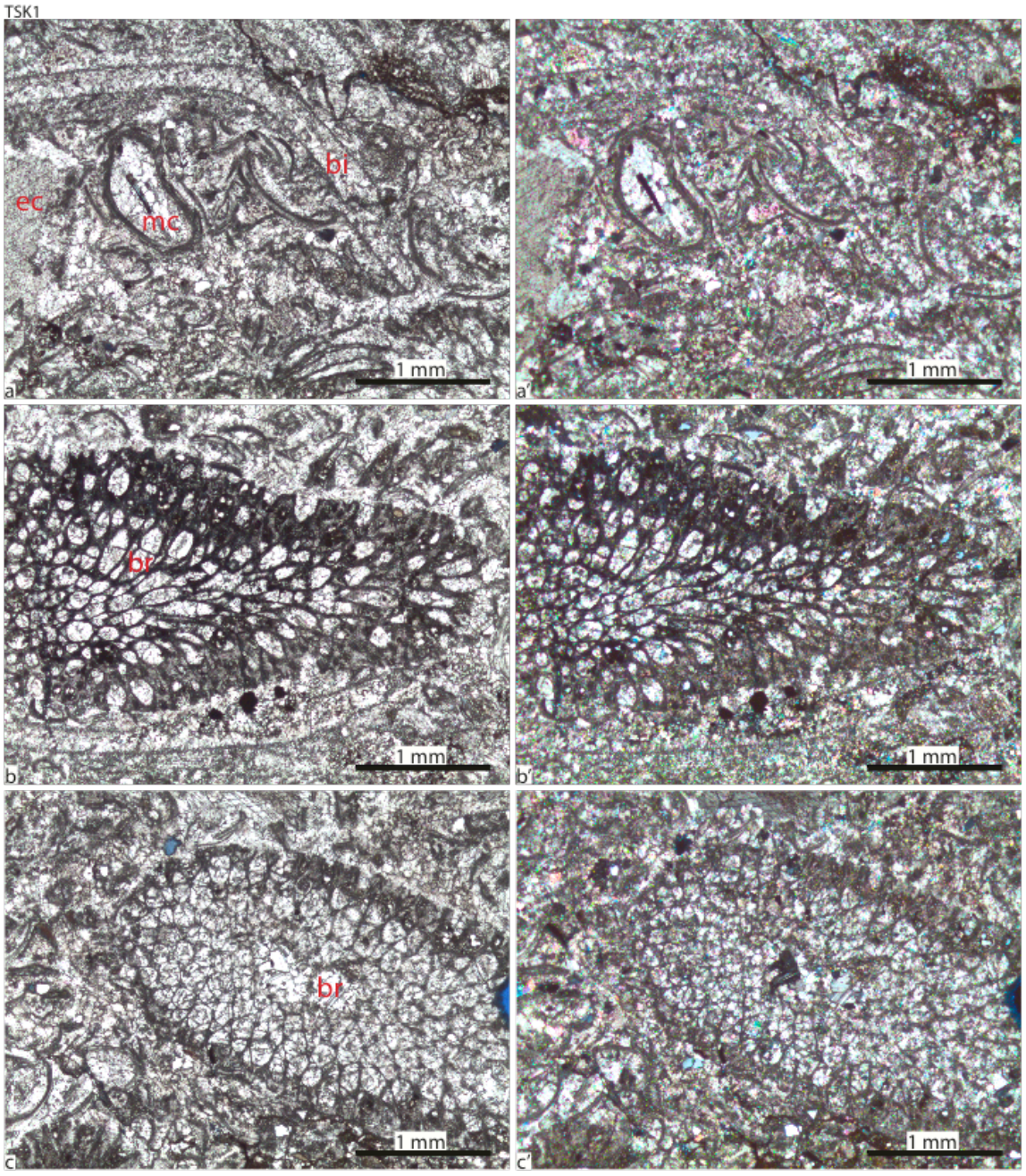

Plate 6 – TSK1

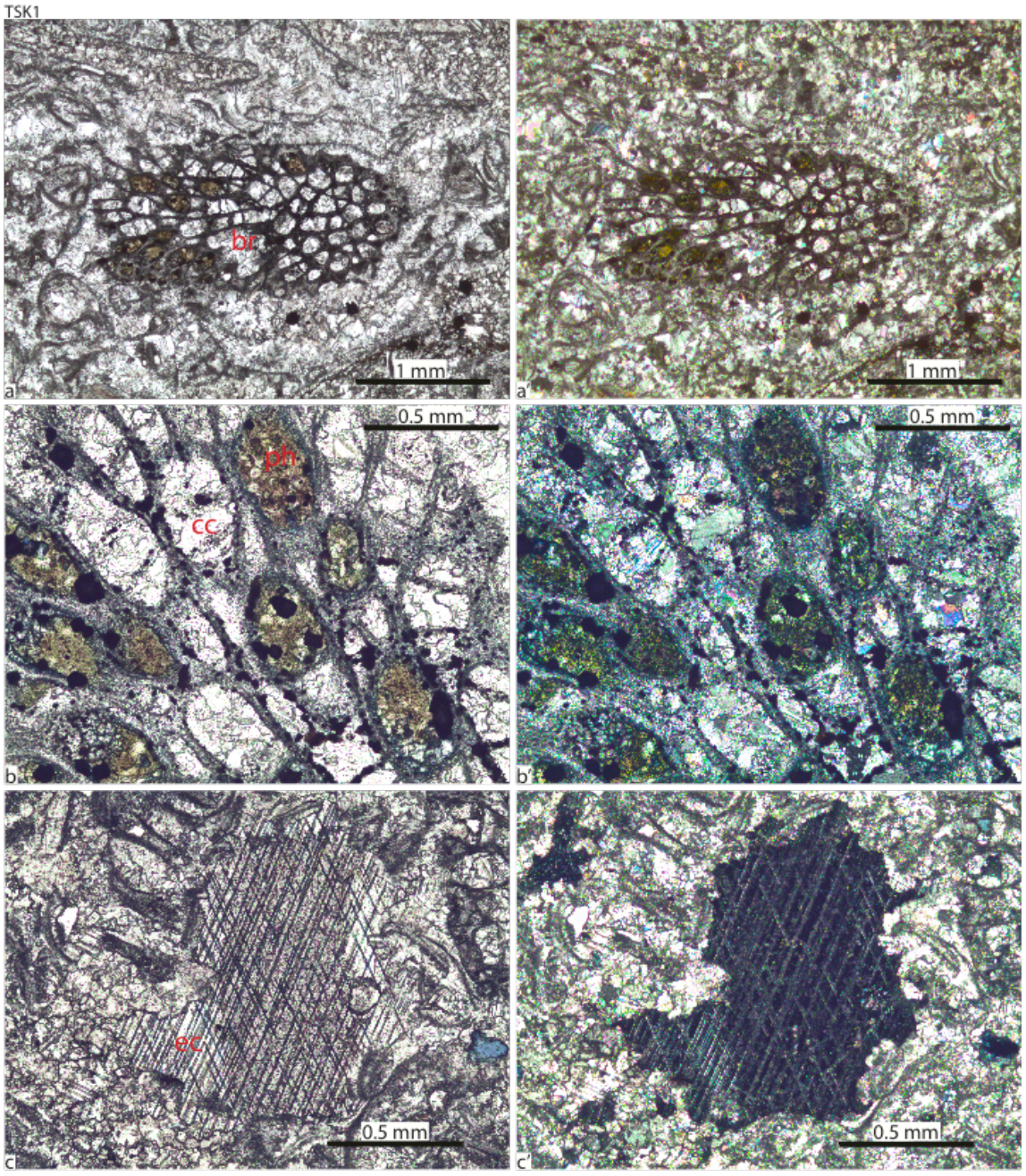

Plate 7 – TSK3

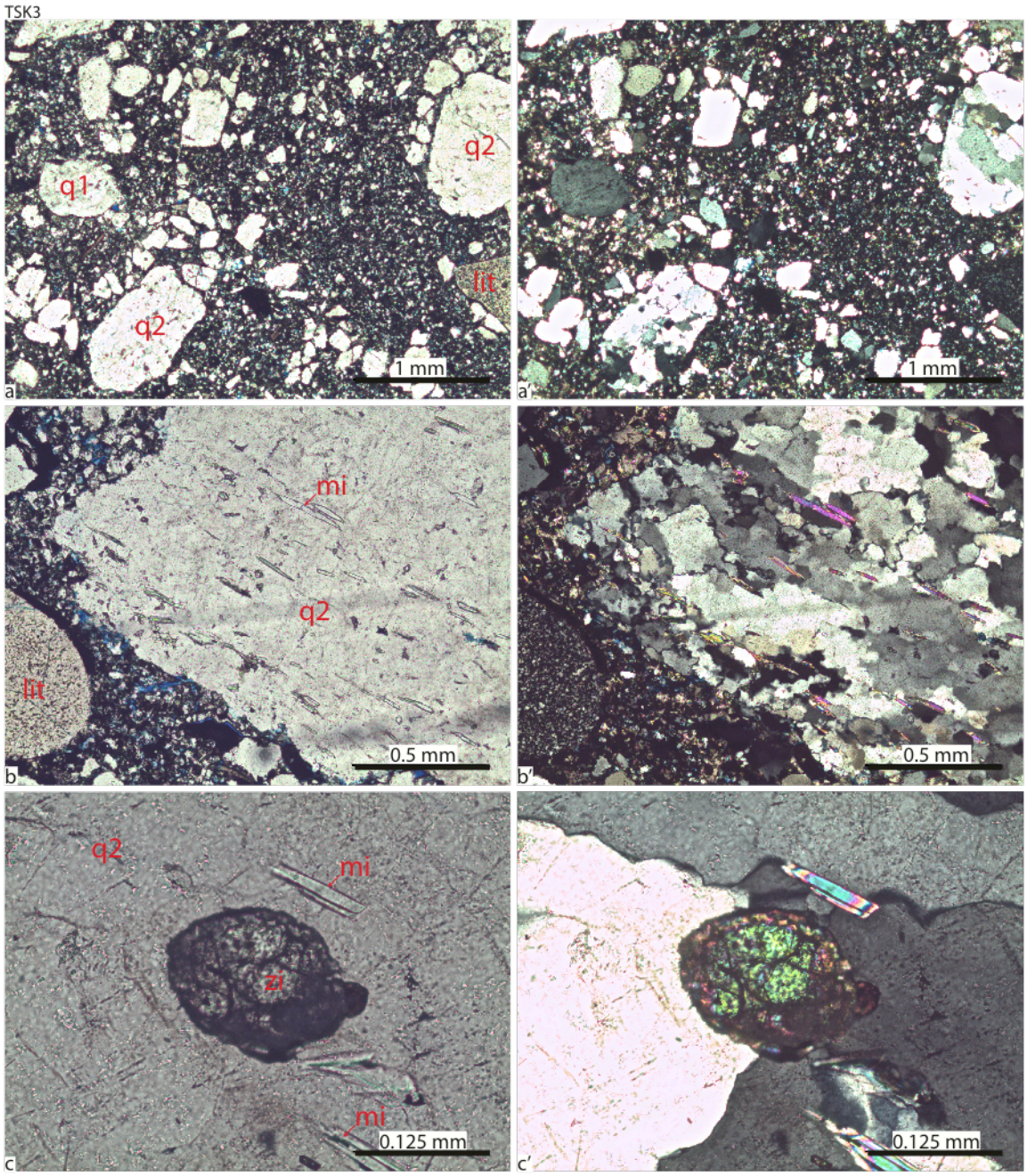
TSK3
q1
q2
lit
q2
1 mm
a
1 mm
a'
mi
q2
lit
0.5 mm
b
0.5 mm
b'
q2
mi
zi
mi
0.125 mm
c
0.125 mm
c'

Plate 8 – TSK4

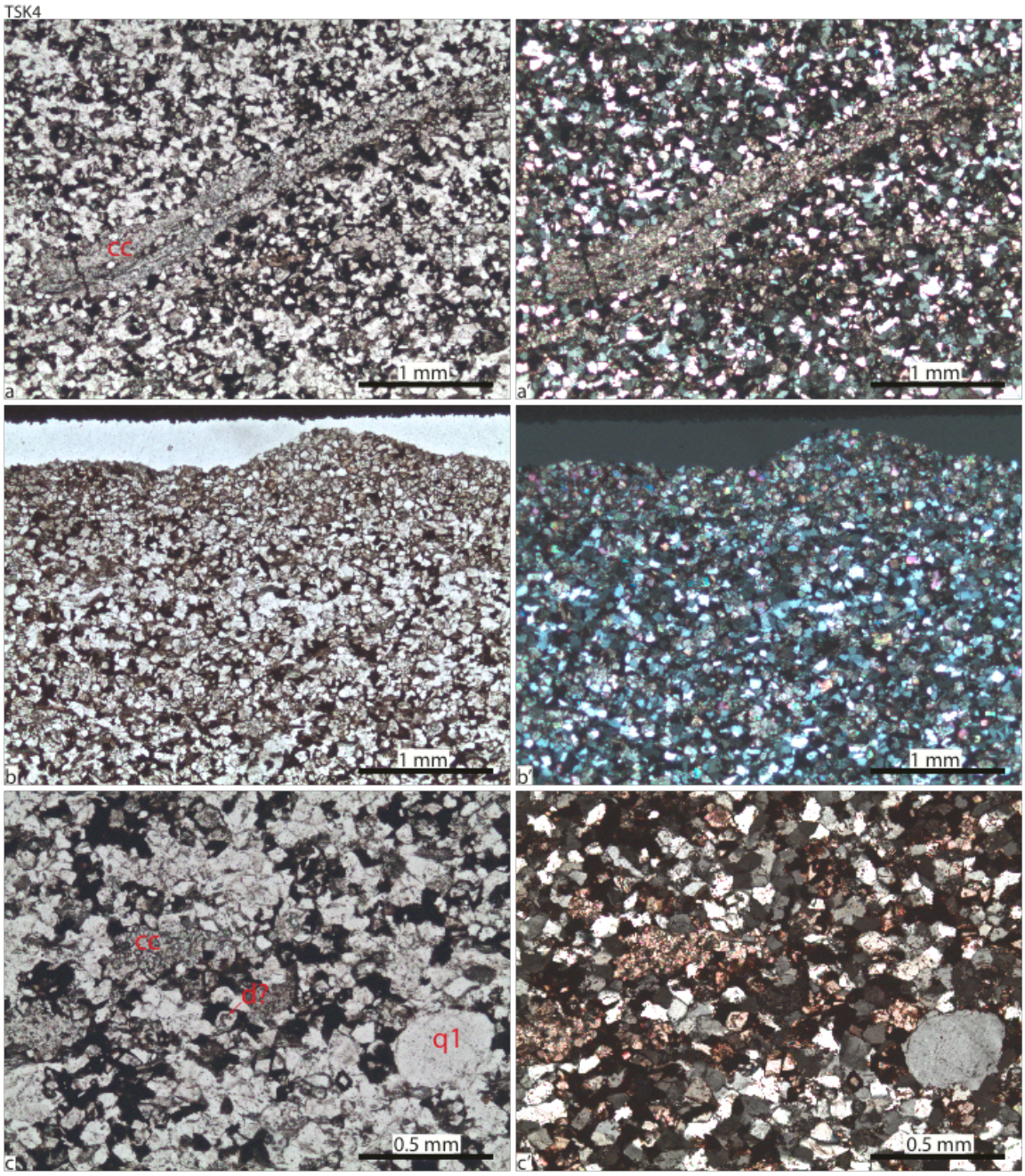

Plate 9 – TSK0

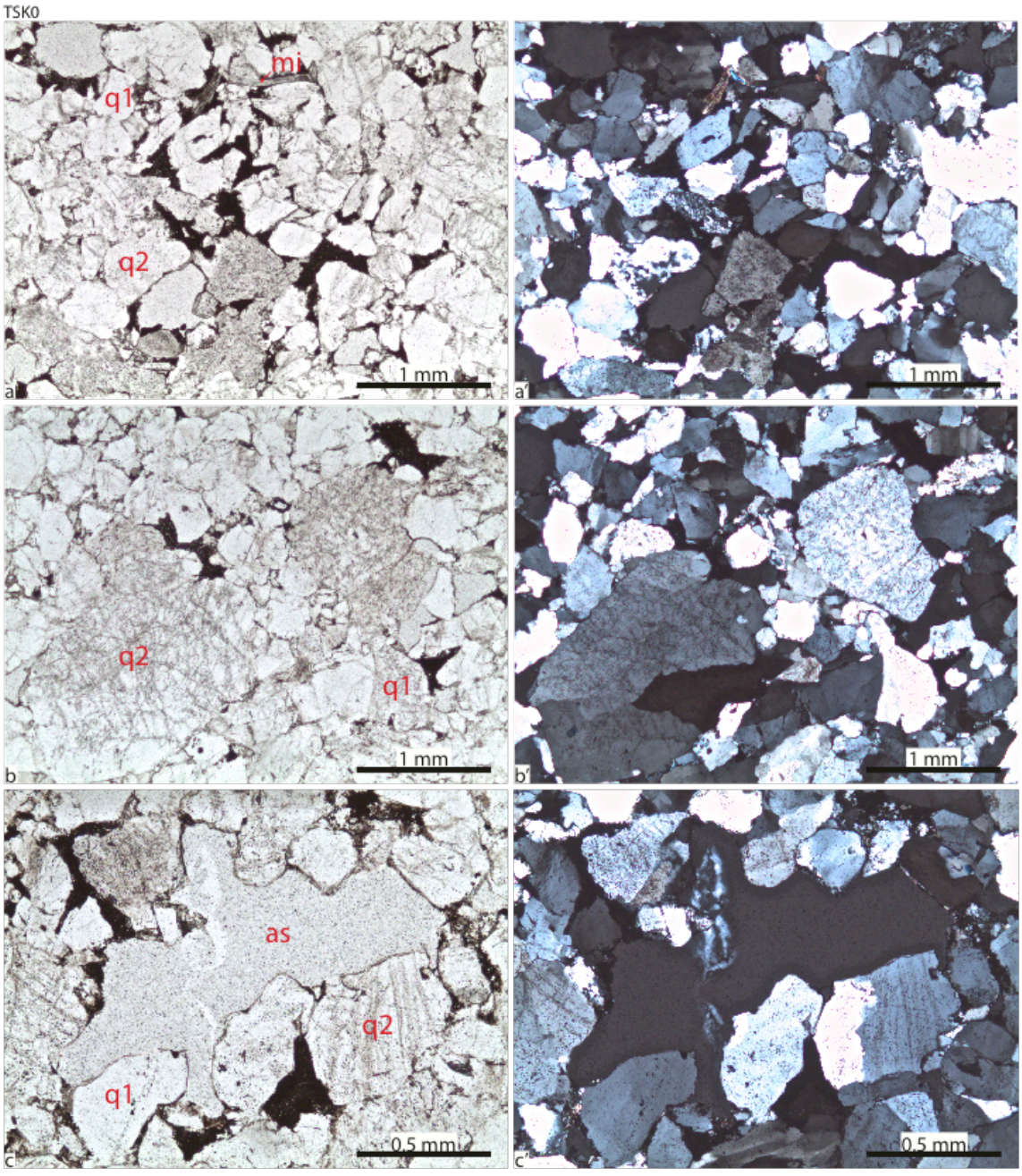

Hornsund, Lidfjellet, Lid-13-1

Plate 10 – Lid-13-1-1: a-c': Microphotographs of a polymictic, grain-supported, quartz-rich conglomerate displaying sub-centimetric, sub-angular, mono-crystalline quartz, centimetric, sub-rounded, poly-crystalline quartz and lithoclasts. Calcitic cement fills the inter-crystalline voids. Brevassfjellet Beds, 13 m above the start of the sedimentary section.

Plate 11 – TSL1: a-c': Medium-grained quartz arenite, relatively similar to TSK0, but with the occurrence of more heavily bended micas, zircons and amorphous silica. Hornsundneset Fm., 6 m above the start of the so-called "missing section".

Plate 12 – TSL0: a-c': Same quartz arenite than TSK0 and TSL1, but with an extremely high number of zircons concentrated at the same level (each red arrow represents a single zircon crystal). Hornsundneset Fm., 11 m above the start of the sedimentary section.

Plate 13 – TSL min 30: a-c': Medium grained quartz arenite similar to TSK0, TSL1 and TSL0. The difference comes from the occurrence of (i) inter-crystalline, pore-filling quartz micro-granules of unknown origin (Qmcg) and (ii) accessory minerals (acm) absent from all the other analysed thin sections. Hornsundneset Fm., 30 m below the start of sedimentary section.

Plate 14 – TSL min 30: a-c': See plate 13. Note the clear boundary between the compact, mono-crystalline quartz zone in the lower half of the thin section, and the upper half, breccia-like, micro-granular quartz-dominated, which might results from unidentified tectonic processes. Hornsundneset Fm., 30 m below the start of sedimentary section.

Plate 10 – Lid-13-1-1

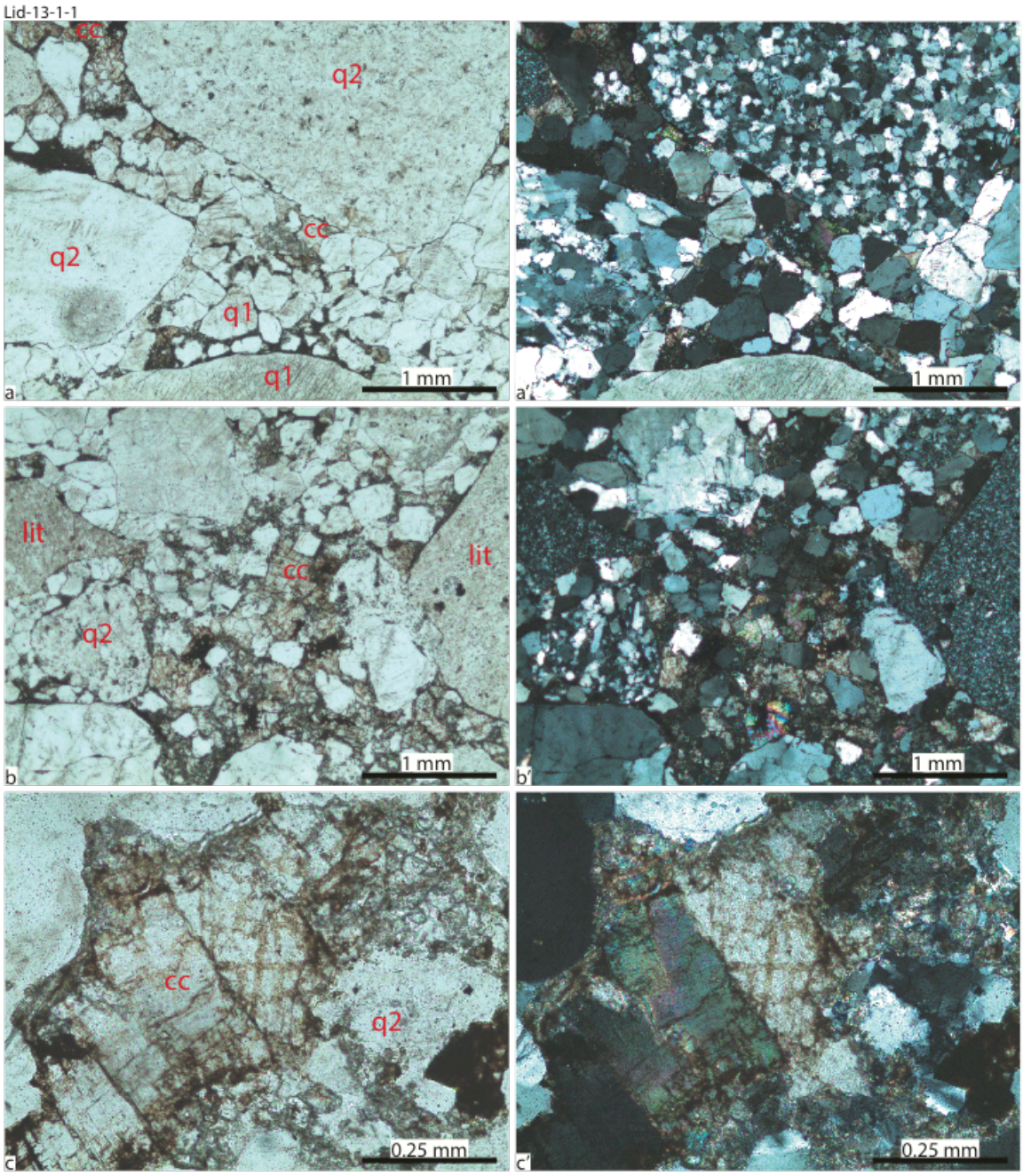

Plate 11 – TSL1

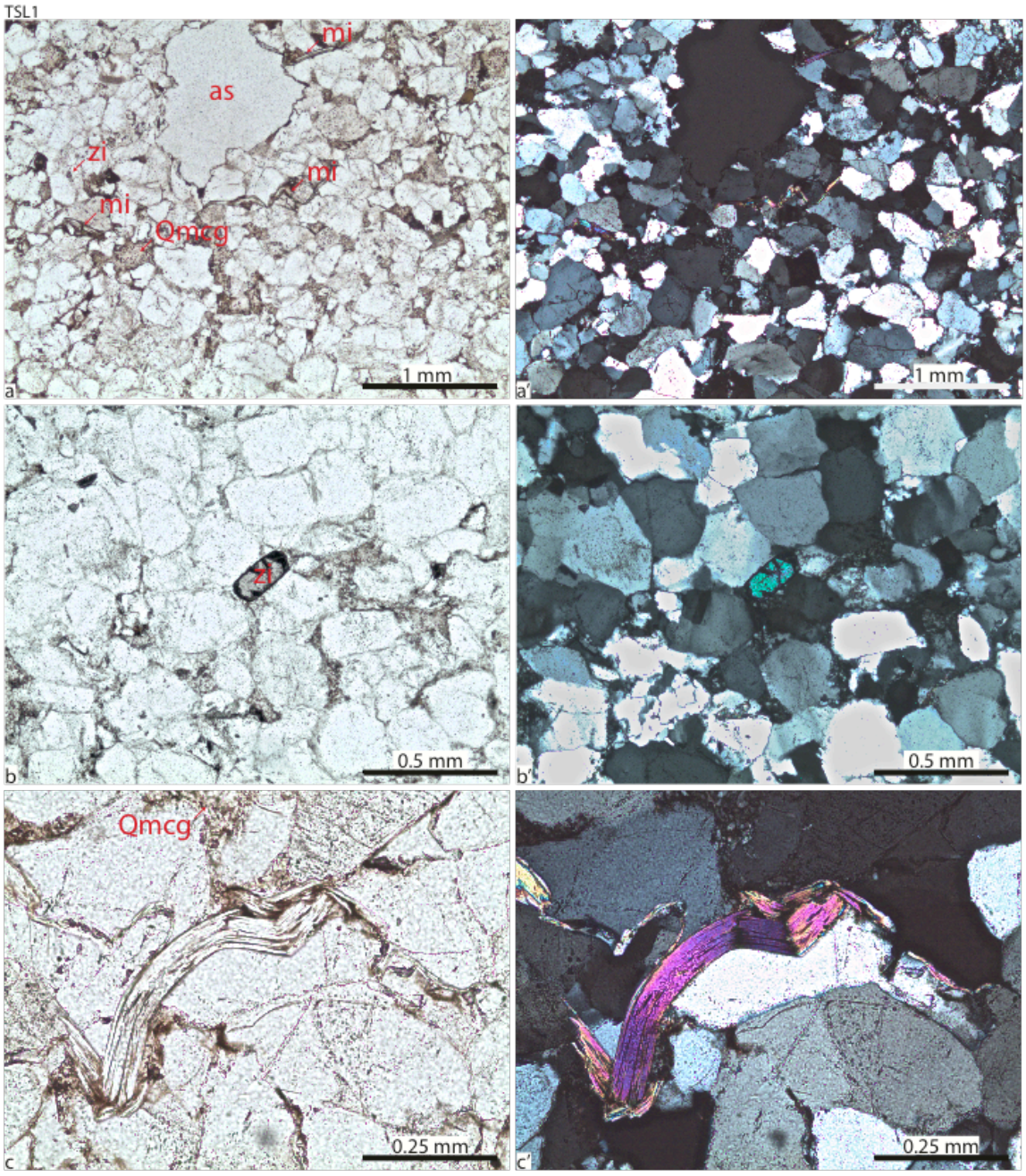

Plate 12 – TSL0

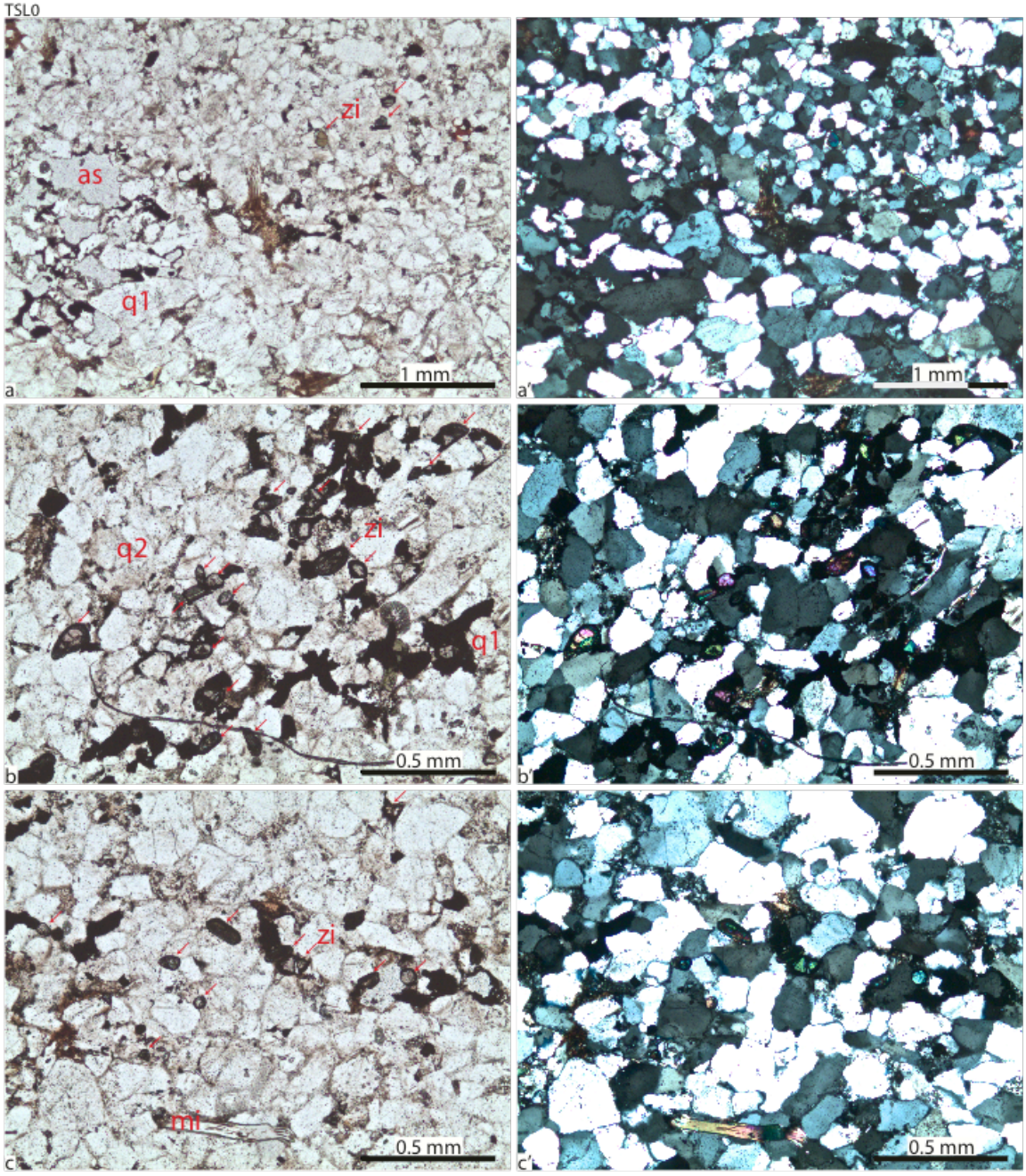

Plate 13 – TSL min 30

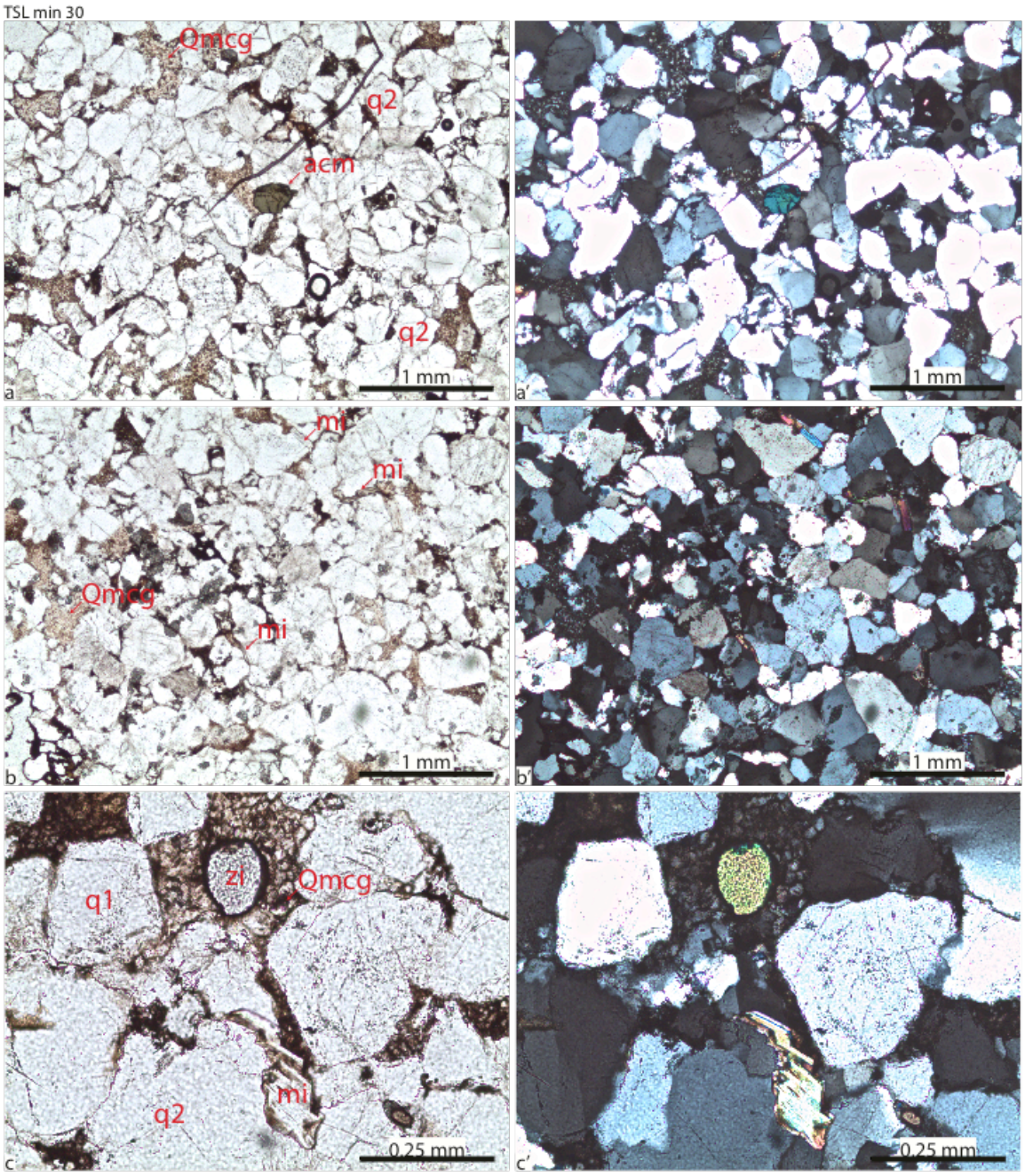

Plate 14 – TSL min 35

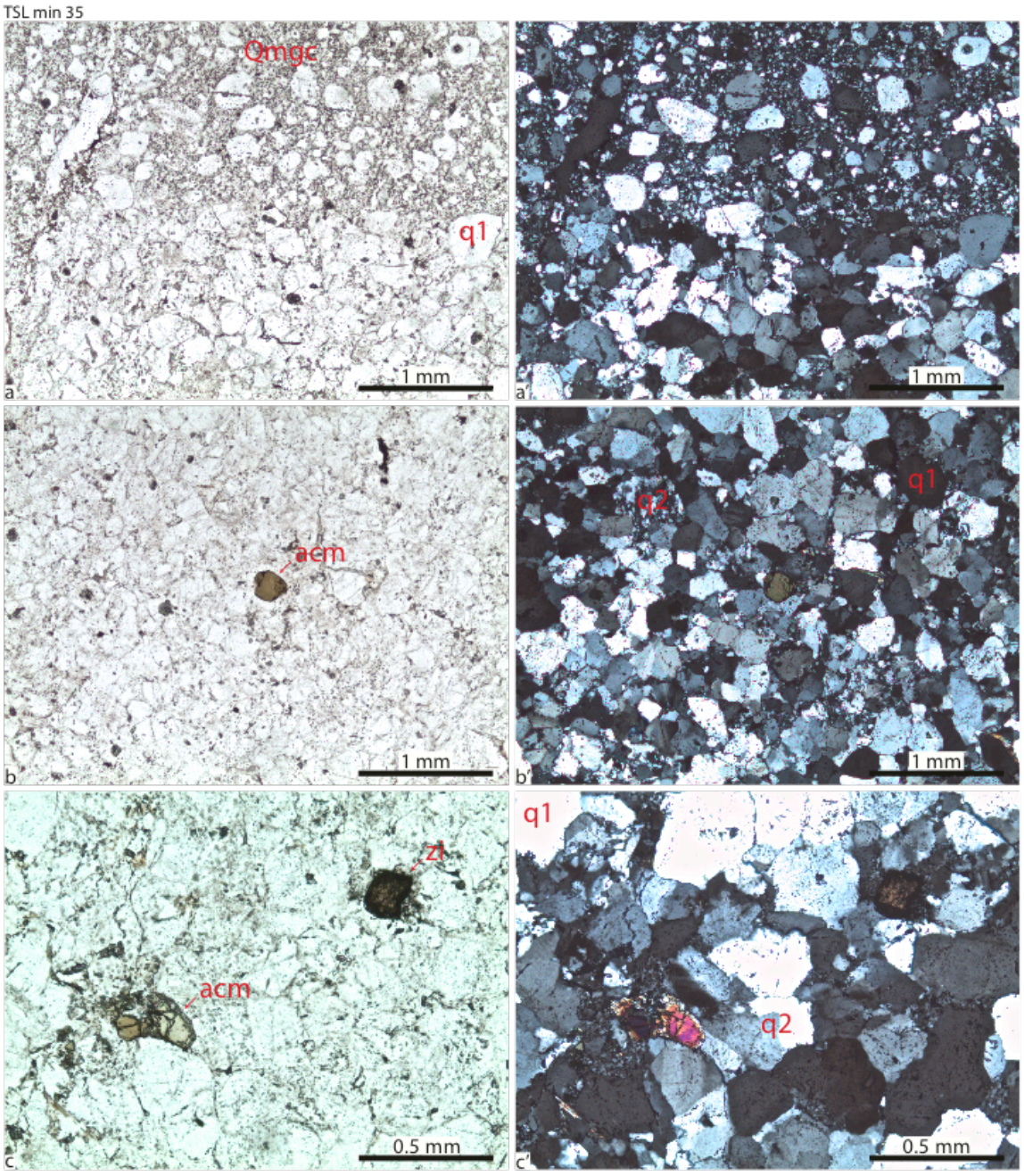

Hornsund, Sergeevfjellet, Serg-2

Plate 15 – TSS2-3: a-c': microphotographs of a polymictic, grain-supported, quartz-rich conglomerate, similar to the one observed in Lid-13-1. Mono- and poly-crystalline quartz grains are present, as well a lithoclasts. Once again, the q2 and the lithoclasts represent the majority of the sub-centimetric grains, while the amount of q1 is high among the sub-millimetric clasts. Zircons and bended micas commonly occur. The inter-crystalline space is filled up by micritic material, potentially sideritic. Brevassfjellet Beds, 15 m above the start of the sedimentary section.

Plate 16 – TSS2-2: a-c': Microphotographs of a gravely sandstone or a sandy conglomerate. Gravels tend to be sub-rounded, while sand-sized clasts are more sub-angular. Glauconite (gl) potentially occurs as accessory minerals. Micritic calcite cement fills the tight void present between the clasts, but also gravel-sized voids. Brevassfjellet Beds, 13.3 m above the start of the sedimentary section.

Plate 17 – TSS2-1: a-b': Microphotographs of a polymictic, grain-supported, quartz-rich conglomerate. Sub-angular mono- and poly-crystalline quartz grains occur together with sub-centimetric lithoclasts. The inter-granular voids is filled with calcitic cements, whose crystals don't reach the critical sparitic dimensions. However, these cement crystals are bigger than the micritic calcite crystals observed in TSS2-2. **c-c':** isopachous cemented crust on the outer rim of the rock. Brevassfjellet Beds, 8.5 m above the start of the sedimentary section.

Plate 18 – TSS2-0: a-c': Heavily folded micas-rich, fine-grained quartz arenite. Micas display two different orientations between the lowest half of the thin section (a-b') and its upper half (c-c'). The phyllosilicate content aside, this thin section shows some similarities with TSK4 on Kovalevskajafjellet. Sergeevfjellet Fm., 1 m above start of the sedimentary section.

Plate 15 – TSS2-3

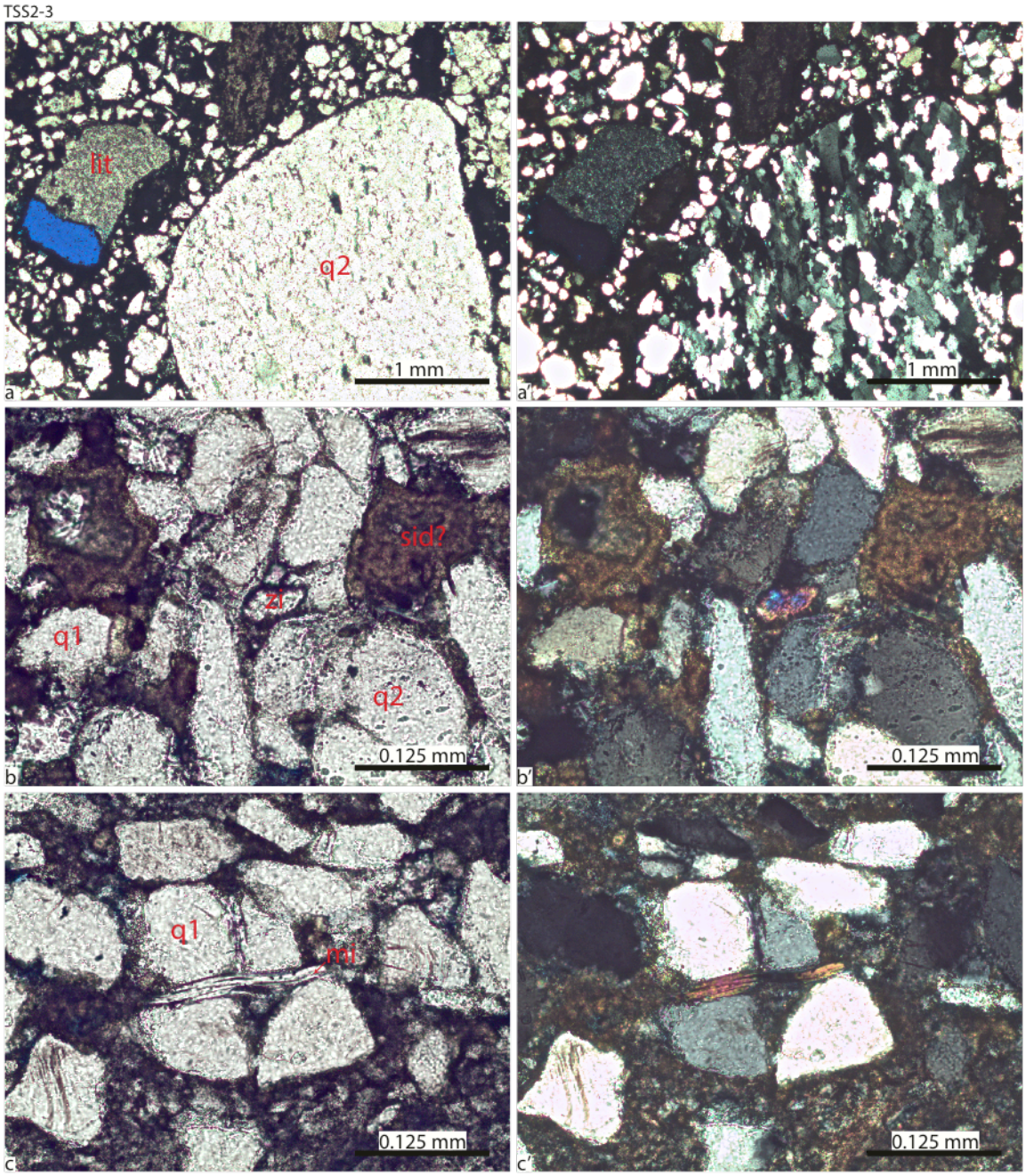

Plate 16 – TSS2-2

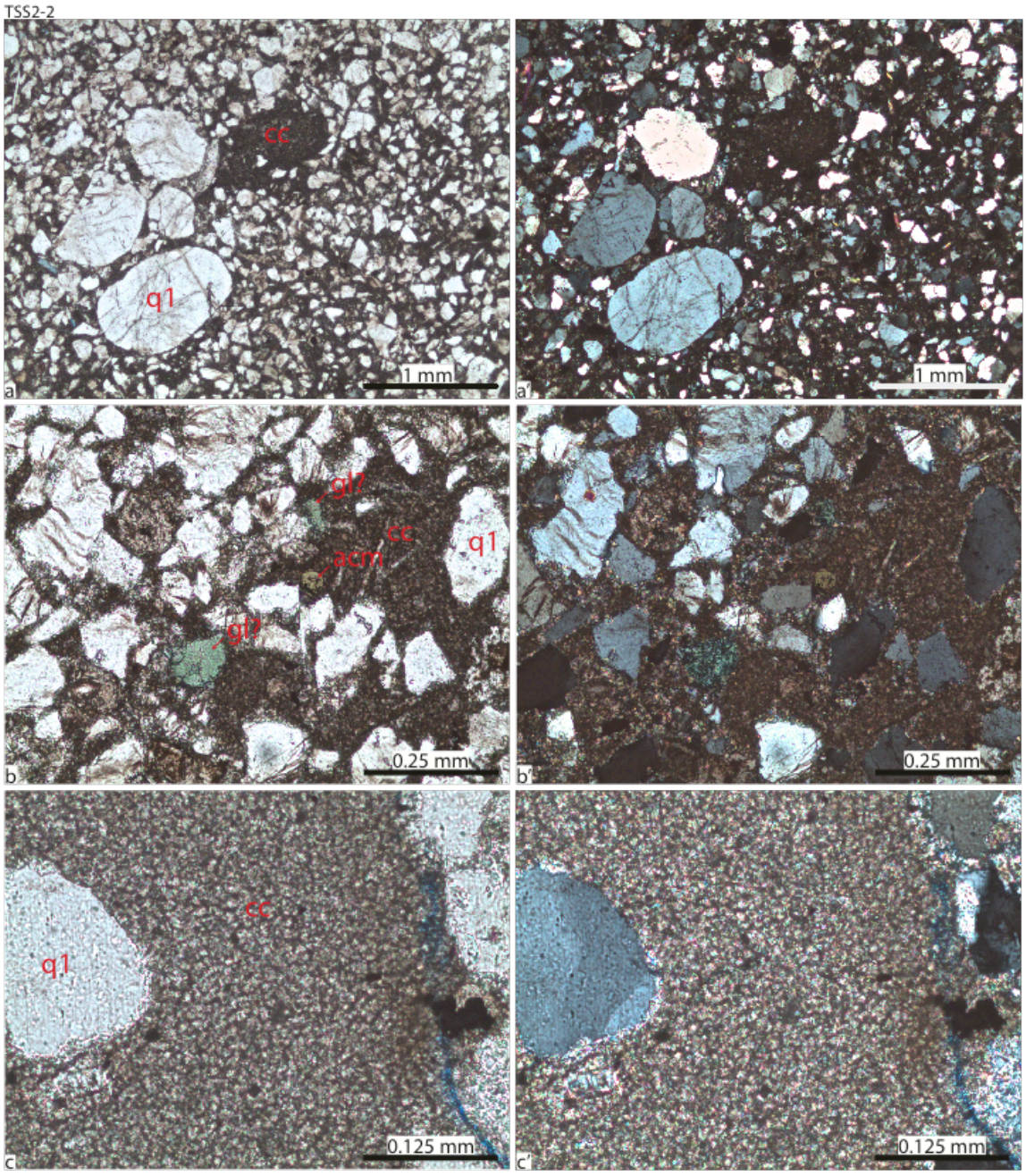

Plate 17 – TSS2-1

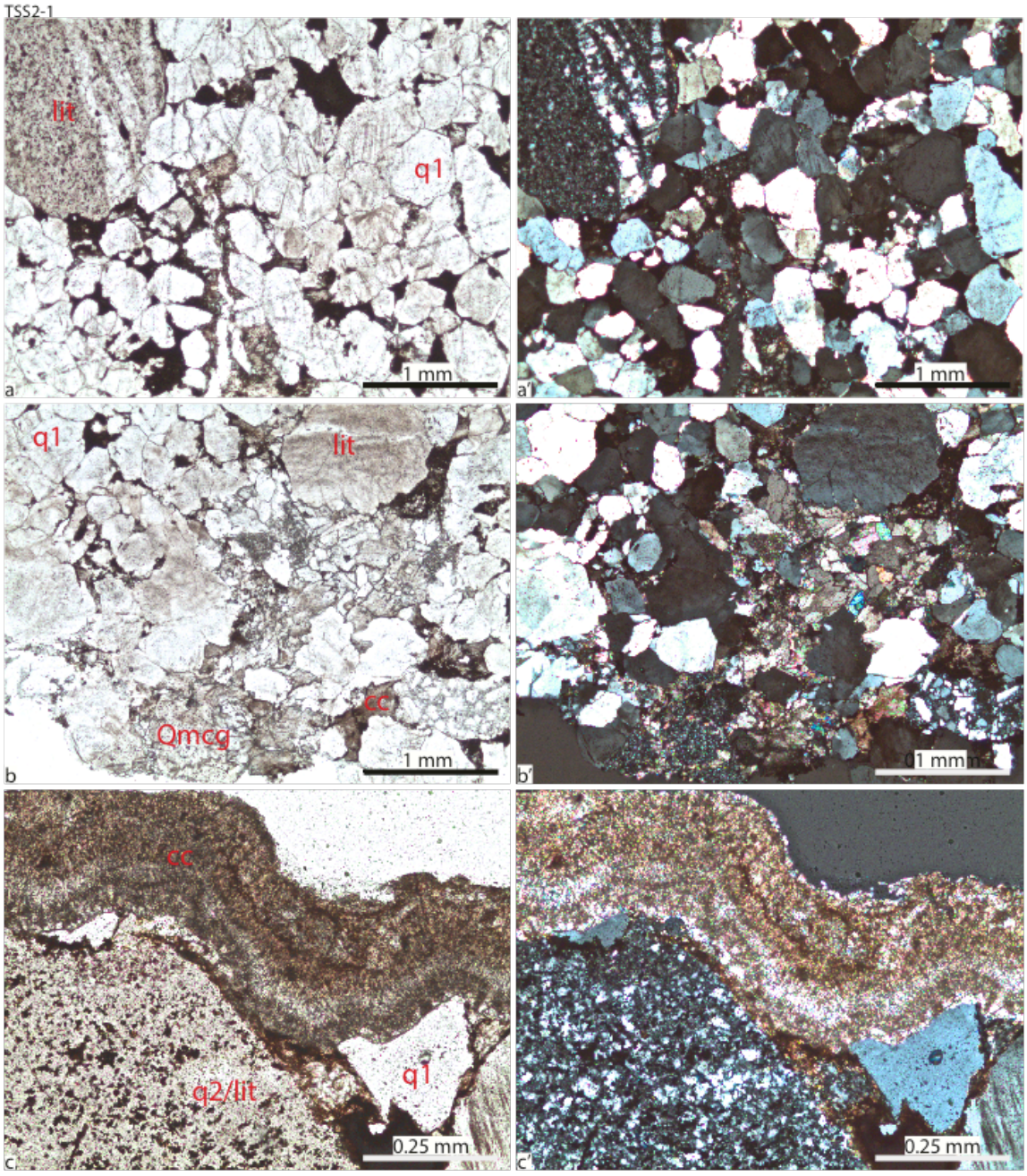

Plate 18 – TSS2-0

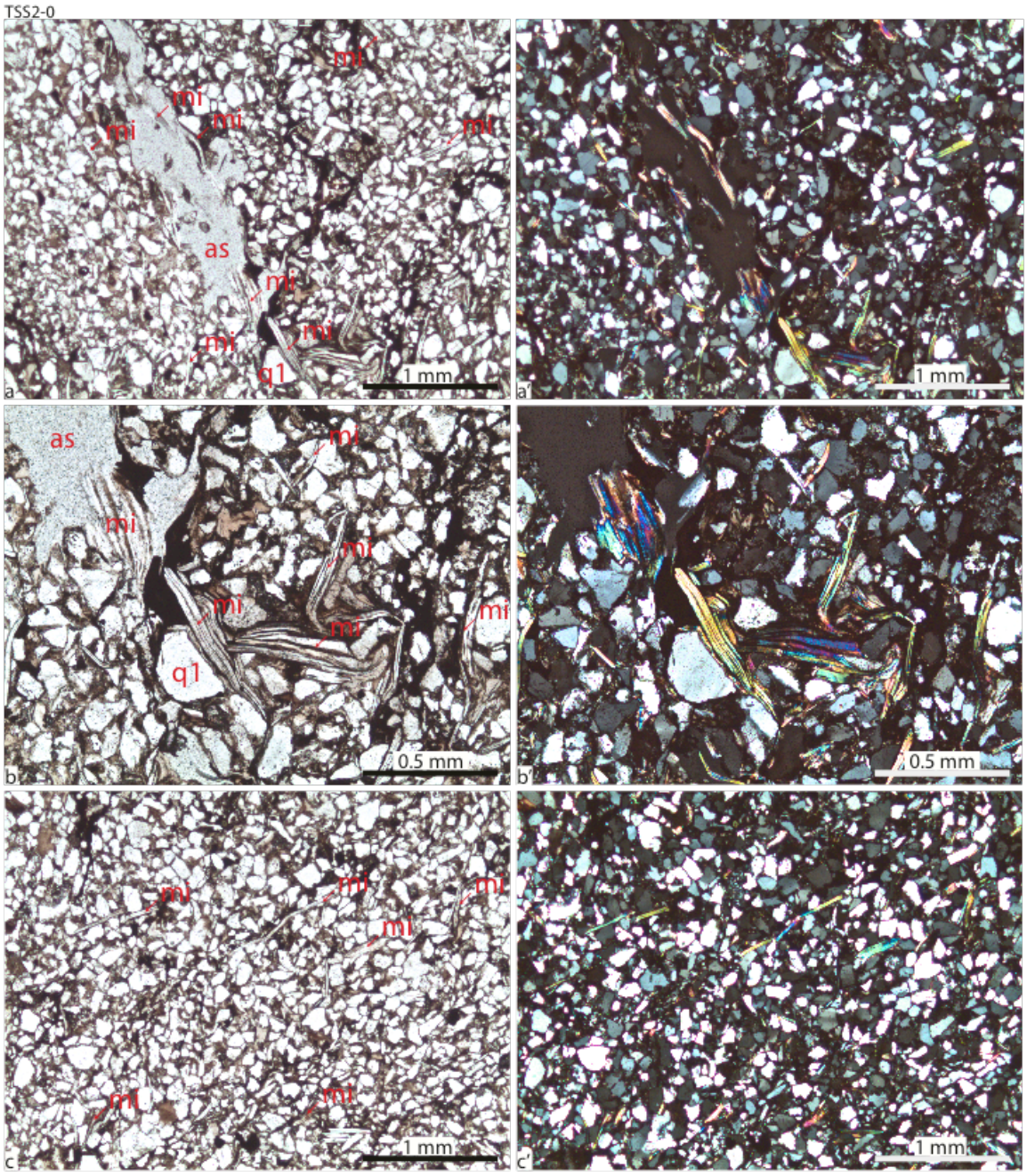

Hornsund, Sergeevfjellet, Serg-3

Plate 19 – TSS3-2: a-a': Microphotographs of an echinoderm remain, surrounded by micritic calcite cement. Minor quartz clasts also sparsely occur in the limestone. **b-b'**: Recrystallized sub-centimetric bivalve shell fragments surrounded by micritic calcite cement. Next to them appears a centimetre-scaled pyritic cluster. The porosity is concentrated within these pyrite-rich masses. **c-c':** Same porous, pyrite-rich horizons than in b-b'. Note that b' and c' are reflected light microphotographs. *Myalina* limestone beds, 15.75 m above the start of the sedimentary section.

Plate 20 – TSS3-1: a-b': Calcareous mudstone only displaying micritic calcite cement. Clasts of any kind are rare. Only a few sub-rounded quartz grains have been observed, as well as sparse micas. *Myalina* limestone beds, 15.6 m above the start of the sedimentary section.

Plate 21 – TSS3-0: a-c': Microphotographs of a low-angle transversal section through a trepostome bryozoans (br) of the *Arcticopora* genus. These sub-rounded fossil fragments show a higher degree of weathering and therefore a longer transport distance than the bryozoan fragments reported from Kovalevskajafjellet. This thin section also displays the (i) highest detrital clast content and (ii) the biggest (twinned) calcite spars of all *Myalina* limestone beds analysed on the Sørkapp-Hornsund High. The size of these calcite spars implies an extremely rapid meteoritic cementation. *Myalina* limestone beds, 15.5 m above the start of the sedimentary section.

Plate 19 – TSS3-2

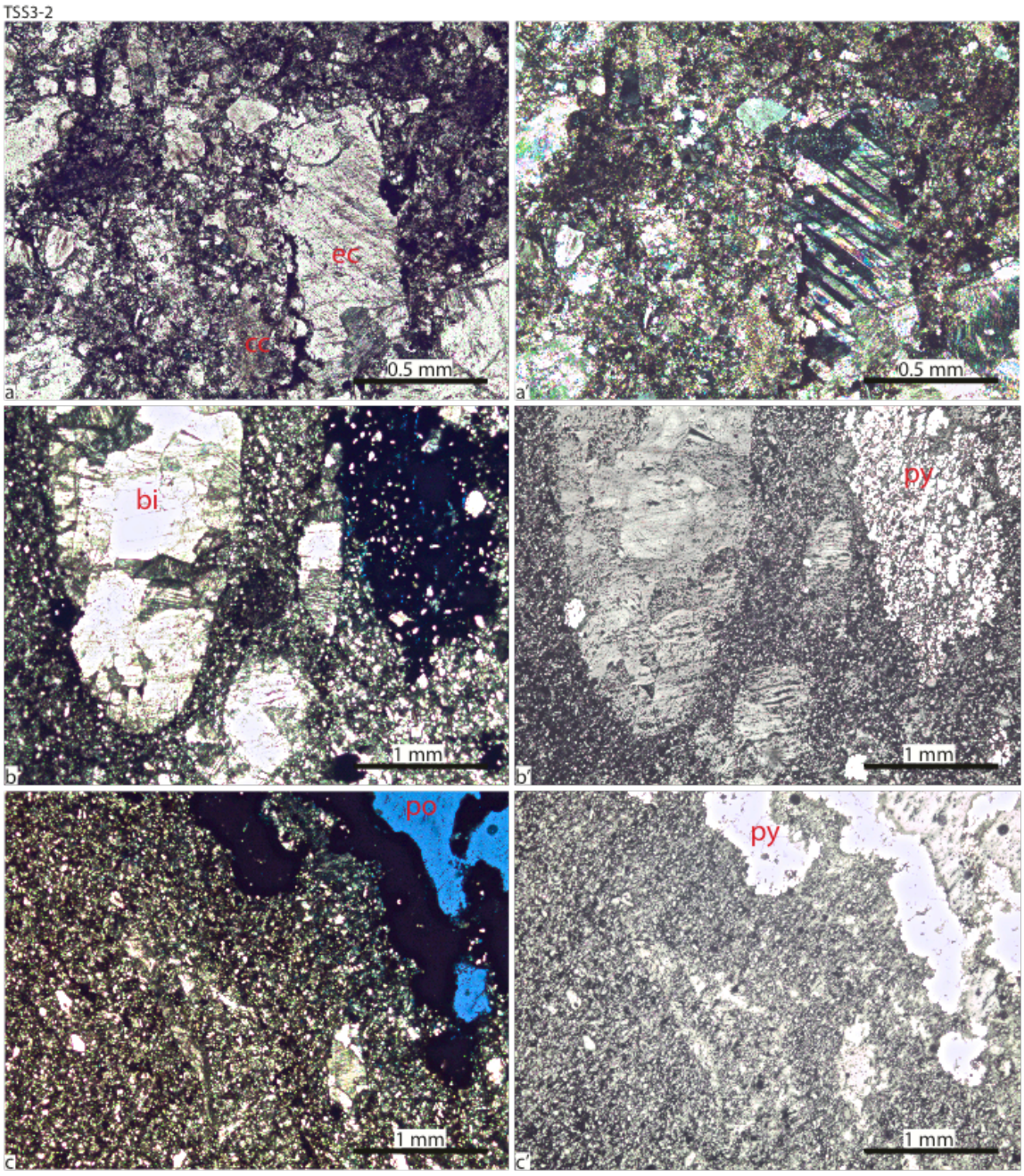

Plate 20 – TSS3-1

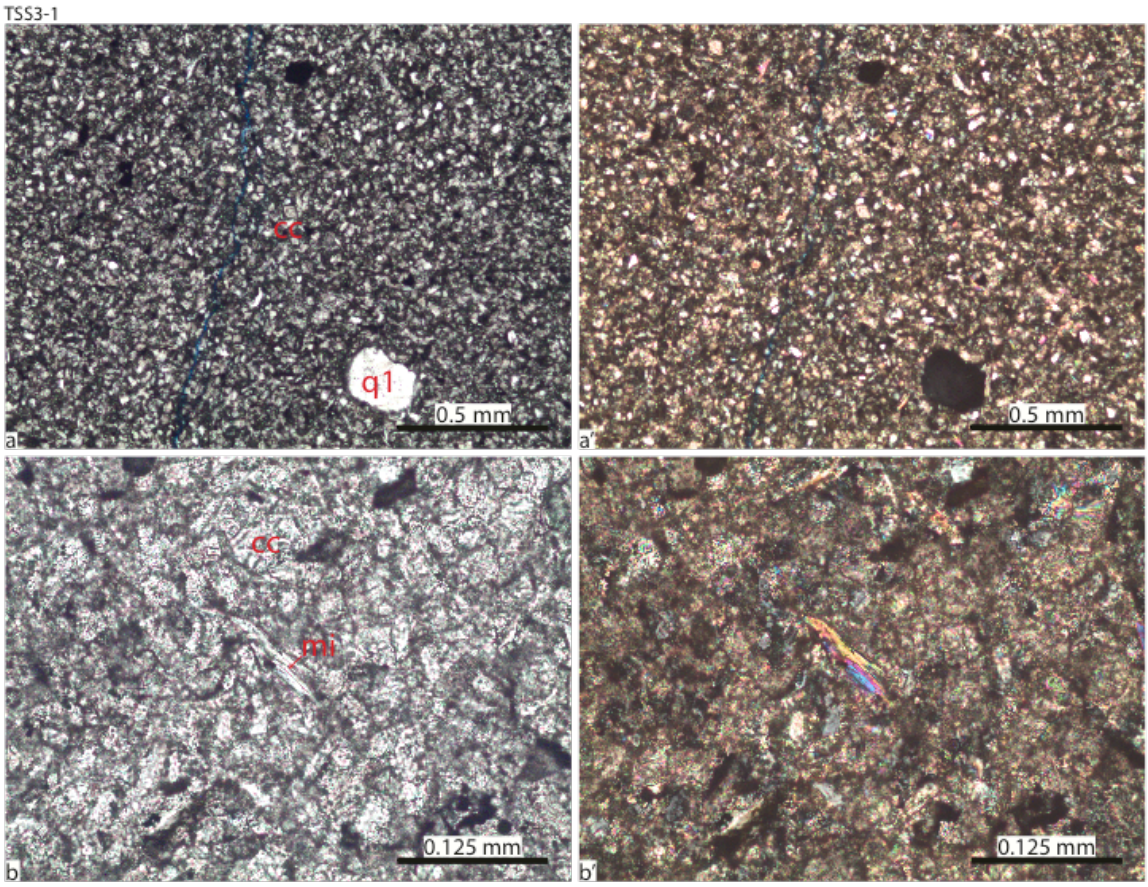

Plate 21 – TSS3-0